

## 18 SMOKE EXCEPTIONAL EVENTS: February 25 – September 25, 2012

### 18.1 Summary of Events

2012, while not considered particularly an active fire season, saw several dates with smoke impacts due to fires in eastern Arizona, southwestern New Mexico and northern Mexico. Readings at the Sunland Park (SPCY) PM<sub>2.5</sub> Partisol monitor were elevated above the annual NAAQS of 12 µg/m<sup>3</sup> on several occasions due to smoke. Table 18-1, below, shows the dates and concentrations of PM<sub>2.5</sub> in µg/m<sup>3</sup> for which smoke from wildfires impacted the monitoring site.

Date of exceedance	SPCY PM <sub>2.5</sub> concentration (µg/m <sup>3</sup> )
4/8/2012	20
4/10/2012	15
4/18/2012	19
4/23/2012	21
4/24/2012	22
5/7/2012	17
5/8/2012	20
5/24/2012	16
5/26/2012	22
6/2/2012	16
6/3/2012	18
6/4/2012	18
6/5/2012	29
6/9/2012	16
6/11/2012	20
6/12/2012	19
6/13/2012	17
6/14/2012	28
6/16/2012	16
6/21/2012	18
6/27/2012	33
6/28/2012	15
8/12/2012	67
9/6/2012	114
9/7/2012	18
9/17/2012	17
9/21/2012	19
9/25/2012	17

Table 18-1. Dates with smoke impacts and corresponding 24-hour average PM<sub>2.5</sub> concentration for the SPCY Partisol monitor.

In effect, New Mexico was surrounded by wildfires for much of this time period. The following images (Figures 18-1 to 18-28), one for each date listed in Table 18-1, are from Weather

Underground's Wundermap® showing satellite-detected fires as red-orange flame icons. Satellites reporting fire detects include GOES-EAST, GOES-WEST, MODIS TERRA, MODIS AQUA, AVHRR METOP-02, AVHRR NOAA-15, AVHRR NOAA-18 AND AVHRR NOAA-19. Times of day vary because satellite coverage times vary. The yellow star superimposed on each map indicates the approximate location of the SPCY Partisol monitor.



Figure 18-1. Wundermap® with satellite detected fires April 8, 2012 at 12:00 pm.

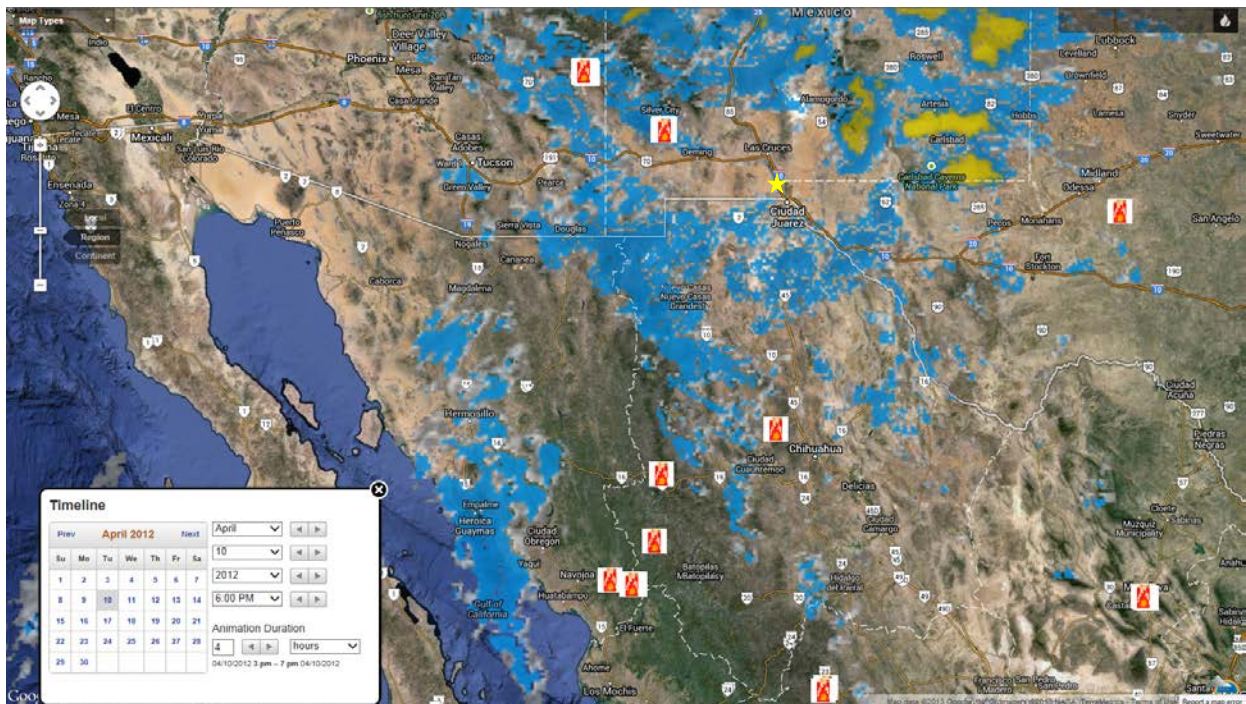


Figure 18-2. Wundermap® with satellite detected fires April 10, 2012 at 6:00 pm.

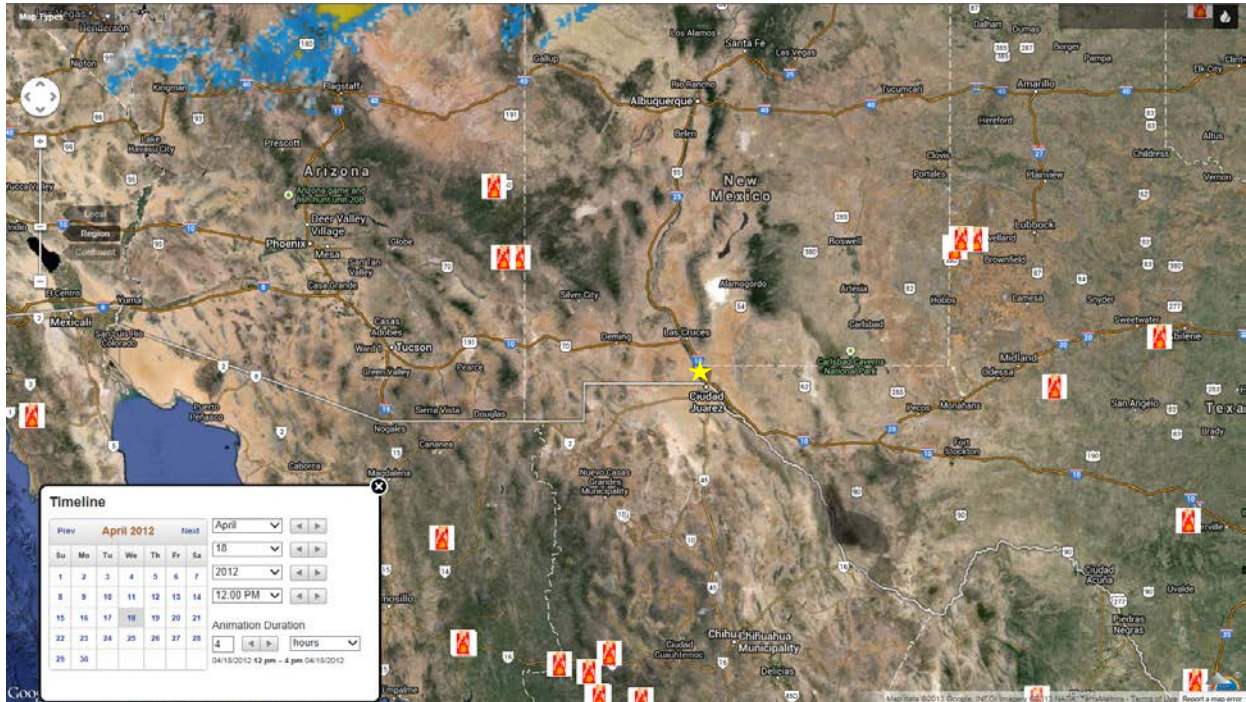


Figure 18-3. Wundermap® with satellite detected fires April 18, 2012 at 12:00 pm.

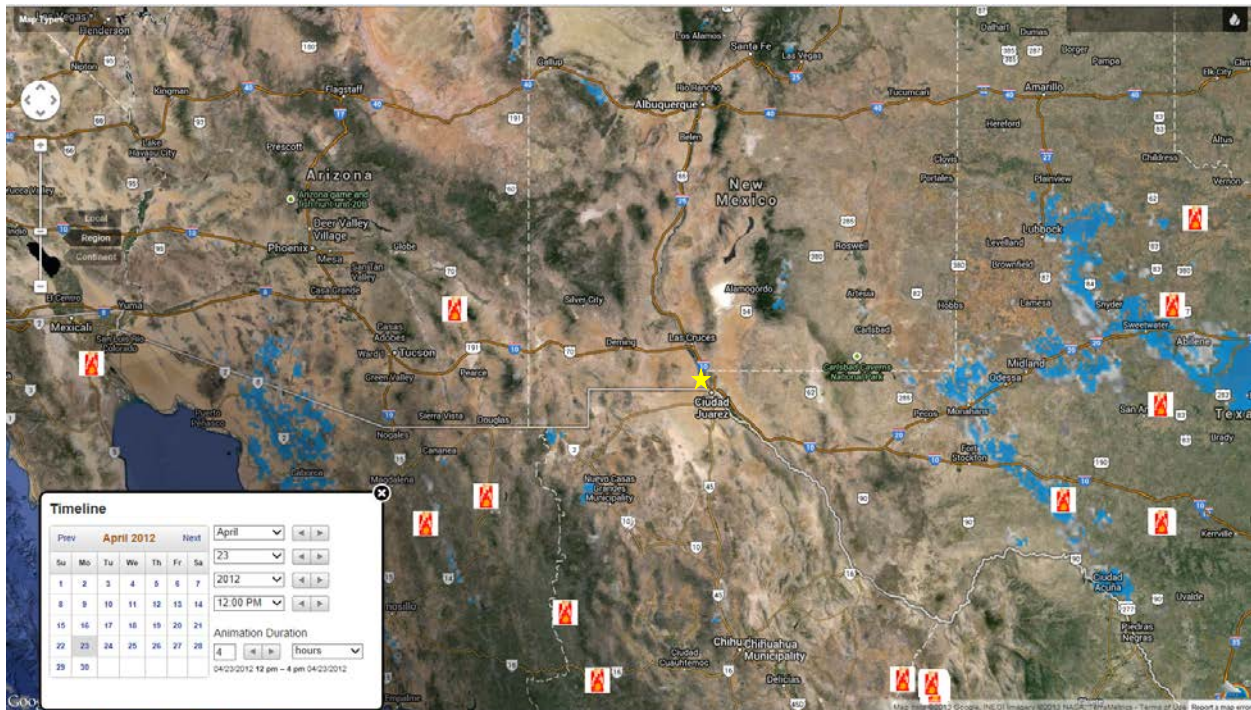


Figure 18-4. Wundermap® with satellite detected fires April 23, 2012 at 12:00 pm.

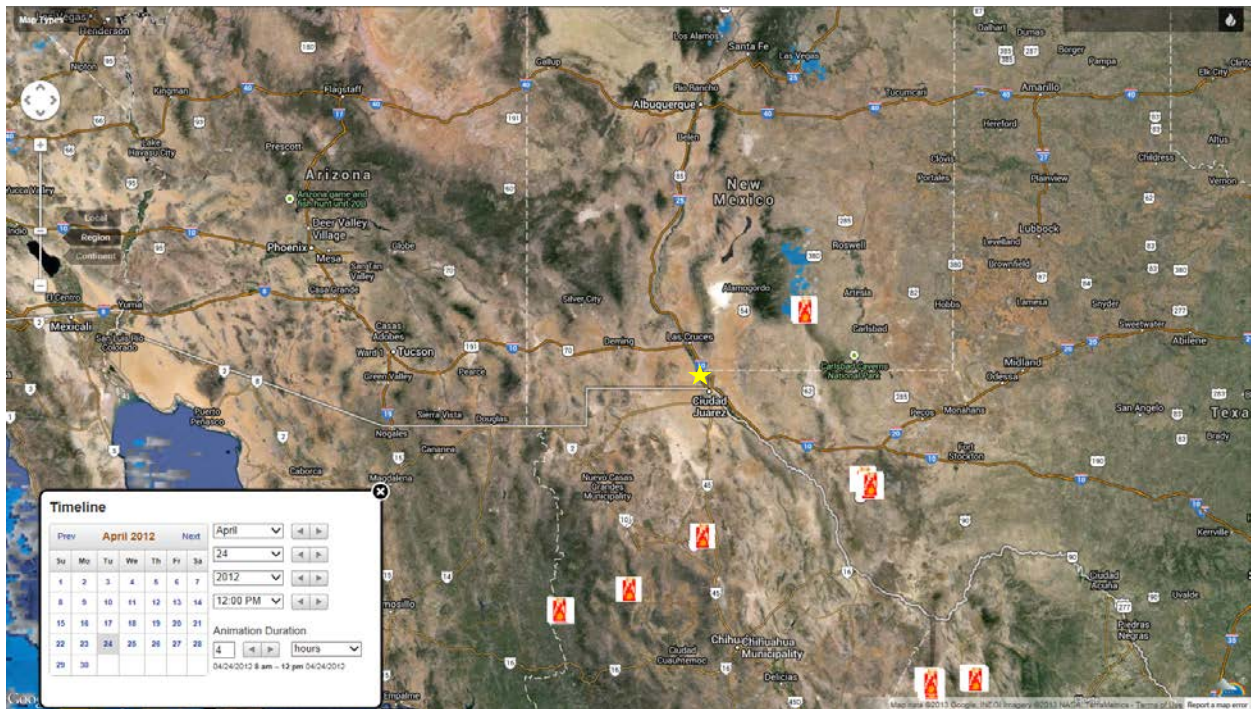


Figure 18-5. Wundermap® with satellite detected fires April 24, 2012 at 12:00 pm.

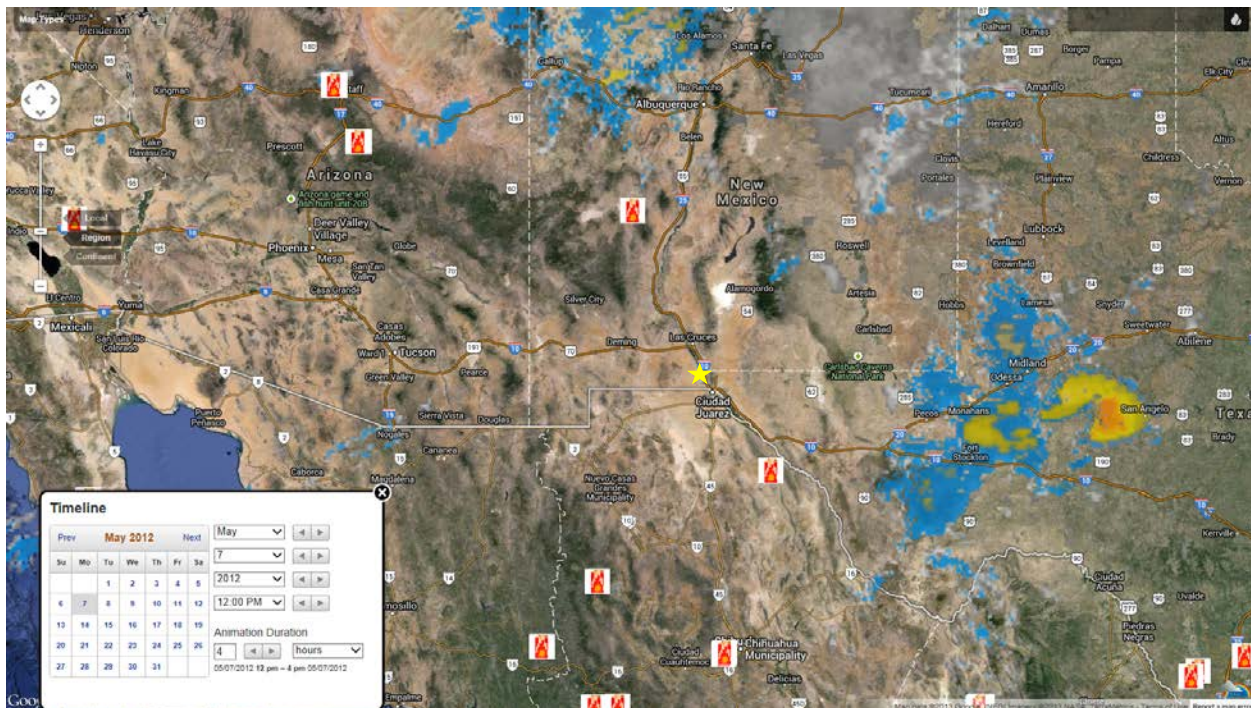


Figure 18-6. Wundermap® with satellite detected fires May 7, 2012 at 12:00 pm.

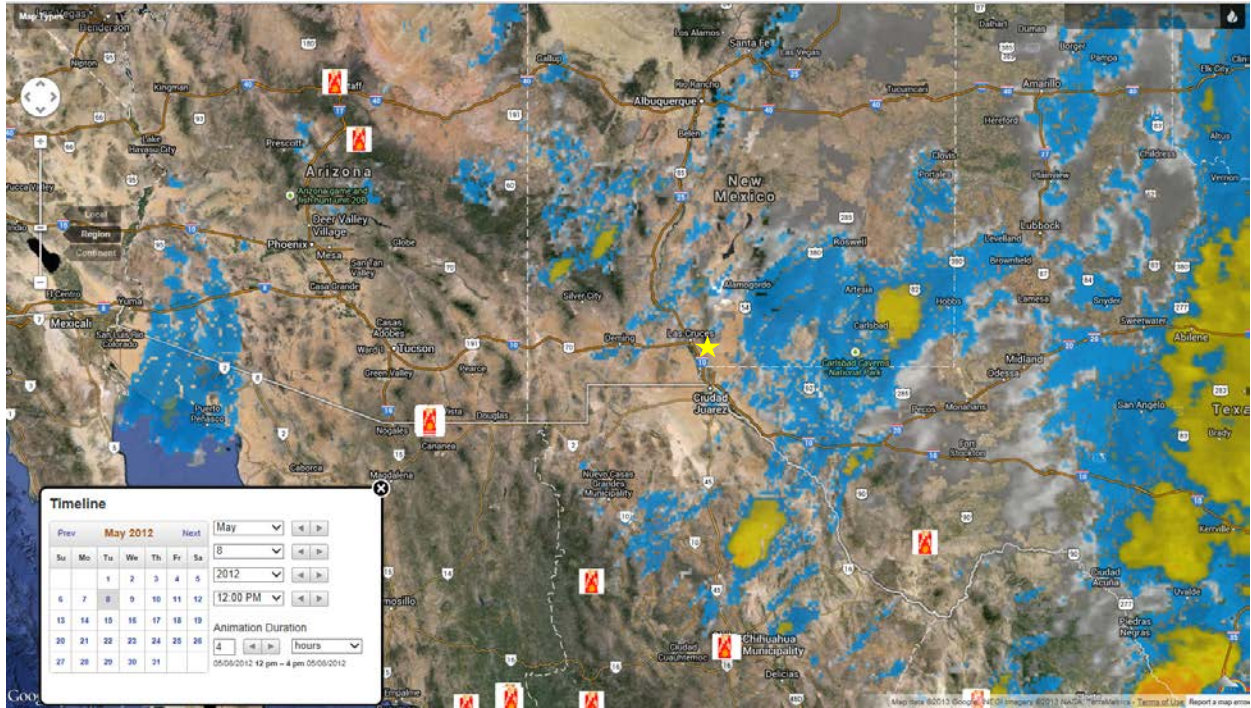


Figure 18-7. Wundermap® with satellite detected fires May 8, 2012 at 12:00 pm.

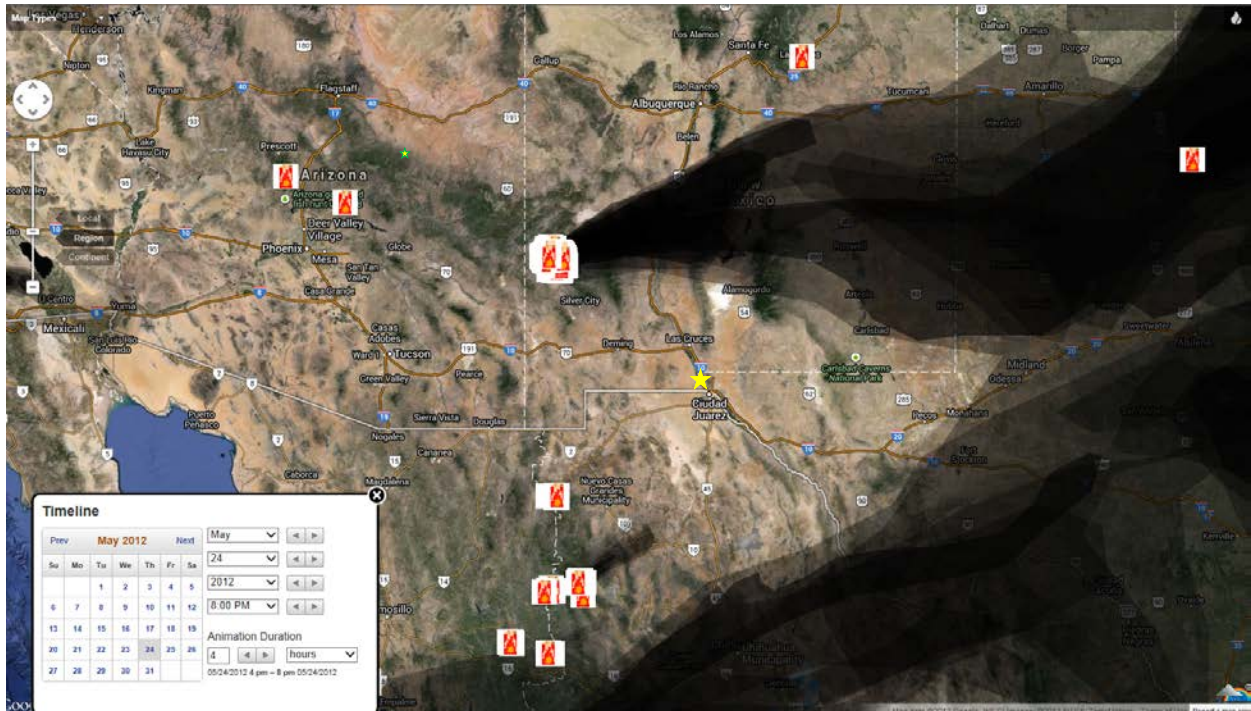


Figure 18-8. Wundermap® with satellite detected fires May 24, 2012 at 8:00 pm.

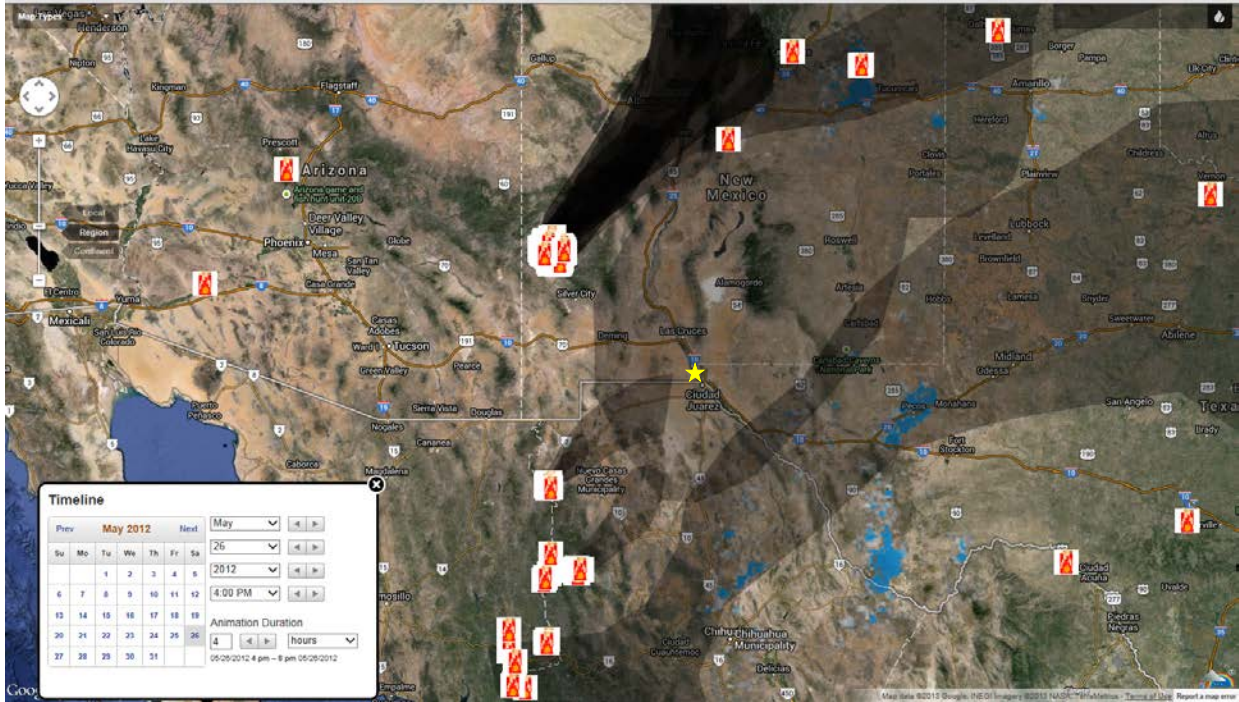


Figure 18-9. Wundermap® with satellite detected fires May 26, 2012 at 4:00 pm.

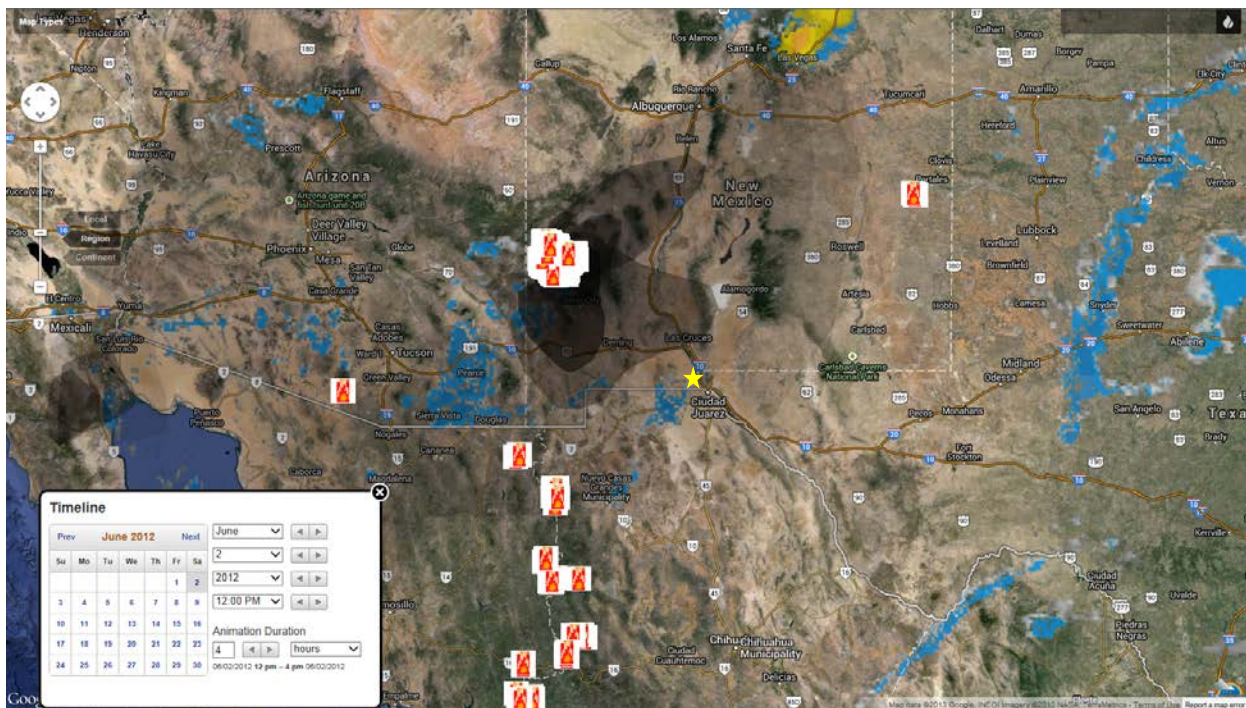


Figure 18-10. Wundermap® with satellite detected fires June 2, 2012 at 12:00 pm.

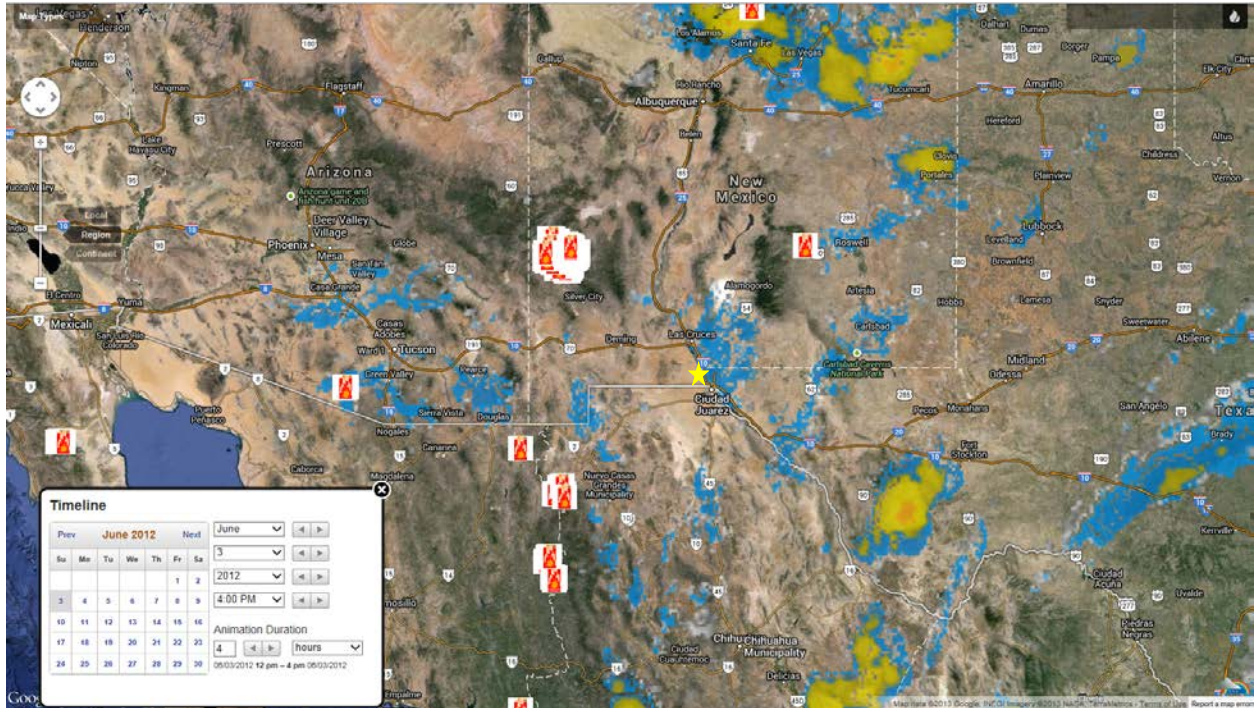


Figure 18-11. Wundermap® with satellite detected fires June 3, 2012 at 4:00 pm.

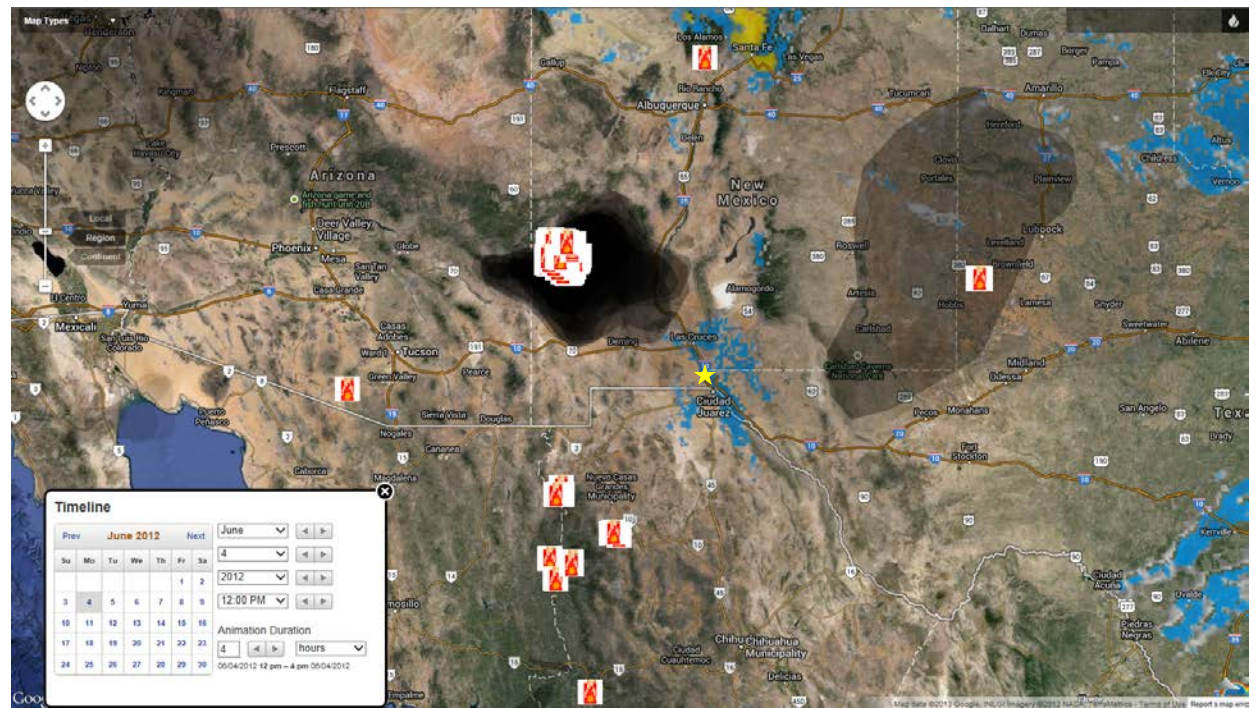


Figure 18-12. Wundermap® with satellite detected fires June 4, 2012 at 12:00 pm.

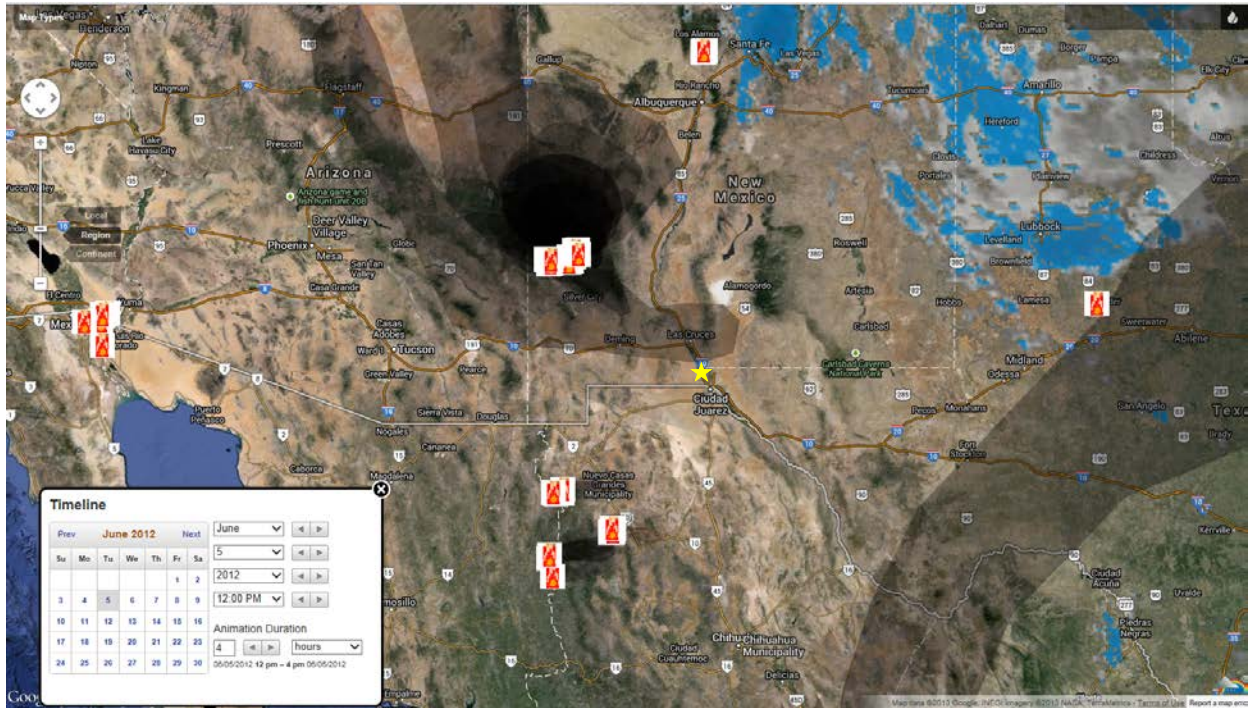


Figure 18-13. Wundermap® with satellite detected fires June 5, 2012 at 12:00 pm.

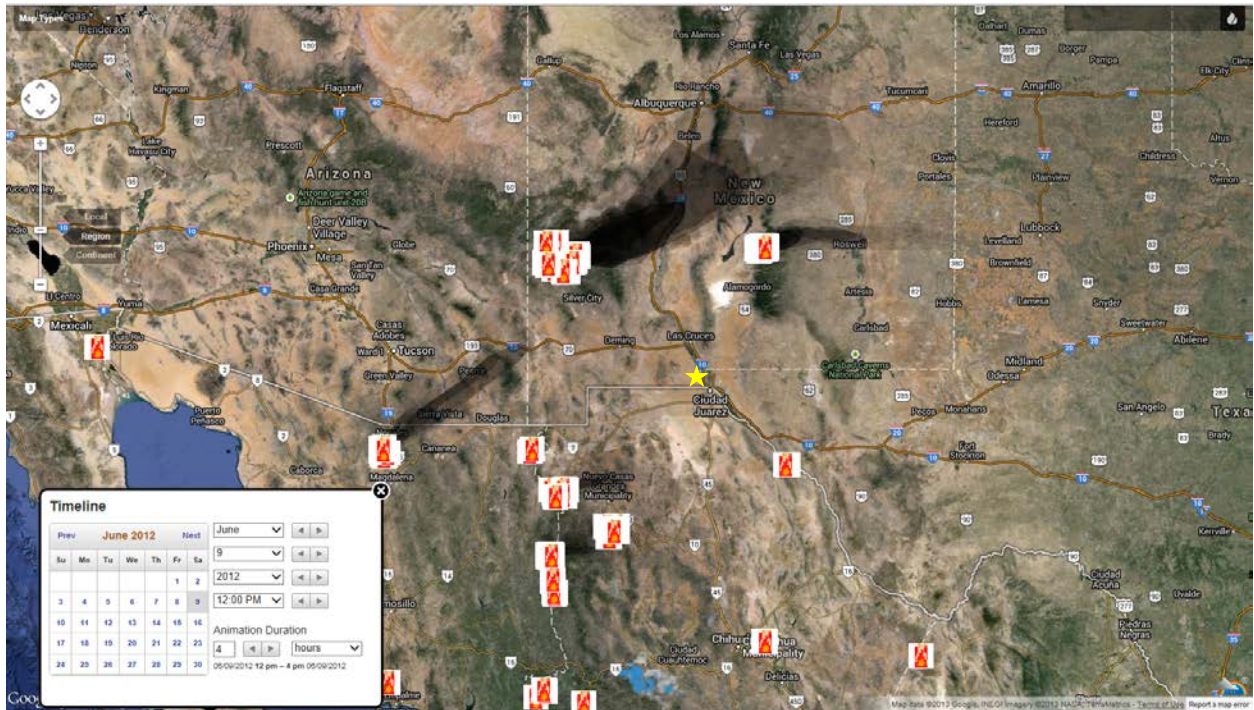


Figure 18-14. Wundermap® with satellite detected fires June 9, 2012 at 12:00 pm.

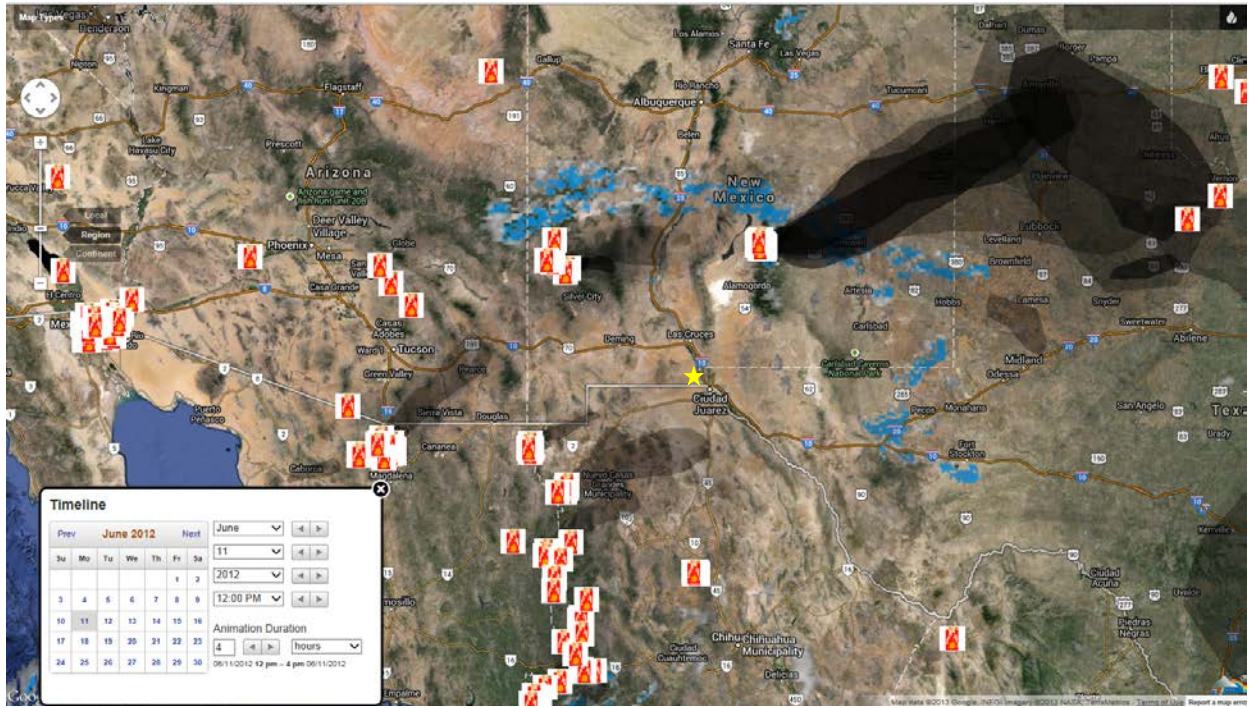


Figure 18-15. Wundermap® with satellite detected fires June 11, 2012 at 12:00 pm.

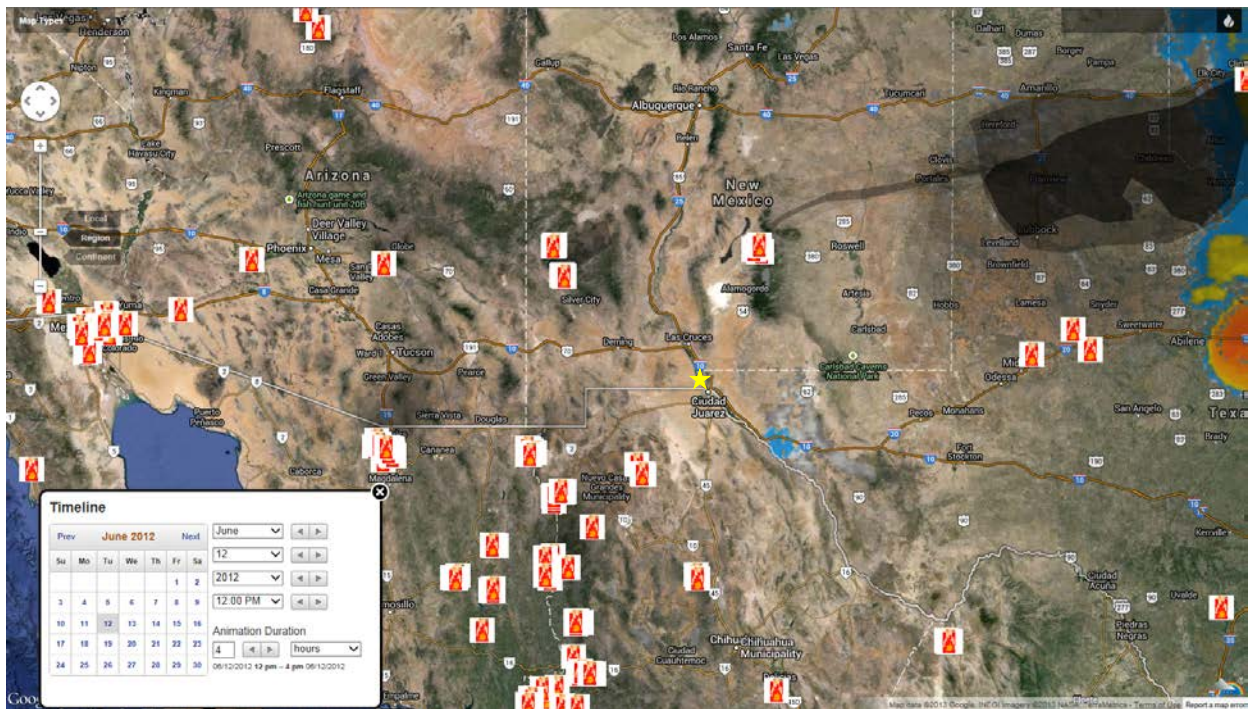


Figure 18-16. Wundermap® with satellite detected fires June 12, 2012 at 12:00 pm.

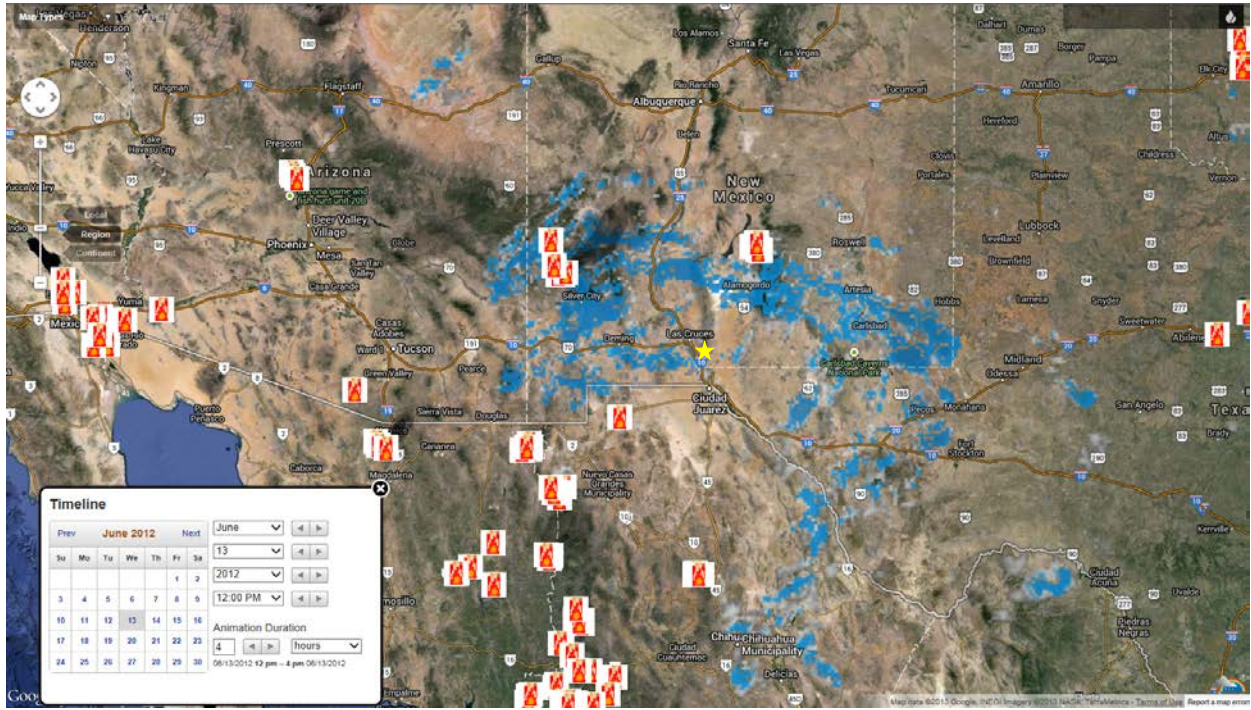


Figure 18-17. Wundermap® with satellite detected fires June 13, 2012 at 12:00 pm.

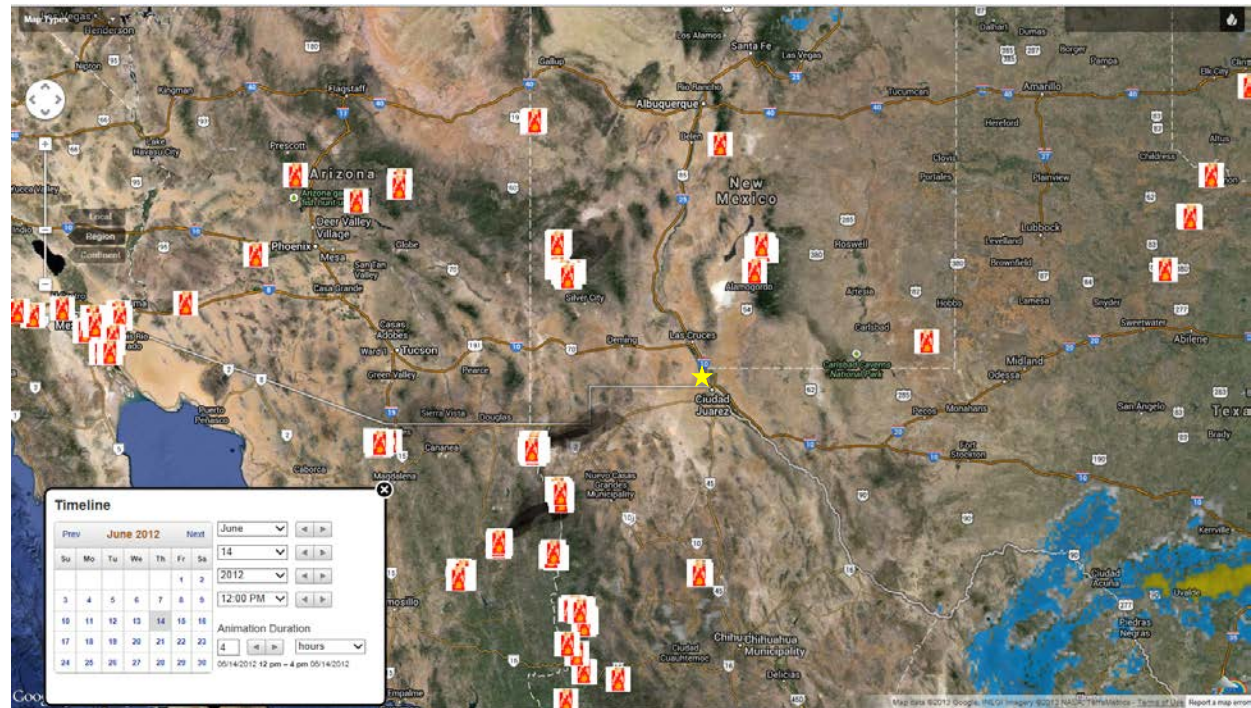


Figure 18-18. Wundermap® with satellite detected fires June 14, 2012 at 12:00 pm.

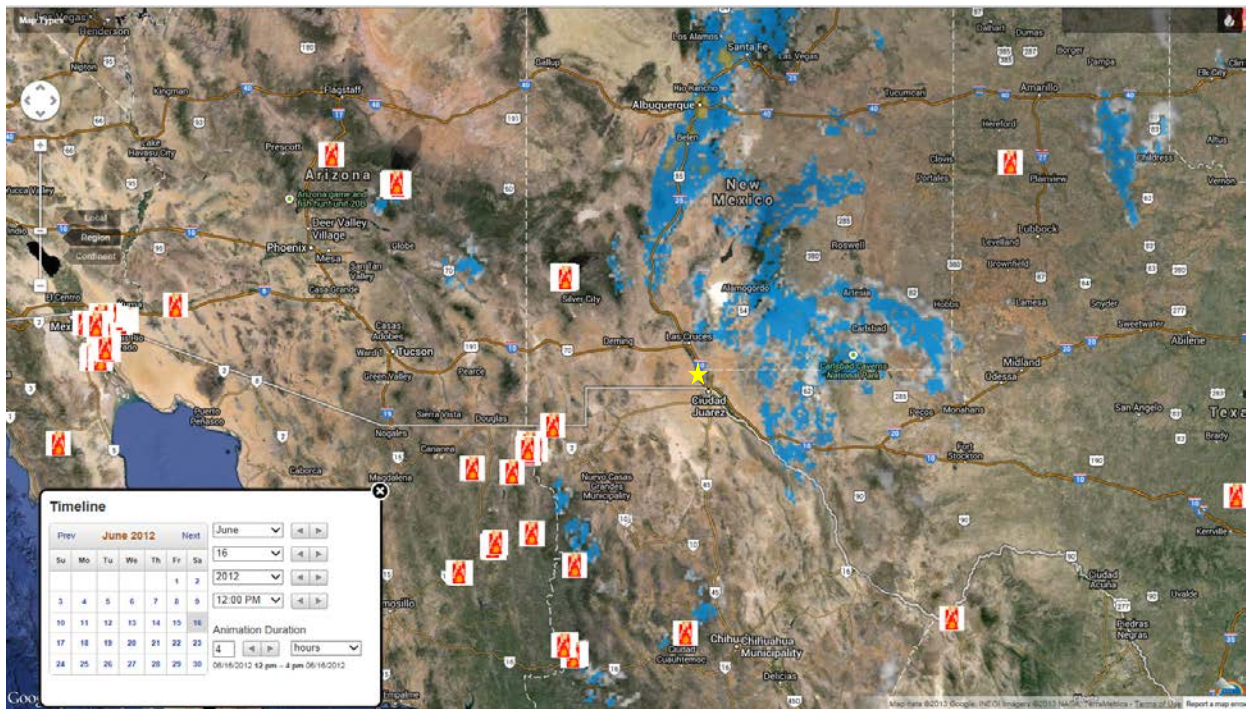


Figure 18-19. Wundermap® with satellite detected fires June 16, 2012 at 12:00 pm.

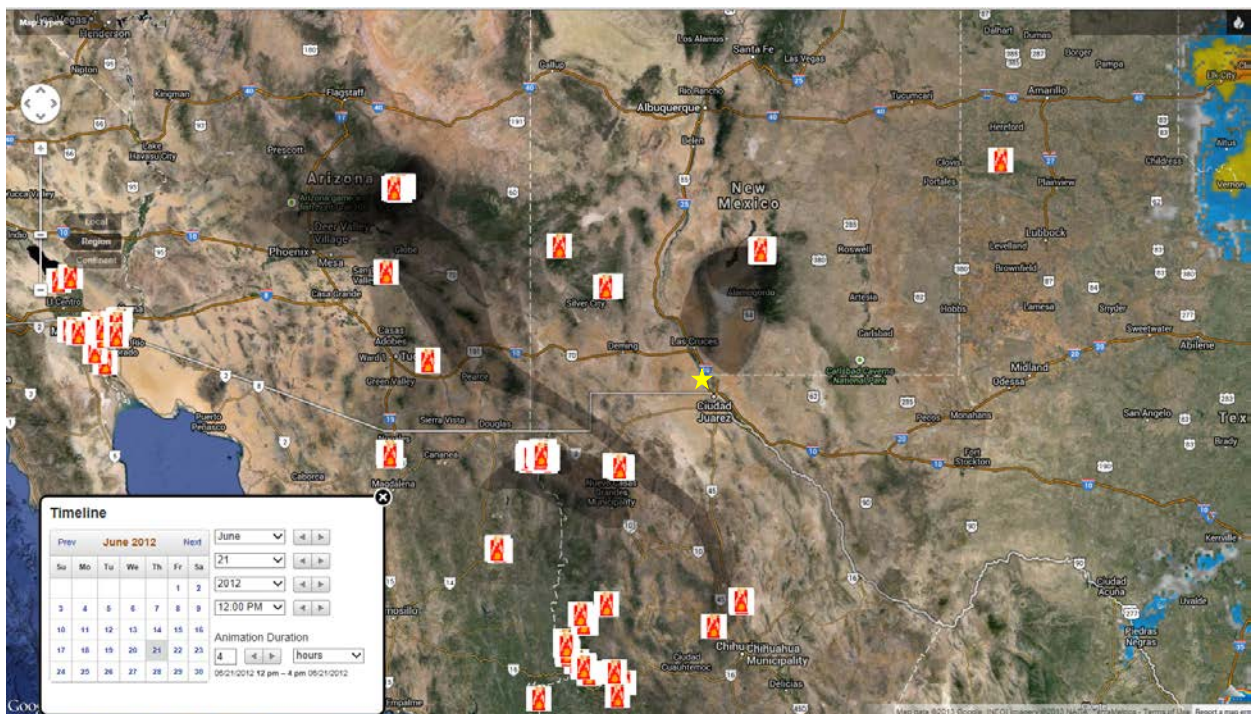


Figure 18-20. Wundermap® with satellite detected fires June 21, 2012 at 12:00 pm.

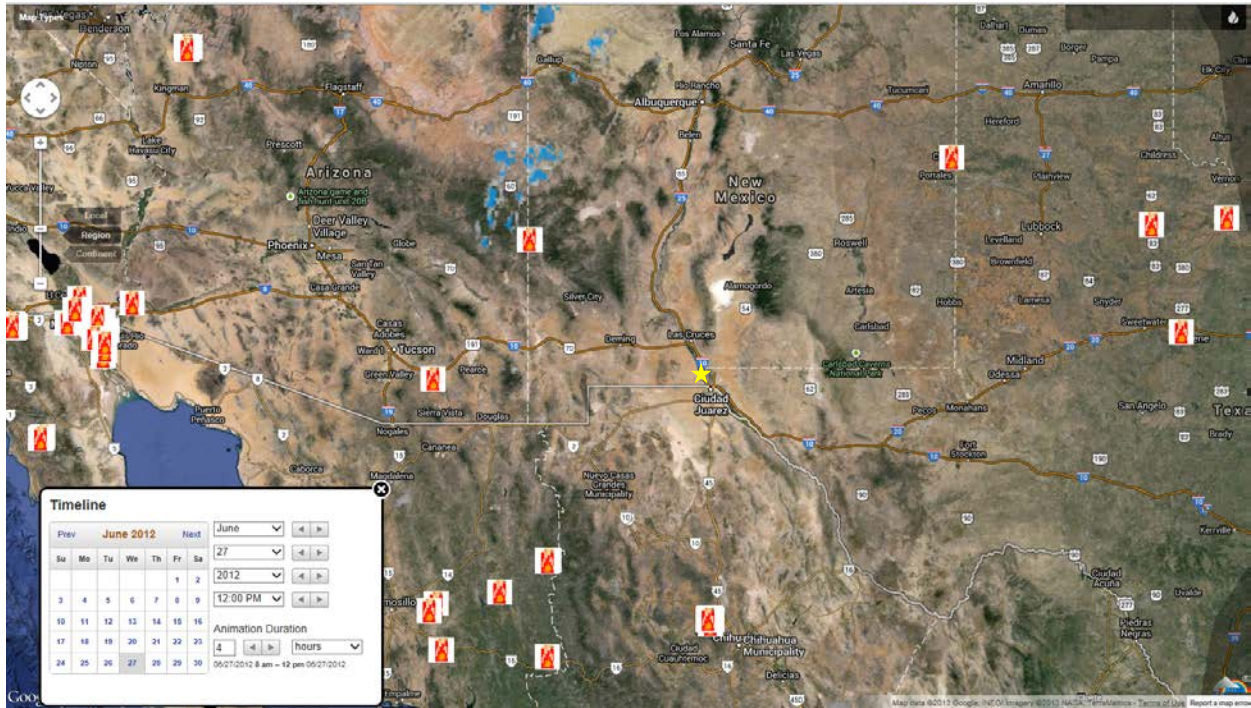


Figure 18-21. Wundermap® with satellite detected fires June 27, 2012 at 12:00 pm.

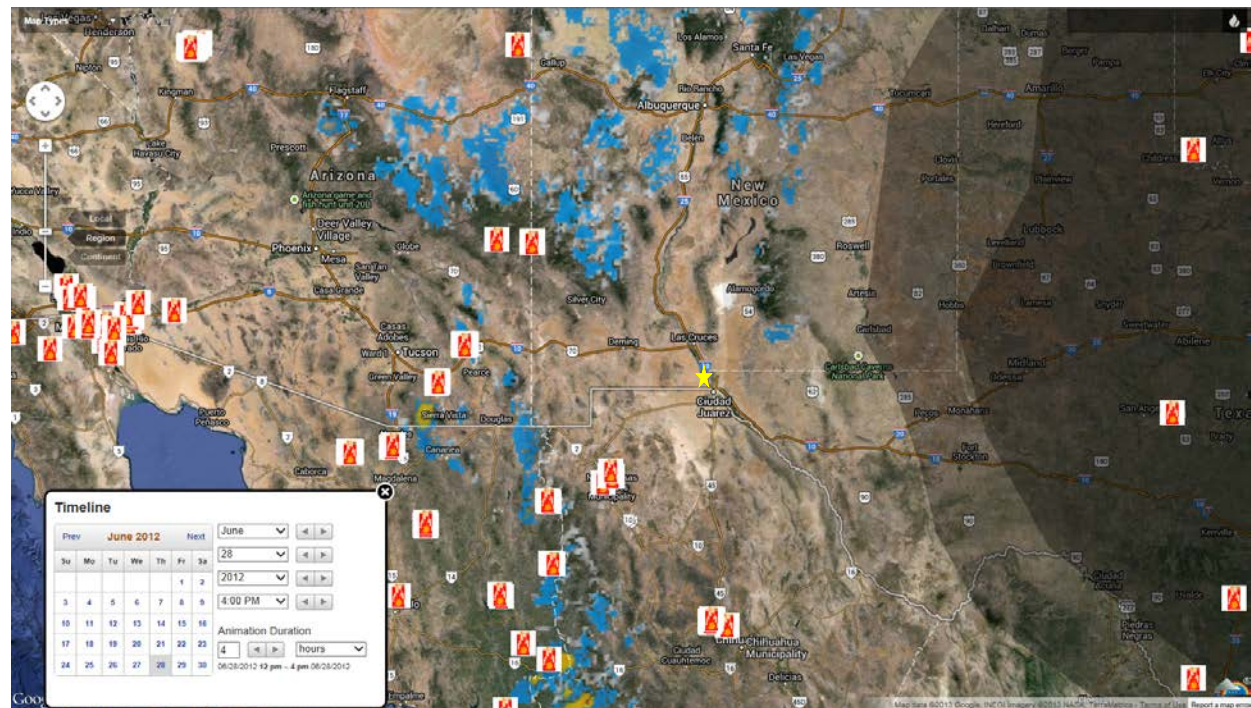


Figure 18-22. Wundermap® with satellite detected fires June 28, 2012 at 4:00 pm.

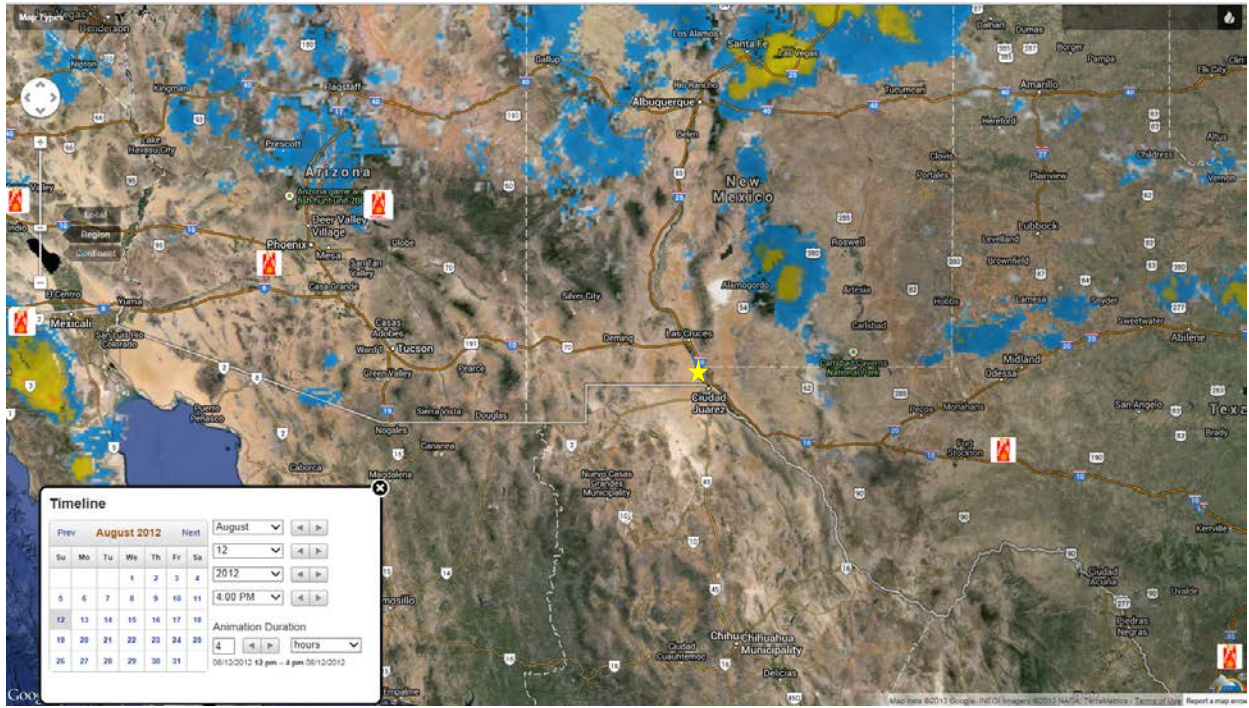


Figure 18-23. Wundermap® with satellite detected fires August 12, 2012 at 4:00 pm.

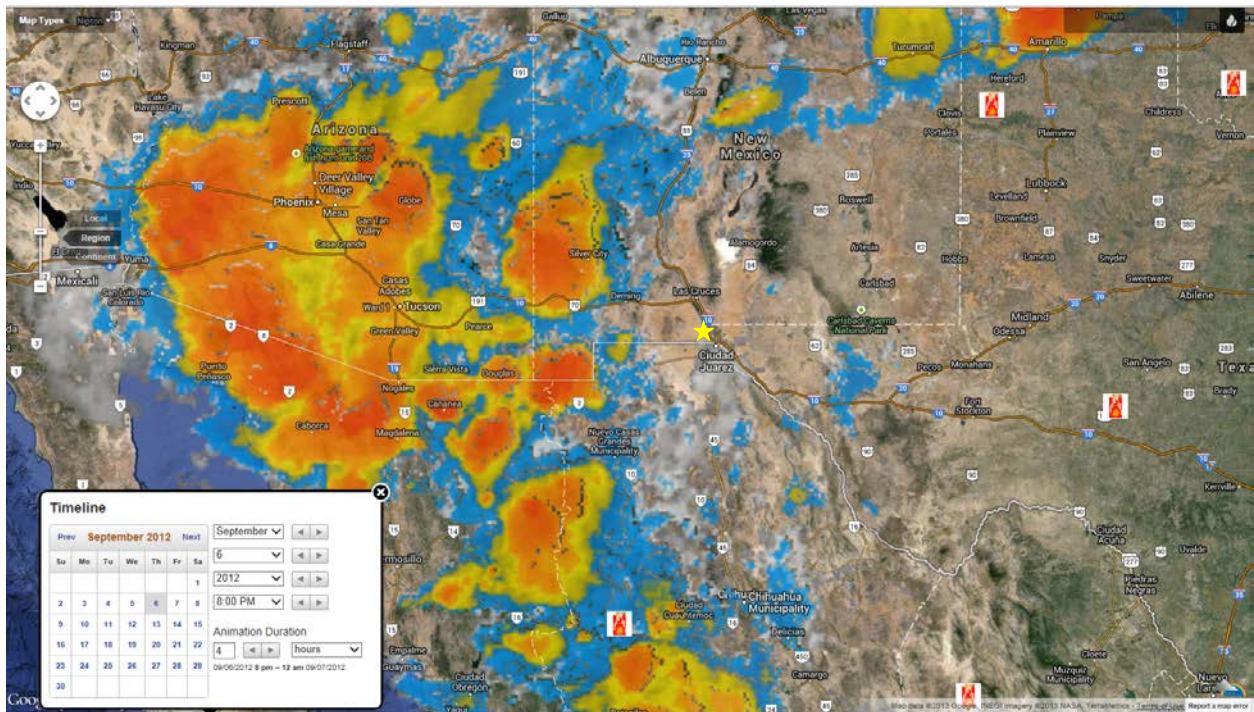


Figure 18-24. Wundermap® with satellite detected fires September 6, 2012 at 8:00 pm.

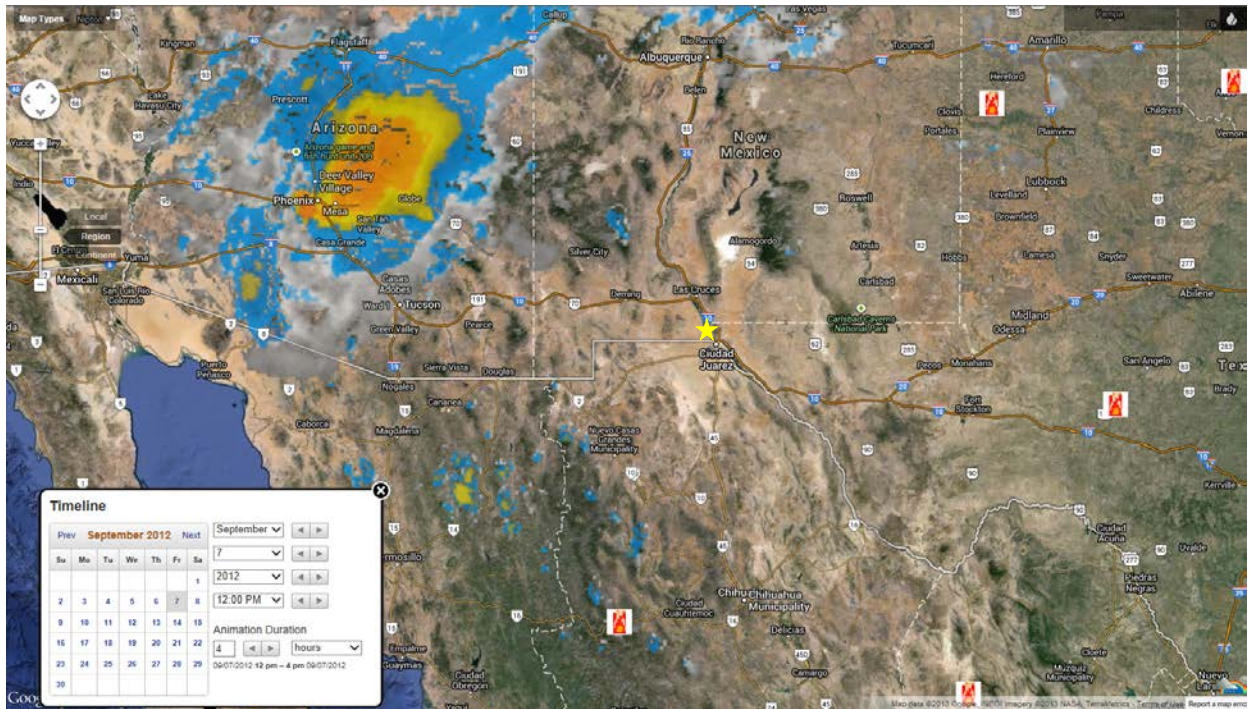


Figure 18-25. Wundermap® with satellite detected fires September 7, 2012 at 12:00 pm.

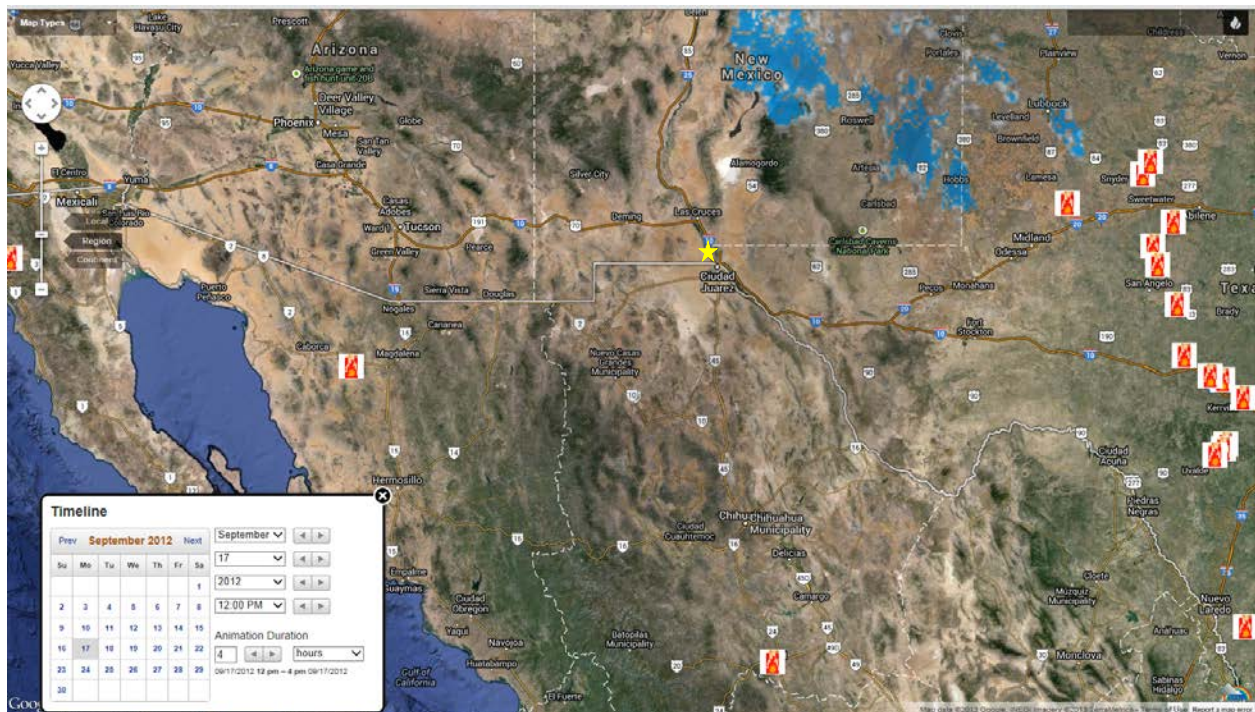


Figure 18-26. Wundermap® with satellite detected fires September 17, 2012 at 12:00 pm.

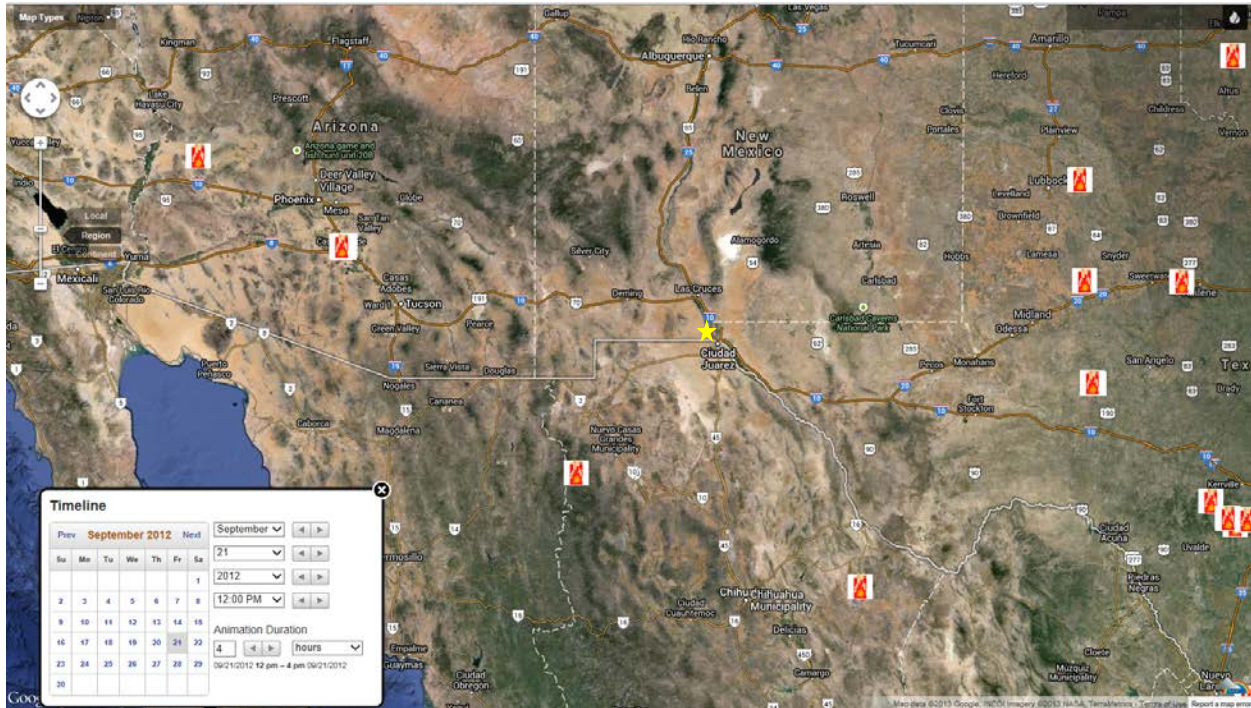


Figure 18-27. Wundermap® with satellite detected fires September 21, 2012 at 12:00 pm.

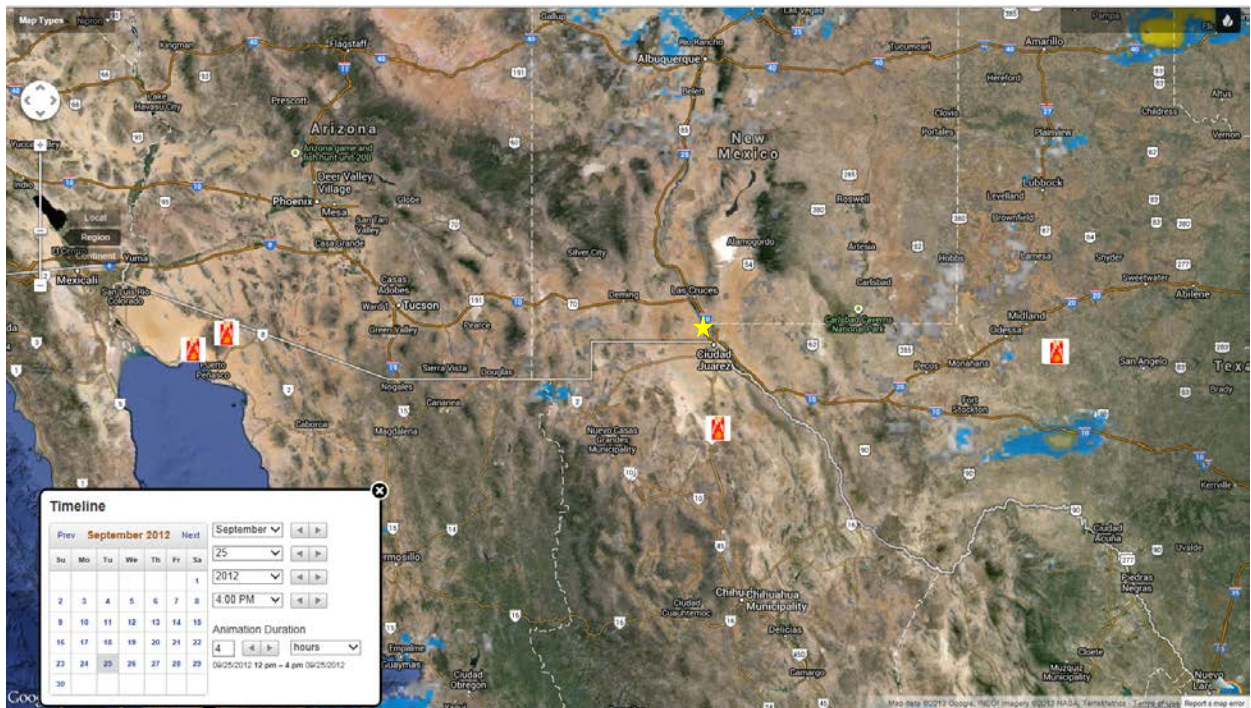


Figure 18-28. Wundermap® with satellite detected fires September 25, 2012 at 4:00 pm.

As can be seen from the images above, smoke was added to the atmosphere beginning in February and building in intensity through June, then decreasing again after June. Fires were still present through August and September; beginning in October smoke was no longer a significant factor for New Mexico’s air quality as indicated by more normalized concentrations at the SPCY PM<sub>2.5</sub> Partisol monitor.

As the events unfolded, winds blew from various directions throughout the border region, carrying smoke from myriad fires into the Sunland Park area. The presence of smoke-producing wildfires, little to no point sources in the area, and the high PM<sub>2.5</sub> concentrations support the assertion that these were exceptional events, specifically natural events caused by wildfire smoke.

## **18.2 Is Not Reasonably Controllable or Preventable**

### 18.2.1 Suspected Source Areas and Categories Contributing to the Event

Sources of smoke contributing to these exceedances include wildfires from eastern Arizona, southwestern New Mexico, and northern Mexico. The largest sources of smoke are from the Whitewater-Baldy fire in southwestern New Mexico and the various fires in northern Mexico, although some contribution may also have been made by several fires in Arizona and New Mexico, depending on the wind directions and speeds on each given date.

The sources of smoke were widespread, often covering large portions of northern Mexico and sometimes nearly half of the contiguous 48 states. Smoke impacts may be due to smoke as far away as California and Central America. Smoke has a relatively high residence time and may remain in the upper atmosphere and then be brought down to the surface as air cools.

### 18.2.2 Recurrence Frequency

The forests, rangelands and grasslands of New Mexico are fire-adapted ecosystems where long absence of fire has led to hazardous fuel and unhealthy forest conditions. Similar conditions exist in Arizona and northern Mexico. Most fires occur during the spring and early summer when conditions are commonly dry and windy. The frequency and intensity of wildfires, including the frequency of catastrophic fires, has been exacerbated by ongoing drought conditions. As Figures 18-29 to 18-36 show, drought conditions have persisted through the end of September. These conditions range from “abnormally dry” to “drought – exceptional” and while these levels ease somewhat from the end of February to the end of September due to precipitation, it is important to note that most of Arizona, New Mexico and Mexico remain in a long-term drought condition.

# North American Drought Monitor

February 29, 2012  
Released: March 13, 2012

<http://www.ncdc.noaa.gov/nadm.html>

Analysts:  
Canada - Trevor Hadwen\*  
Richard Rieger  
Mallory MacDonald  
Mexico - Reynaldo Pascual  
Adelina Albanil  
U.S.A. - Mark Svoboda

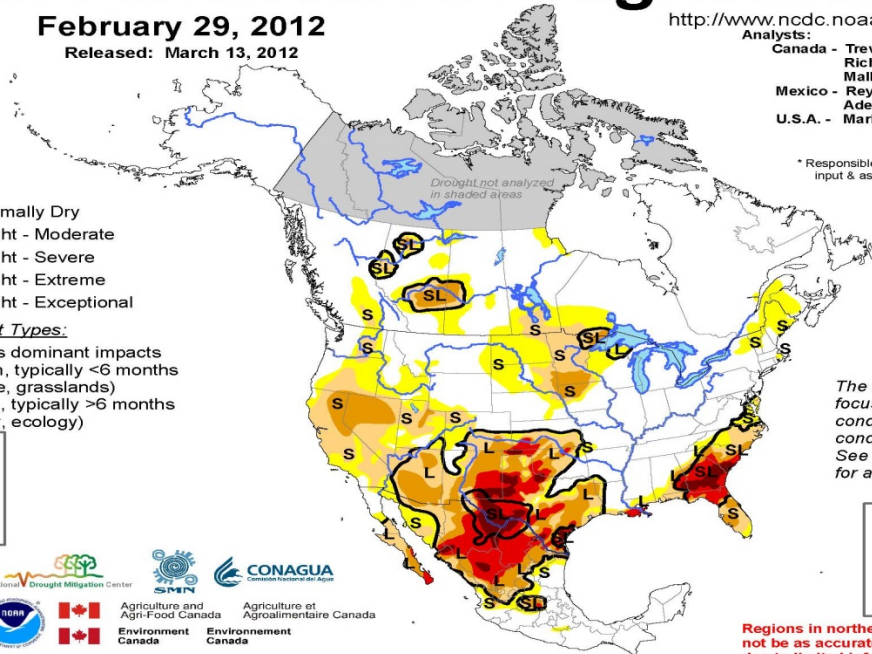
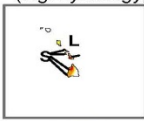
\* Responsible for collecting analysts' input & assembling the NA-DM map

**Intensity:**

- D0 Abnormally Dry
- D1 Drought - Moderate
- D2 Drought - Severe
- D3 Drought - Extreme
- D4 Drought - Exceptional

**Drought Impact Types:**

- ~ Delineates dominant impacts
- S = Short-Term, typically <6 months (e.g. agriculture, grasslands)
- L = Long-Term, typically >6 months (e.g. hydrology, ecology)



The Drought Monitor focuses on broad-scale conditions. Local conditions may vary. See accompanying text for a general summary.



Regions in northern Canada may not be as accurate as other regions due to limited information.

Figure 18-29. North American Drought Monitor map analyzed as of February 29, 2012. Severe to exceptional drought conditions dominate New Mexico and Mexico with mostly long-term impacts. Arizona conditions may be classified as moderate to severe, also with long-term impacts.

# North American Drought Monitor

March 31, 2012  
Released: April 18, 2012

<http://www.ncdc.noaa.gov/nadm.html>

Analysts:  
Canada - Trevor Hadwen  
Richard Rieger  
Mexico - Reynaldo Pascual  
Adelina Albanil  
U.S.A. - Brian Fuchs  
Brad Pugh\*

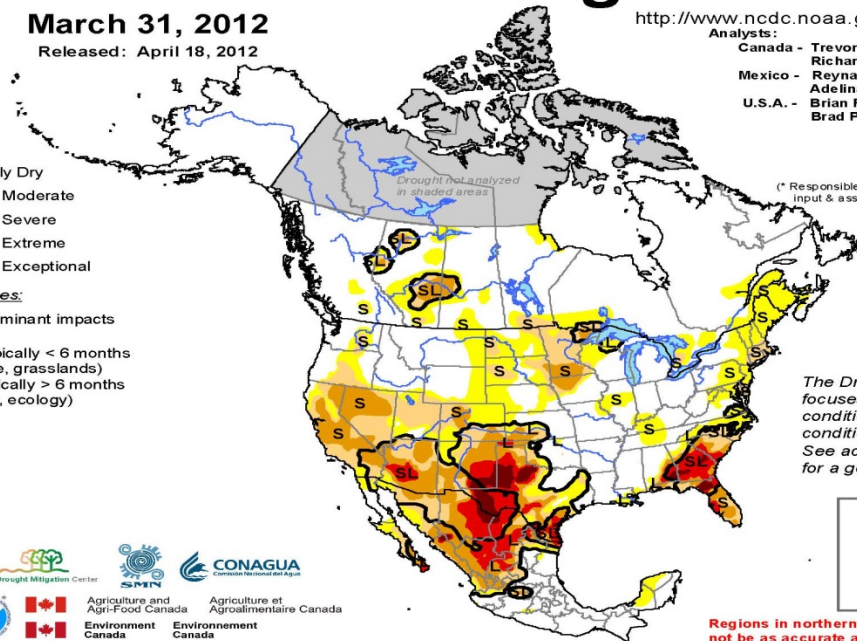
\* Responsible for collecting analysts' input & assembling the NA-DM map

**Intensity:**

- D0 Abnormally Dry
- D1 Drought - Moderate
- D2 Drought - Severe
- D3 Drought - Extreme
- D4 Drought - Exceptional

**Drought Impact Types:**

- ~ Delineates dominant impacts
- S = Short-Term, typically < 6 months (e.g. agriculture, grasslands)
- L = Long-Term, typically > 6 months (e.g. hydrology, ecology)



The Drought Monitor focuses on broad-scale conditions. Local conditions may vary. See accompanying text for a general summary.



Regions in northern Canada may not be as accurate as other regions due to limited information.

Figure 18-30. North American Drought Monitor map analyzed as of March 31, 2012. Much of New Mexico and Mexico are classified as severe to exceptional conditions with mostly long-term impacts. In Arizona, conditions have worsened since February. In this analysis, most of Arizona is classified as severe to extreme, with both short and long term impacts.

# North American Drought Monitor

April 30, 2012

Released: Thursday, May 10, 2012

<http://www.ncdc.noaa.gov/nadm.html>

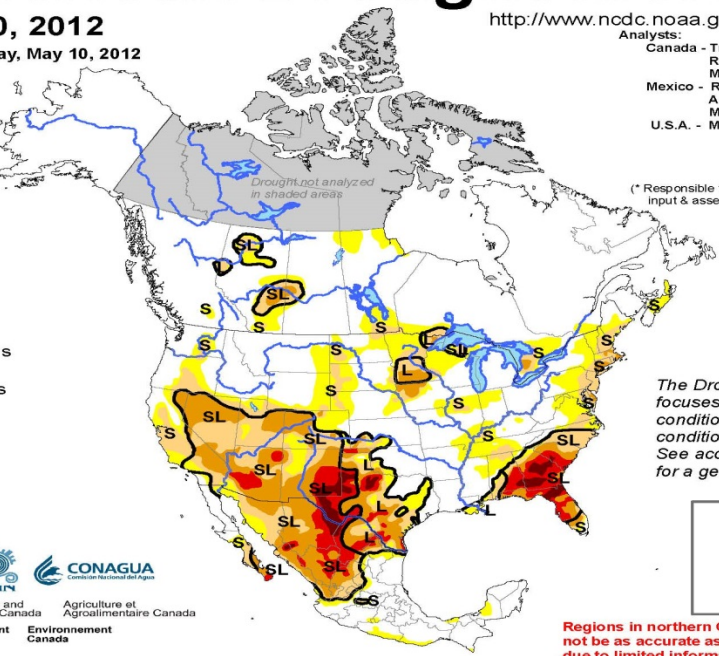
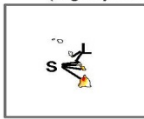
Analysts:  
 Canada - Trevor Hadwen  
 Richard Rieger  
 Malory MacDonald  
 Mexico - Reynaldo Pascual\*  
 Adelina Albanil\*  
 Minerva López\*  
 U.S.A. - Matthew Rosencrans

**Intensity:**

- D0 Abnormally Dry
- D1 Drought - Moderate
- D2 Drought - Severe
- D3 Drought - Extreme
- D4 Drought - Exceptional

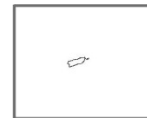
**Drought Impact Types:**

- ~ Delineates dominant impacts
- S = Short-Term, typically <6 months  
(e.g. agriculture, grasslands)
- L = Long-Term, typically >6 months  
(e.g. hydrology, ecology)



(\* Responsible for collecting analysts' input & assembling the NA-DM map)

The Drought Monitor focuses on broad-scale conditions. Local conditions may vary. See accompanying text for a general summary.



Regions in northern Canada may not be as accurate as other regions due to limited information.

Figure 18-31. North American Drought Monitor map analyzed as of April 30, 2012. Conditions have eased somewhat for Mexico, although most of the country remains classified as severe to extreme. New Mexico is still mostly severe to exceptional and Arizona is still mostly severe to extreme. Most areas are now classified as having both short- and long-term impacts.

# North American Drought Monitor

May 31, 2012

Released: Tuesday, June 12, 2012

<http://www.ncdc.noaa.gov/nadm.html>

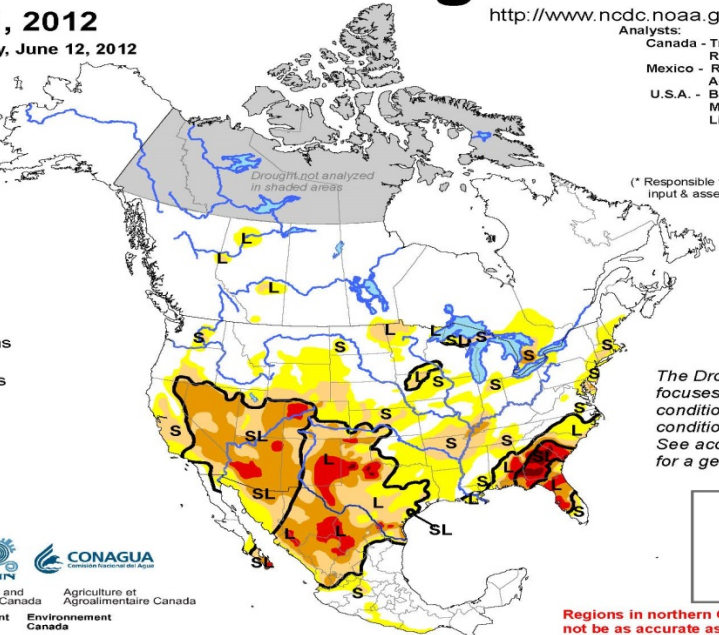
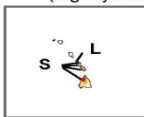
Analysts:  
 Canada - Trevor Hadwen  
 Richard Rieger  
 Mexico - Reynaldo Pascual  
 Adelina Albanil  
 U.S.A. - Brad Rippey  
 Michael Brewer\*  
 Liz Love-Brotak

**Intensity:**

- D0 Abnormally Dry
- D1 Drought - Moderate
- D2 Drought - Severe
- D3 Drought - Extreme
- D4 Drought - Exceptional

**Drought Impact Types:**

- ~ Delineates dominant impacts
- S = Short-Term, typically <6 months  
(e.g. agriculture, grasslands)
- L = Long-Term, typically >6 months  
(e.g. hydrology, ecology)



(\* Responsible for collecting analysts' input & assembling the NA-DM map)

The Drought Monitor focuses on broad-scale conditions. Local conditions may vary. See accompanying text for a general summary.



Regions in northern Canada may not be as accurate as other regions due to limited information.

Figure 18-32. North American Drought Monitor map analyzed as of May 31, 2012. Conditions continue to ease for New Mexico, although, as with Arizona and Mexico, severe to extreme conditions persist. Most of New Mexico and Mexico expect long-term impacts while Arizona expects both short- and long-term impacts.

# North American Drought Monitor

June 30, 2012

Released: Thursday July 19, 2012

<http://www.ncdc.noaa.gov/nadm.html>

Analysts:

Canada - Trevor Hadwen  
Dwayne Chobanik  
Richard Rieger  
Mexico - Reynaldo Pascual  
Adelina Albanil  
U.S.A. - Mark Svoboda\*  
Rich Tinker

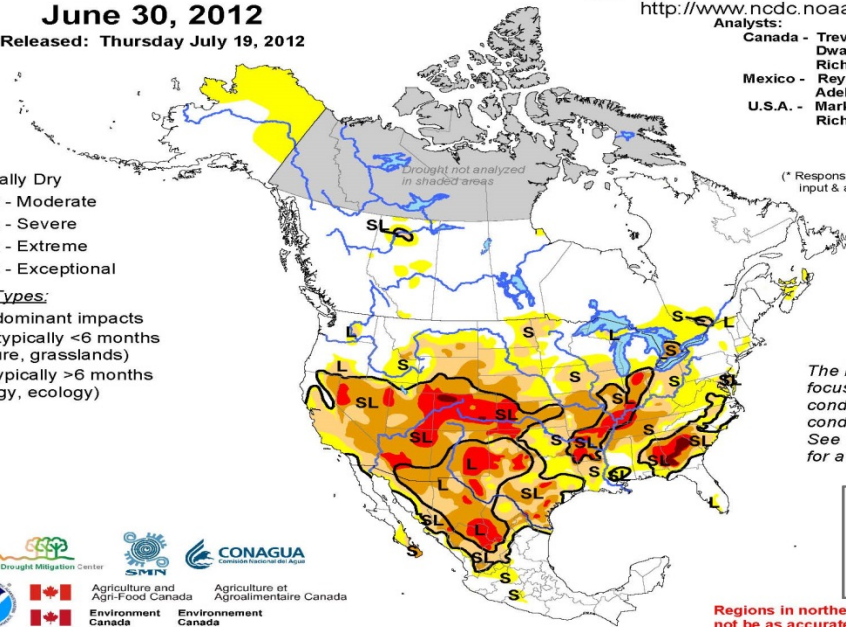
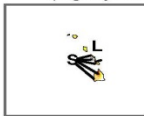
(\* Responsible for collecting analysts' input & assembling the NA-DM map)

**Intensity:**

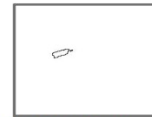
- D0 Abnormally Dry
- D1 Drought - Moderate
- D2 Drought - Severe
- D3 Drought - Extreme
- D4 Drought - Exceptional

**Drought Impact Types:**

- ~ Delineates dominant impacts
- S = Short-Term, typically <6 months (e.g. agriculture, grasslands)
- L = Long-Term, typically >6 months (e.g. hydrology, ecology)



The Drought Monitor focuses on broad-scale conditions. Local conditions may vary. See accompanying text for a general summary.



Regions in northern Canada may not be as accurate as other regions due to limited information.



Figure 18-33. North American Drought Monitor map analyzed as of June 30, 2012. Most of Arizona, New Mexico and Mexico are classified as severe to extreme. Long-term impact areas have increased, however, now also including parts of Arizona. Most of Arizona still expects both short- and long-term impacts.

# North American Drought Monitor

July 31, 2012

Released: Tuesday, August 14, 2012

<http://www.ncdc.noaa.gov/nadm.html>

Analysts:

Canada - Trevor Hadwen  
Richard Rieger  
Mexico - Adelina Albanil  
Reynaldo Pascual  
U.S.A. - Mark Svoboda  
Mark Brusberg\*  
Brad Rippey\*

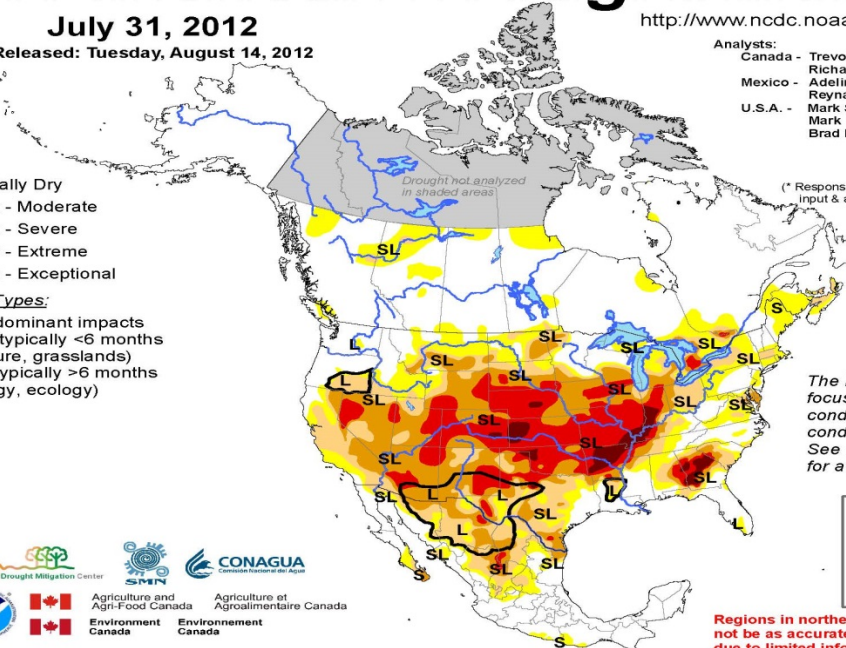
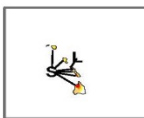
(\* Responsible for collecting analysts' input & assembling the NA-DM map)

**Intensity:**

- D0 Abnormally Dry
- D1 Drought - Moderate
- D2 Drought - Severe
- D3 Drought - Extreme
- D4 Drought - Exceptional

**Drought Impact Types:**

- ~ Delineates dominant impacts
- S = Short-Term, typically <6 months (e.g. agriculture, grasslands)
- L = Long-Term, typically >6 months (e.g. hydrology, ecology)



The Drought Monitor focuses on broad-scale conditions. Local conditions may vary. See accompanying text for a general summary.



Regions in northern Canada may not be as accurate as other regions due to limited information.



Figure 18-34. North American Drought Monitor map analyzed as of July 31, 2012. Conditions for New Mexico and Arizona are similar to June's analysis, although a larger portion of New Mexico has moved to short- and long-term impacts. Mexico's conditions have improved and now is mainly classified as moderate to severe, although with much of the country expecting long-term impacts.

# North American Drought Monitor

August 31, 2012

Released: Thursday, September 13, 2012

<http://www.ncdc.noaa.gov/nadm.html>

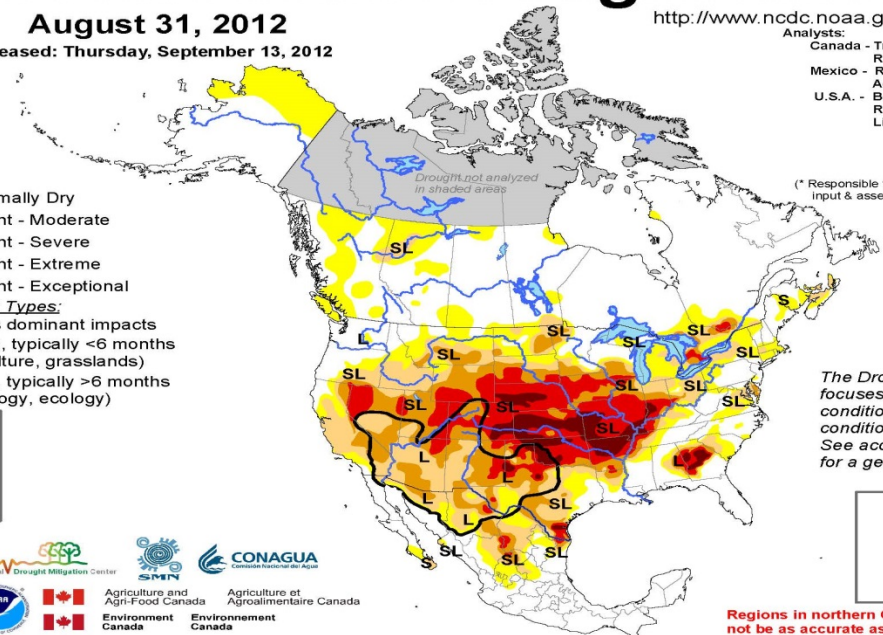
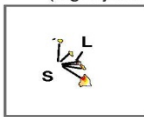
Analysts:  
 Canada - Trevor Hadwen  
 Richard Rieger  
 Mexico - Reynaldo Pascual  
 Adelina Albanil  
 U.S.A. - Brian Fuchs  
 Richard Heim\*  
 Liz Love-Brotak

**Intensity:**

- D0 Abnormally Dry
- D1 Drought - Moderate
- D2 Drought - Severe
- D3 Drought - Extreme
- D4 Drought - Exceptional

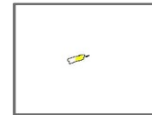
**Drought Impact Types:**

- ~ Delineates dominant impacts
- S = Short-Term, typically <6 months (e.g. agriculture, grasslands)
- L = Long-Term, typically >6 months (e.g. hydrology, ecology)



(\* Responsible for collecting analysts' input & assembling the NA-DM map)

The Drought Monitor focuses on broad-scale conditions. Local conditions may vary. See accompanying text for a general summary.



Regions in northern Canada may not be as accurate as other regions due to limited information.

Figure 18-35. North American Drought Monitor map analyzed as of August 31, 2012. Most of New Mexico, Arizona and Mexico conditions are classified as moderate to severe, with a few areas classified as extreme. Nearly all of Arizona and New Mexico expect long-term impacts while Mexico expects both long- and short-term impacts.

# North American Drought Monitor

September 30, 2012

Released: Thursday, Oct 11, 2012

<http://www.ncdc.noaa.gov/nadm.html>

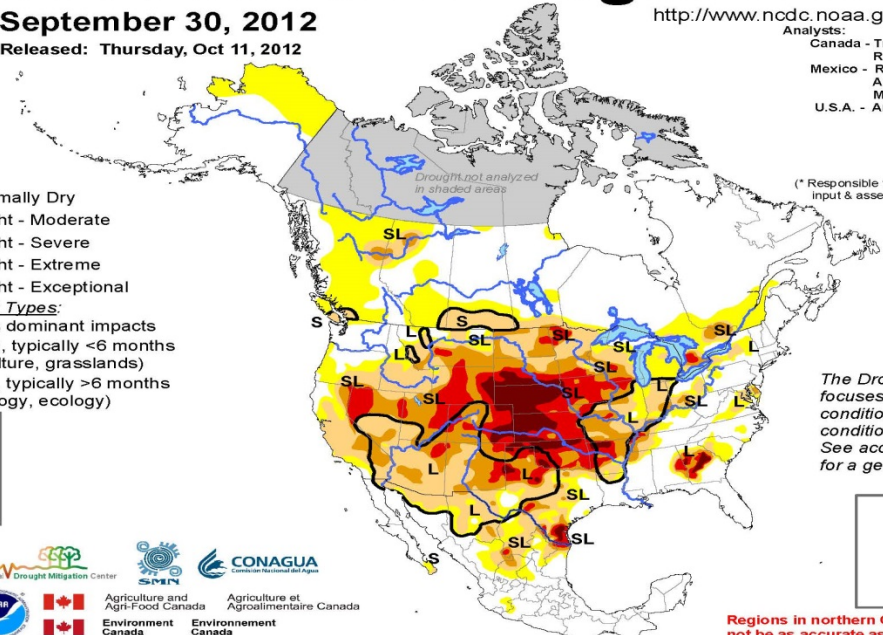
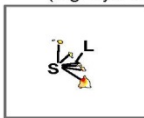
Analysts:  
 Canada - Trevor Hadwen  
 Richard Rieger  
 Mexico - Reynaldo Pascual  
 Adelina Albanil  
 Minerva López\*  
 U.S.A. - Anthony Artusa

**Intensity:**

- D0 Abnormally Dry
- D1 Drought - Moderate
- D2 Drought - Severe
- D3 Drought - Extreme
- D4 Drought - Exceptional

**Drought Impact Types:**

- ~ Delineates dominant impacts
- S = Short-Term, typically <6 months (e.g. agriculture, grasslands)
- L = Long-Term, typically >6 months (e.g. hydrology, ecology)



(\* Responsible for collecting analysts' input & assembling the NA-DM map)

The Drought Monitor focuses on broad-scale conditions. Local conditions may vary. See accompanying text for a general summary.



Regions in northern Canada may not be as accurate as other regions due to limited information.

Figure 18-36. North American Drought Monitor map analyzed as of September 30, 2012. Conditions for Arizona and New Mexico are similar to August's analysis of mostly moderate to severe with mainly long-term impacts. For Mexico, conditions are mostly abnormally dry to moderate, with both short- and long-term impacts.

Drought conditions are predicted to intensify and temperatures are predicted to increase. If fires are located in remote and rugged terrain, the ability to contain fires is dramatically reduced. While the recurrence frequency for exceptional events resulting from smoke cannot be estimated, such events will continue to recur and may increase.

### 18.2.3 Controls Analysis

In the United States, various agencies are responsible for land management, including the management of forests. These agencies include the Bureau of Land Management, U.S. Forest Service, State Forest agencies, and State Land Offices. Lands where fires may occur also include private land. As such, the individual managers make decisions on forest thinning for the purpose of wildfire prevention. Agencies or private land owners may use controlled burns to manage grasslands, forests and agricultural residue.

Further, when public lands are in extremely dry conditions, managers may close them to public use in order to minimize the risk of human-induced fires. However, no control strategy is 100% effective and further, lightning strikes are completely uncontrollable. Lightning-induced wildfires account for widely varying percentages of total acreage burned. For 2012, lightning-induced fires accounted for approximately 80% of total acreage burned in the southwest. Data are not available for Mexico fires.

## **18.3 Historical Fluctuations Analysis**

A historical record of the number and burned acreage of wildfires in Arizona, New Mexico and western Texas (Figure 18-37) has been documented by the Southwest Coordination Center. While there is significant variability in the number of fires, the general trend is toward fewer fires. Significant variability also exists in the number of acres burned. The Whitewater-Baldy fire in the Gila National Forest northwest of the SPCY Partisol monitor, contributed nearly 300,000 of the 500,000 acres burned in 2012. These historical data suggest that, even though fewer fires may start, drought conditions – especially when coupled with an exceptionally windy fire season – will promote conditions conducive to extensive wild land burning.

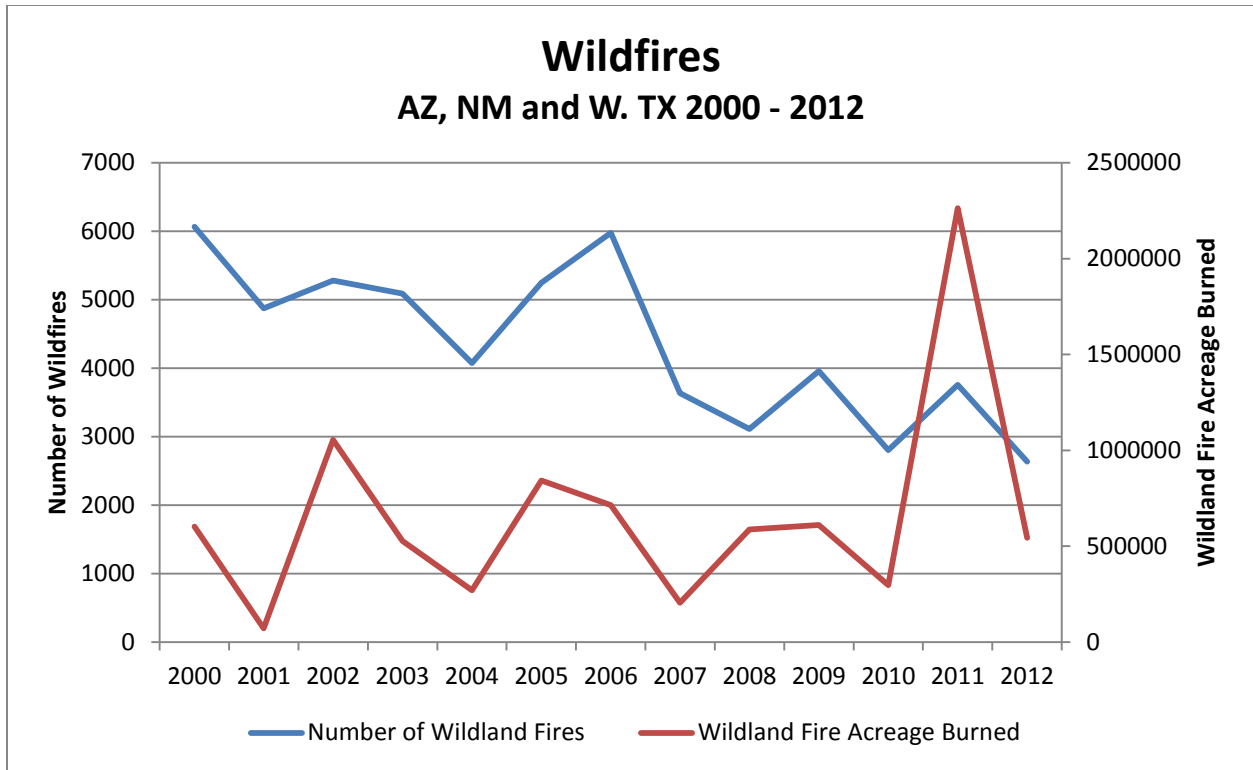


Figure 18-37. Historical record based on data from the Southwest Coordination Center, showing the number and acreage burned of wildfires in Arizona, New Mexico and western Texas for the years 2000 through 2012. Data are not available for Mexico.

### 18.4 Clear Causal Relationship

Fires in Arizona, New Mexico and northern Mexico caused significant amounts of smoke to be entrained in the atmosphere beginning as early as February and continuing through September.

For each of the dates listed in Table 18-1, a Naval Research Laboratory’s Navy Aerosol Analysis and Prediction System (NAAPS) product is available in 6-hour increments. This product breaks down the aerosols, using the AOD data, fire locations, weather data, and microchemistry and physics, into sulfates, dust and smoke and projects these onto a map. The following images show, from the NAAPS Archive, that for each of these dates, smoke was present and affected the SPCY PM<sub>2.5</sub> Partisol monitor. (Figures 18-38 to 18-65) While only one image is shown for each date, many dates have several available confirming images. These analyses show that smoke impacts were seen for each of these dates.

Smoke Surface Concentration ( $\mu\text{g}/\text{m}^3$ )  
for 00:00Z 09 Apr 2012

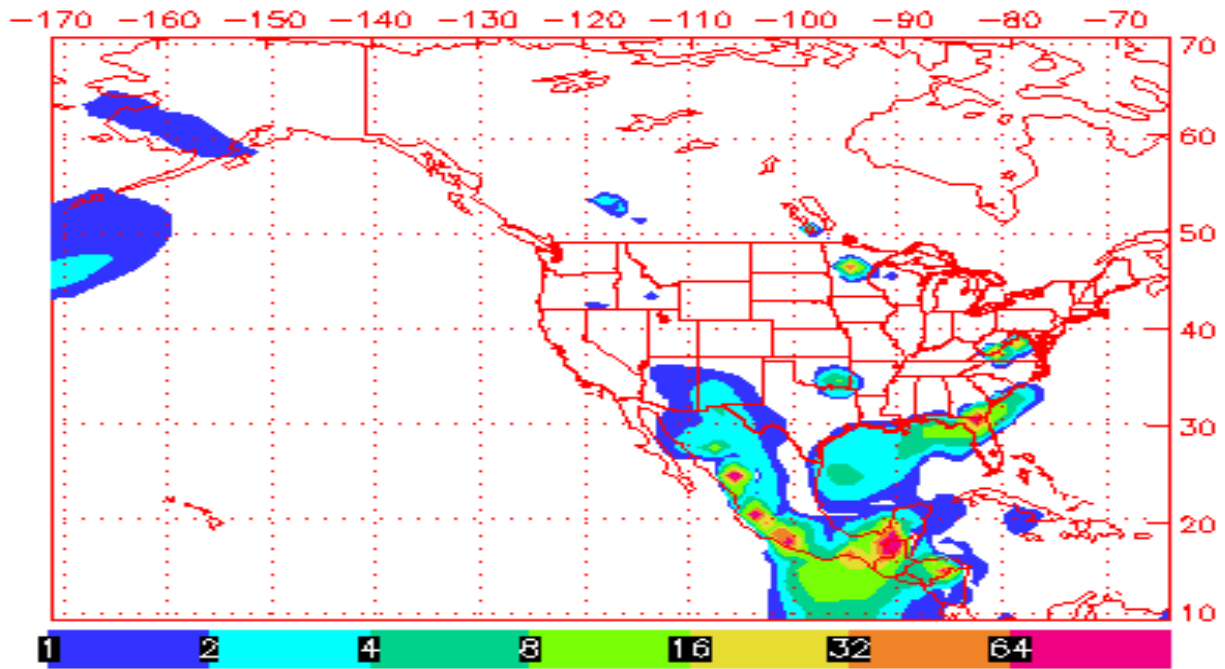


Figure 18-38. Smoke surface concentration for April 8, 2012 at 6:00 pm MDT

Smoke Surface Concentration ( $\mu\text{g}/\text{m}^3$ )  
for 00:00Z 11 Apr 2012

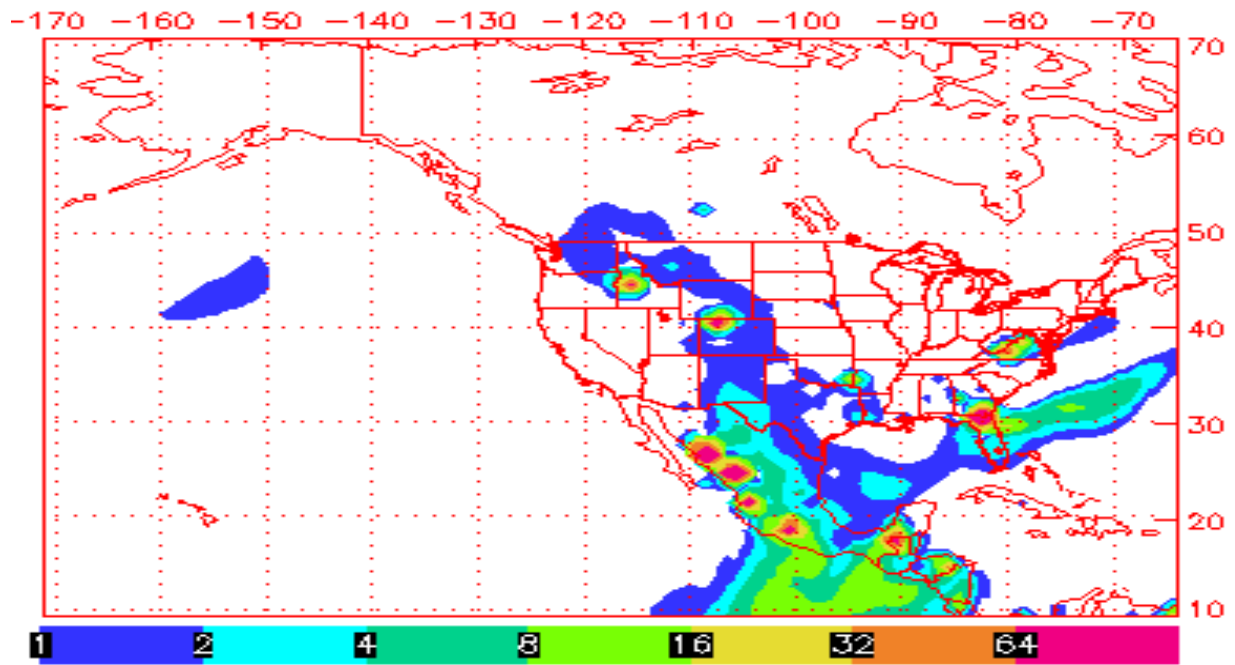


Figure 18-39. Smoke Surface Concentration for April 18, 2012 at 6:00 pm MDT.

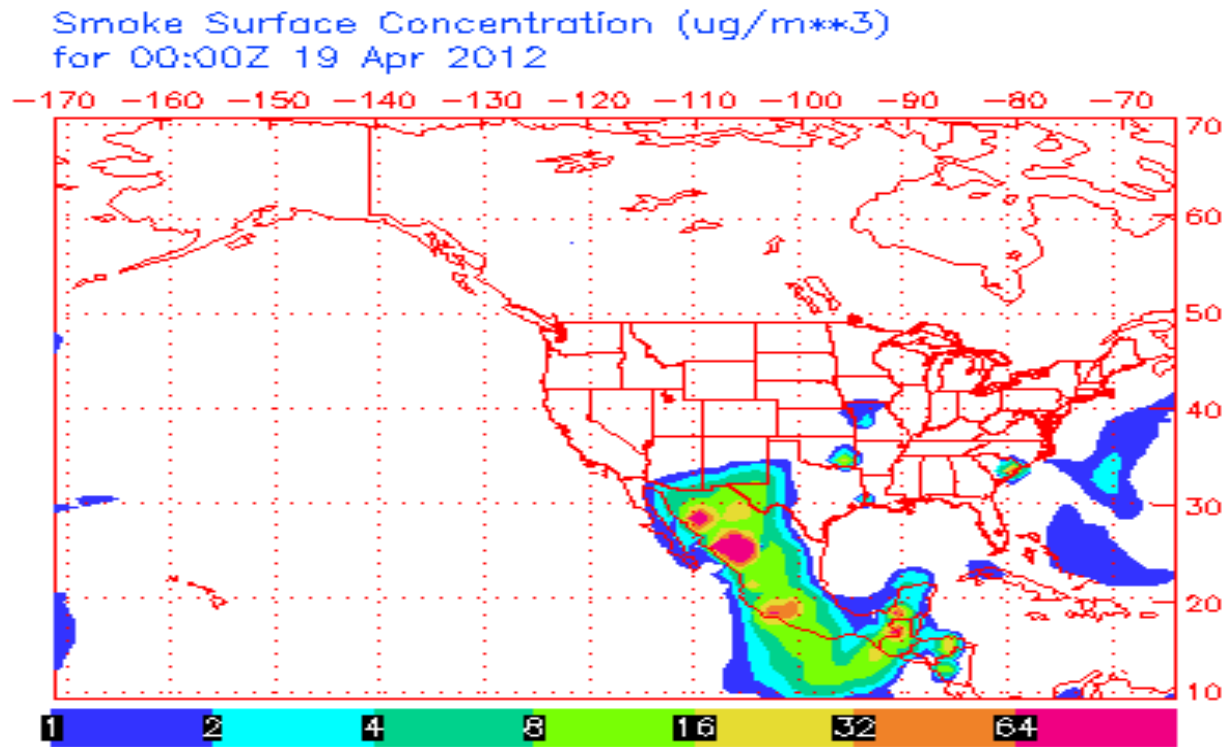


Figure 18-40. Smoke Surface Concentration for April 19, 2012 at 6:00 pm MDT.

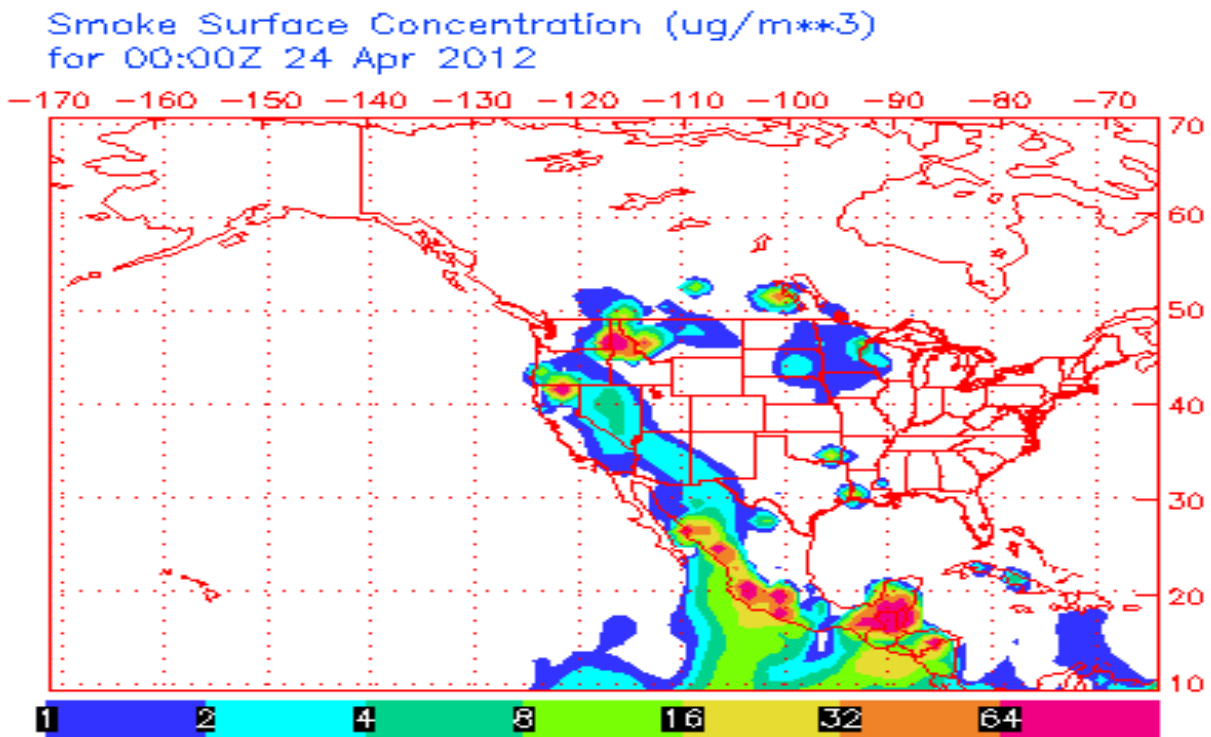


Figure 18-41. Smoke Surface Concentration for April 23, 2012 at 6:00 pm MDT.

Smoke Surface Concentration ( $\mu\text{g}/\text{m}^3$ )  
for 18:00Z 24 Apr 2012

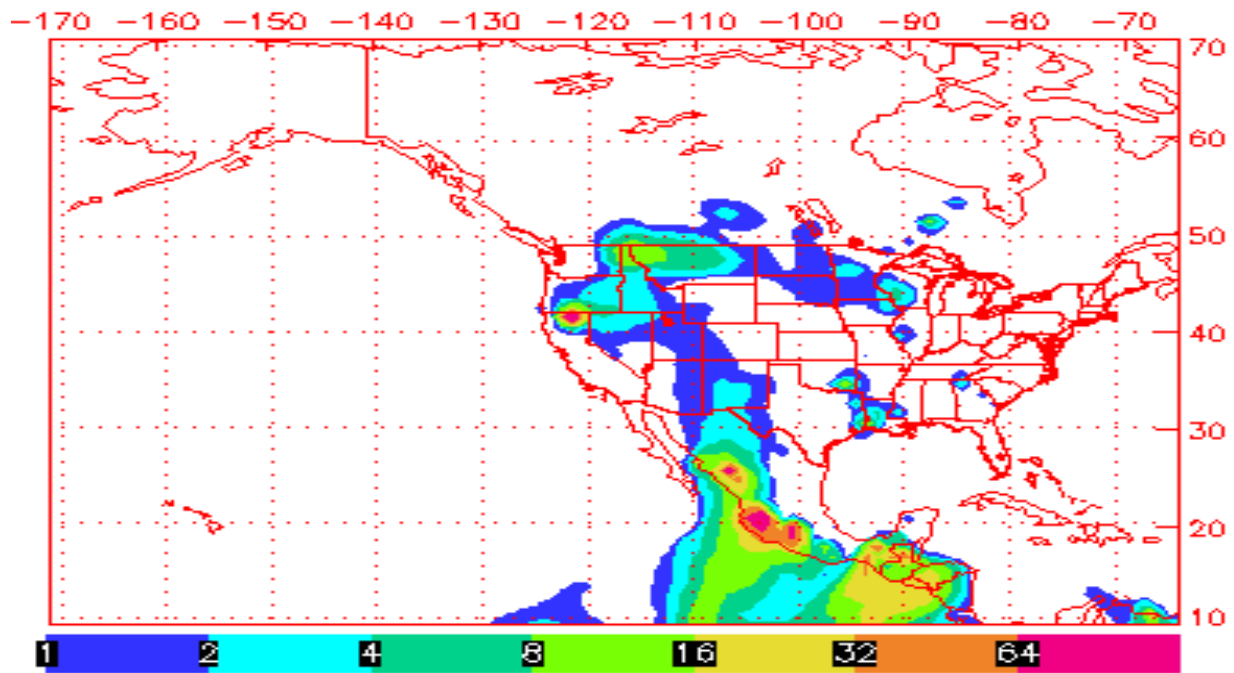


Figure 18-42. Smoke Surface Concentration for April 24, 2012 at 12:00 pm MDT.

Smoke Surface Concentration ( $\mu\text{g}/\text{m}^3$ )  
for 18:00Z 07 May 2012

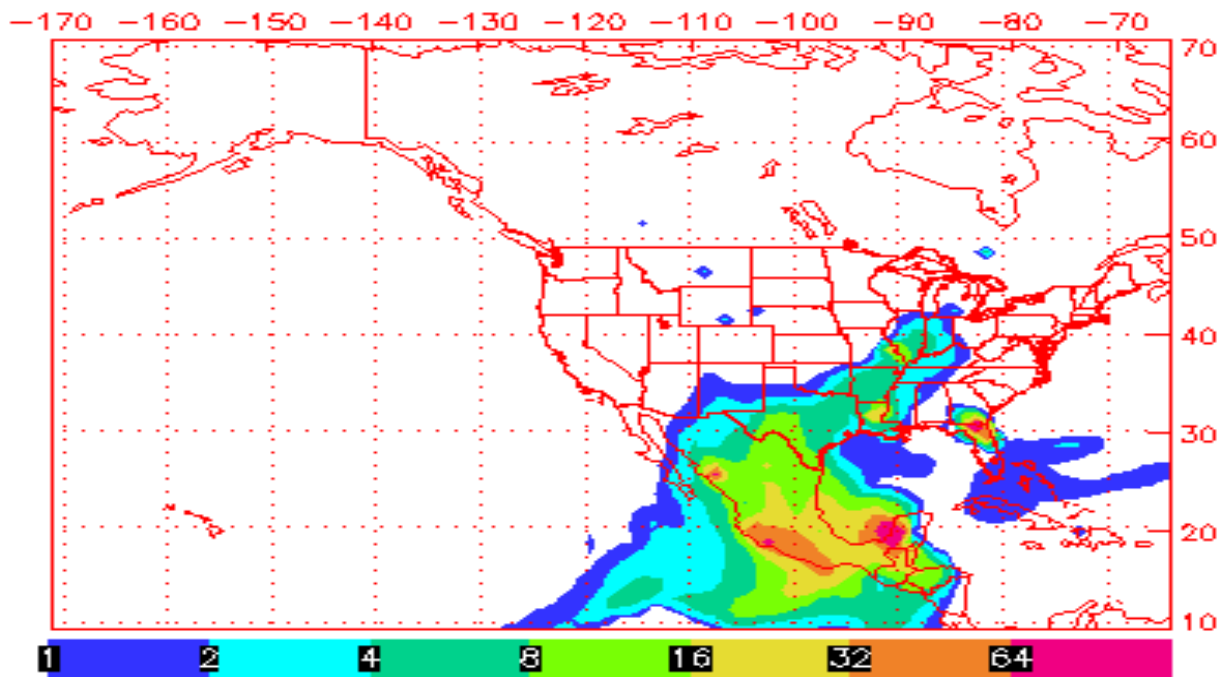


Figure 18-43. Smoke Surface Concentration for May 7, 2012 at 12:00 pm MDT.

Smoke Surface Concentration (ug/m\*\*3)  
for 12:00Z 08 May 2012

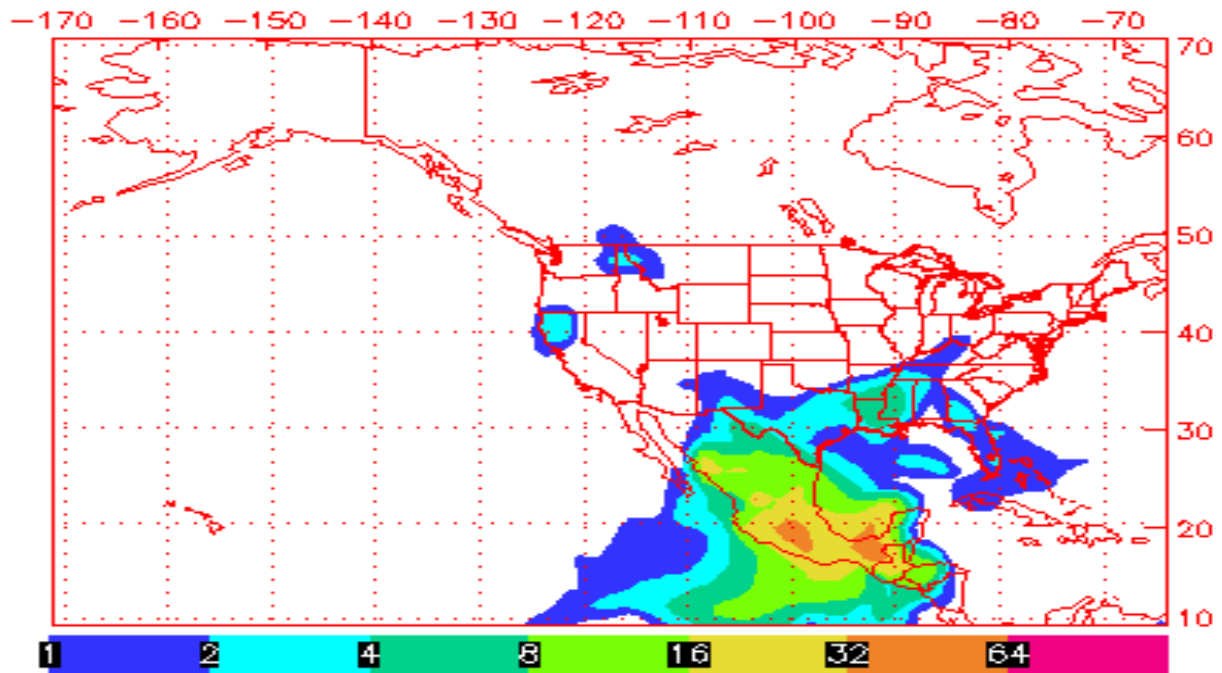


Figure 18-44. Smoke Surface Concentration for May 8, 2012 at 6:00 am MDT.

Smoke Surface Concentration (ug/m\*\*3)  
for 12:00Z 24 May 2012

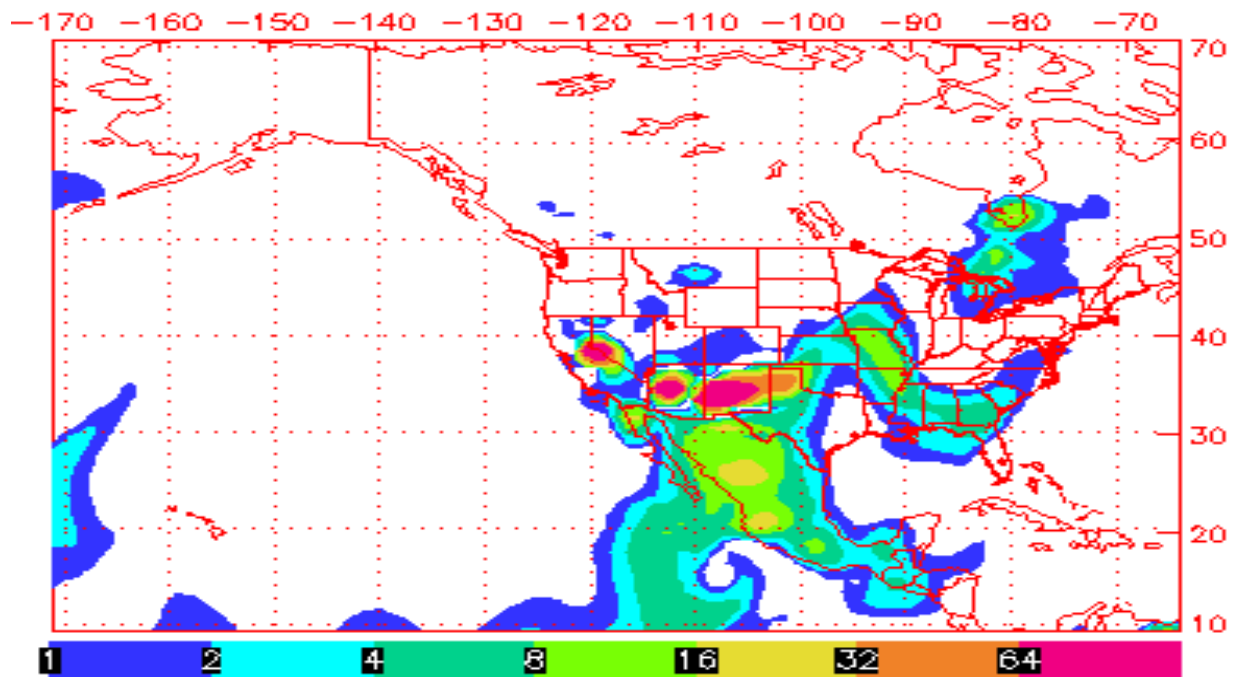


Figure 18-45. Smoke Surface Concentration for May 24, 2012 at 6:00 am MDT

Smoke Surface Concentration ( $\mu\text{g}/\text{m}^3$ )  
for 18:00Z 26 May 2012

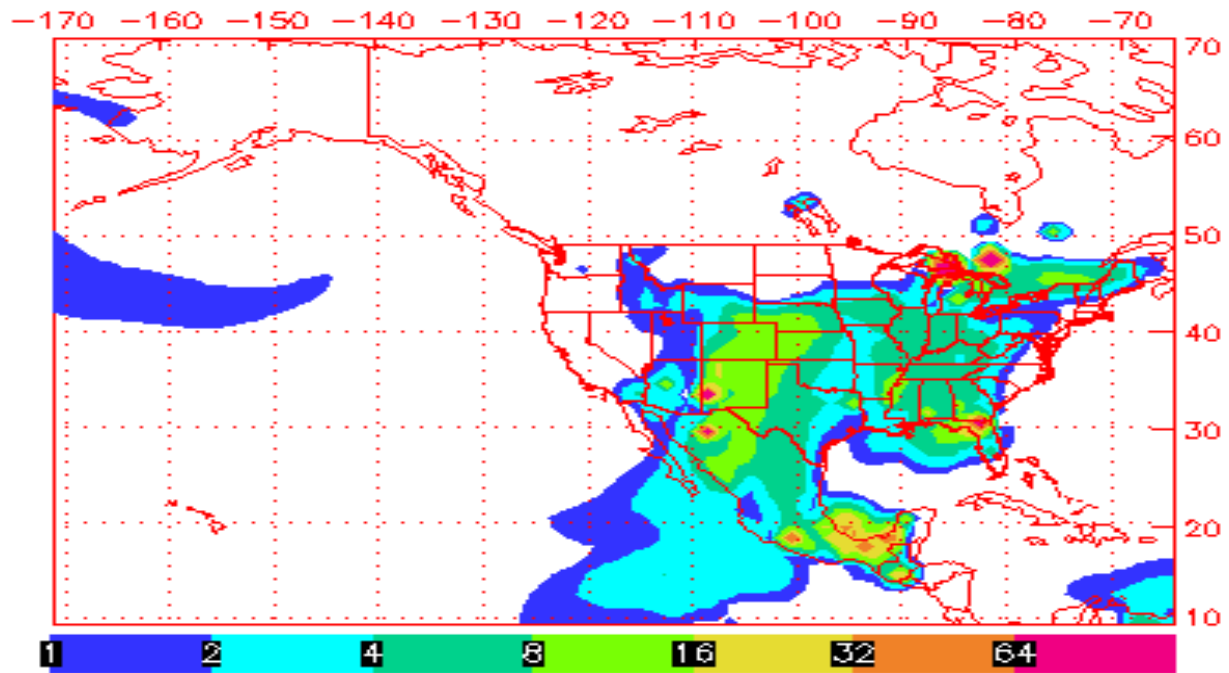


Figure 18-46. Smoke Surface Concentration for May 26, 2012 at 12:00 pm MDT

Smoke Surface Concentration ( $\mu\text{g}/\text{m}^3$ )  
for 00:00Z 03 Jun 2012

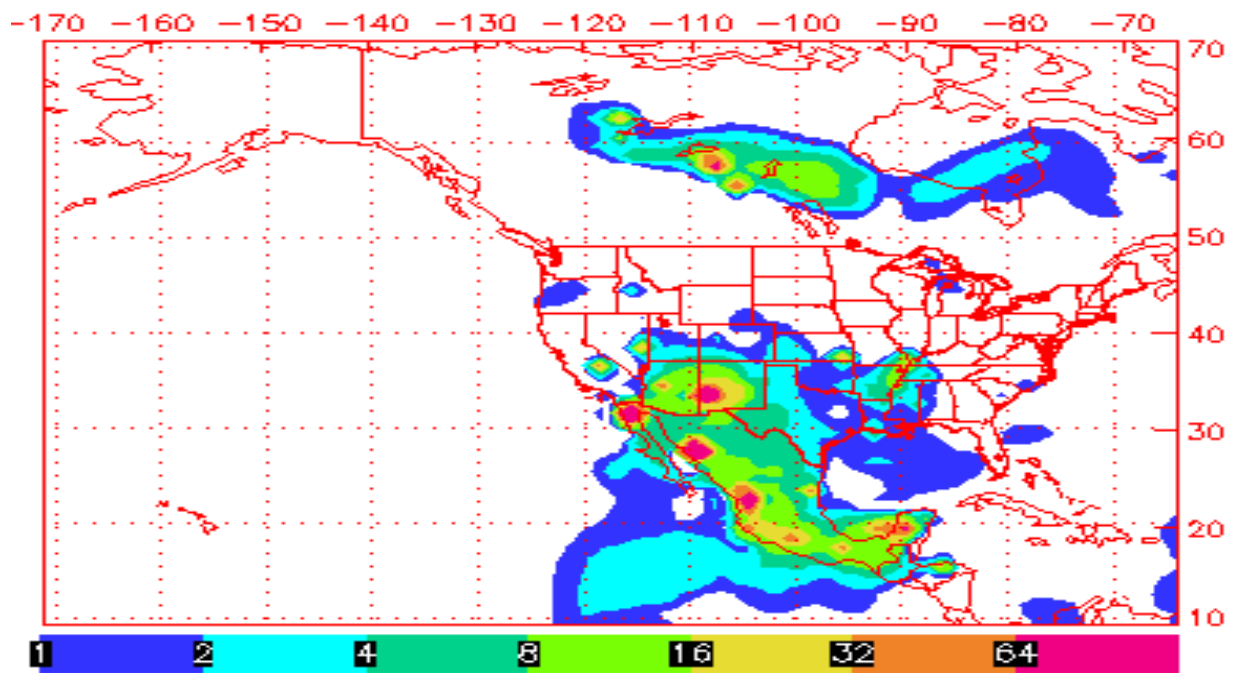


Figure 18-47. Smoke Surface Concentration for June 2, 2012 at 6:00 pm MDT

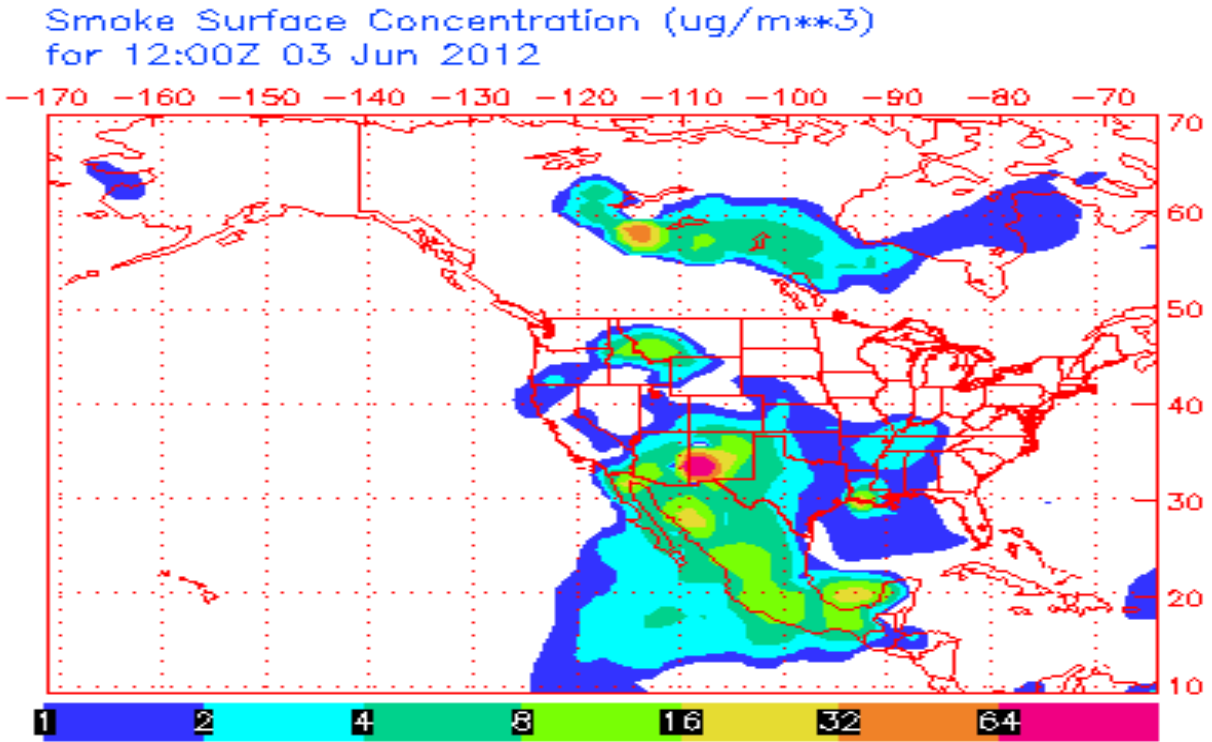


Figure 18-48. Smoke Surface Concentration for June 3, 2012 at 6:00 am MDT

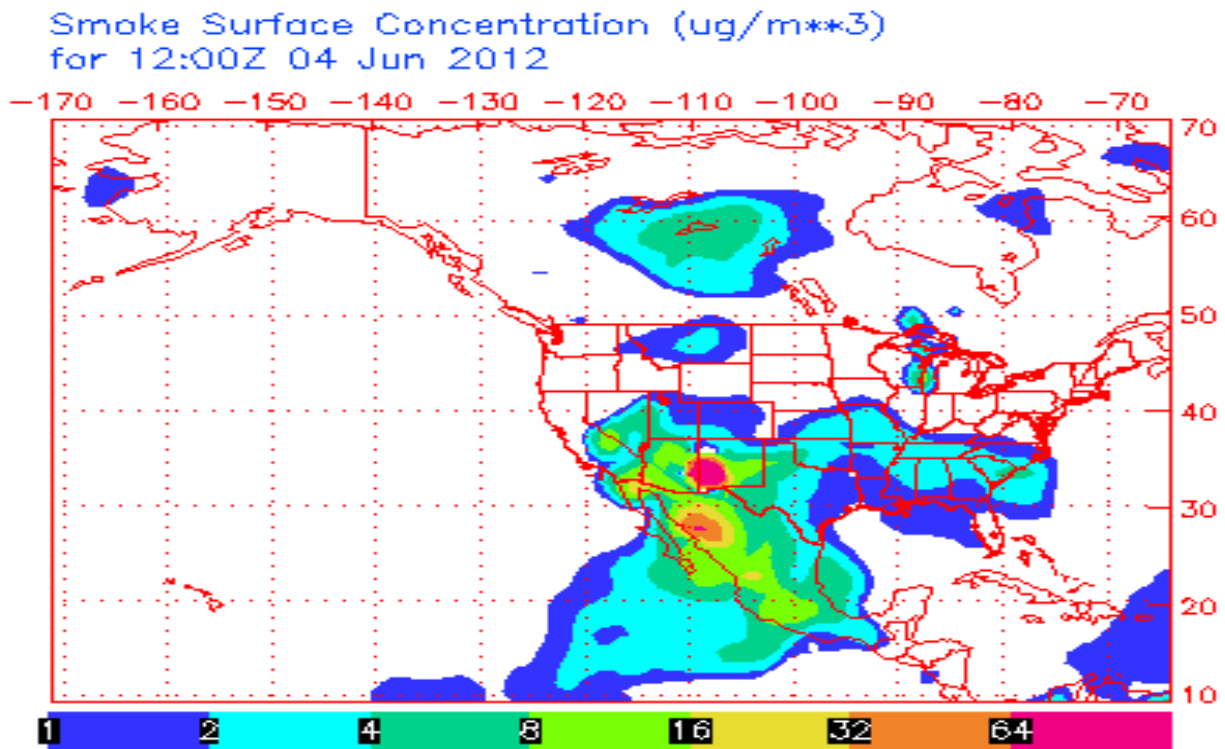


Figure 18-49. Smoke Surface Concentration for June 4, 2012 at 6:00 am MDT

Smoke Surface Concentration ( $\mu\text{g}/\text{m}^3$ )  
for 12:00Z 05 Jun 2012

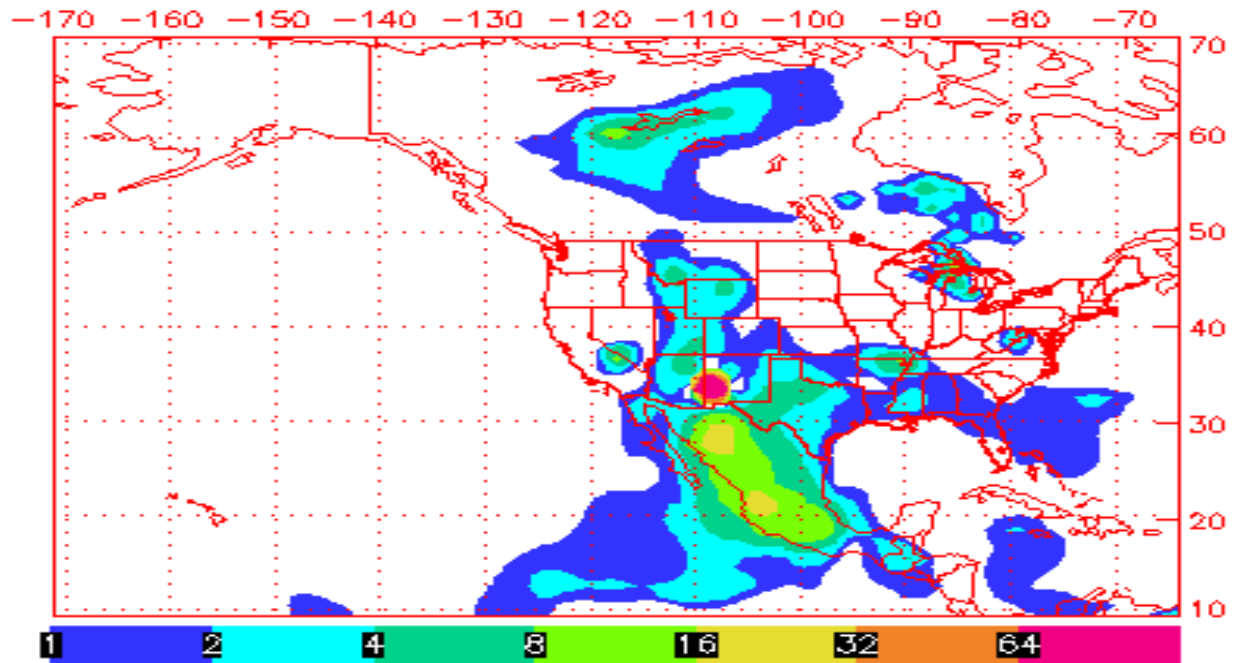


Figure 18-50. Smoke Surface Concentration for June 5, 2012 at 6:00 am MDT

Smoke Surface Concentration ( $\mu\text{g}/\text{m}^3$ )  
for 12:00Z 09 Jun 2012

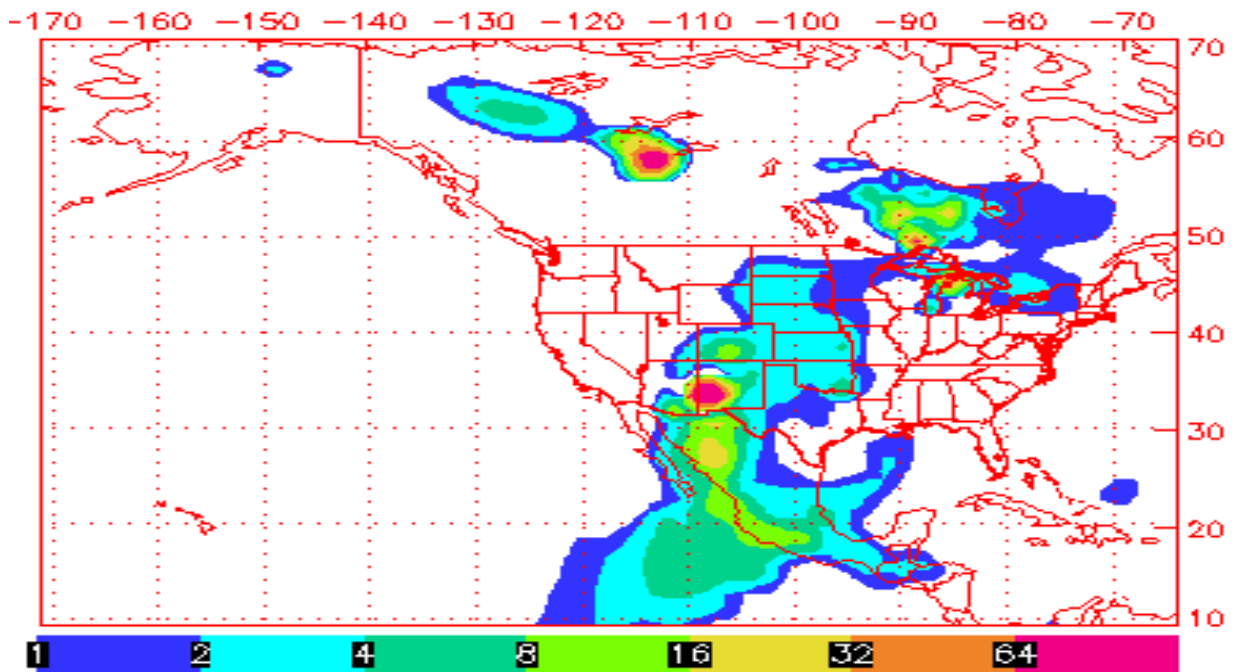


Figure 18-51. Smoke Surface Concentration for June 9, 2012 at 6:00 am MDT

Smoke Surface Concentration ( $\mu\text{g}/\text{m}^3$ )  
for 12:00Z 11 Jun 2012

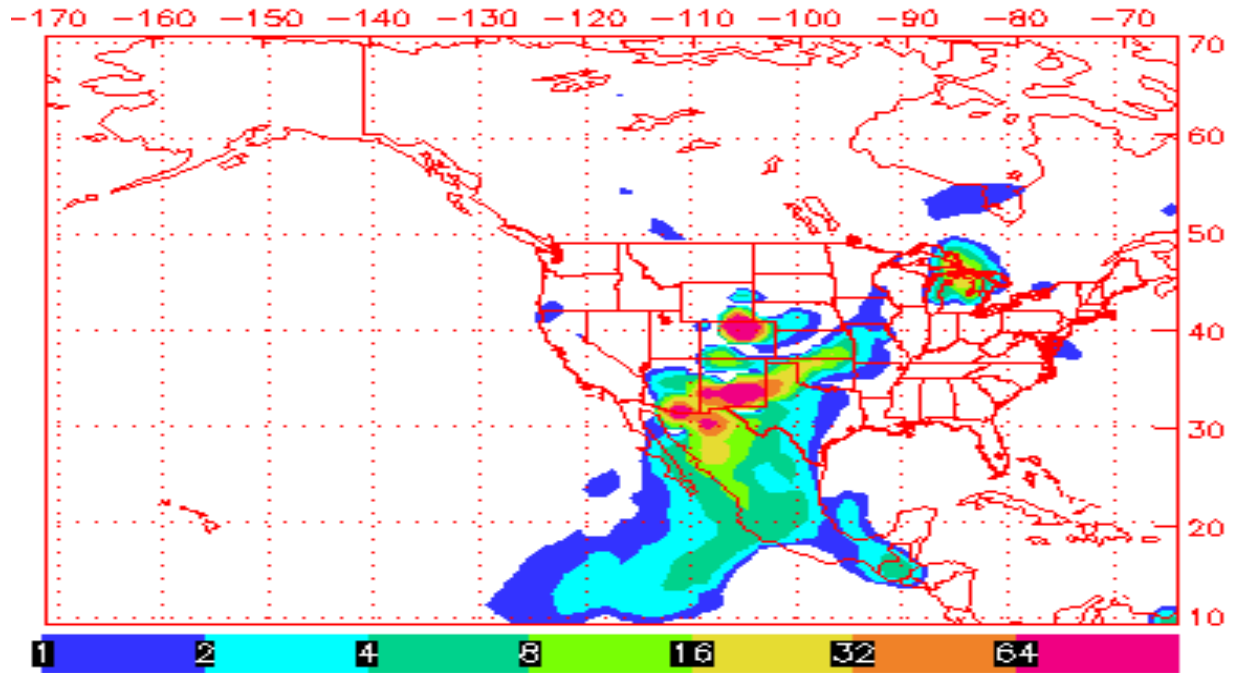


Figure 18-52. Smoke Surface Concentration for June 11, 2012 at 6:00 am MDT

Smoke Surface Concentration ( $\mu\text{g}/\text{m}^3$ )  
for 12:00Z 12 Jun 2012

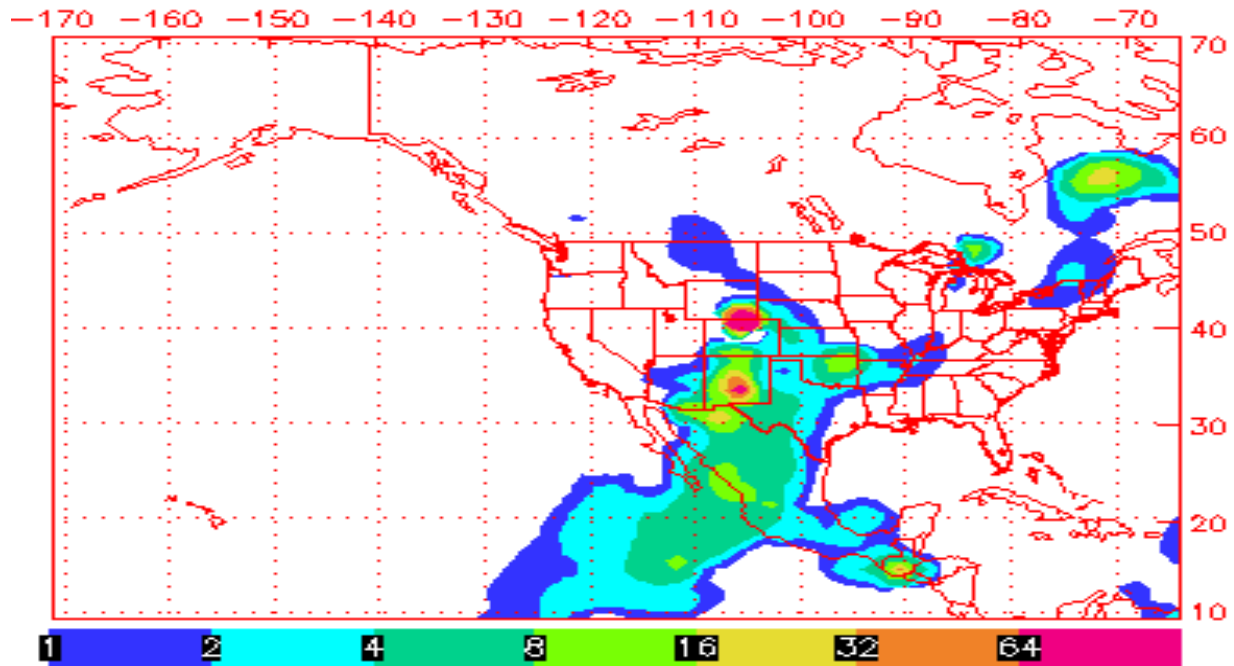


Figure 18-53. Smoke Surface Concentration for June 12, 2012 at 6:00 am MDT

Smoke Surface Concentration ( $\mu\text{g}/\text{m}^3$ )  
for 12:00Z 13 Jun 2012

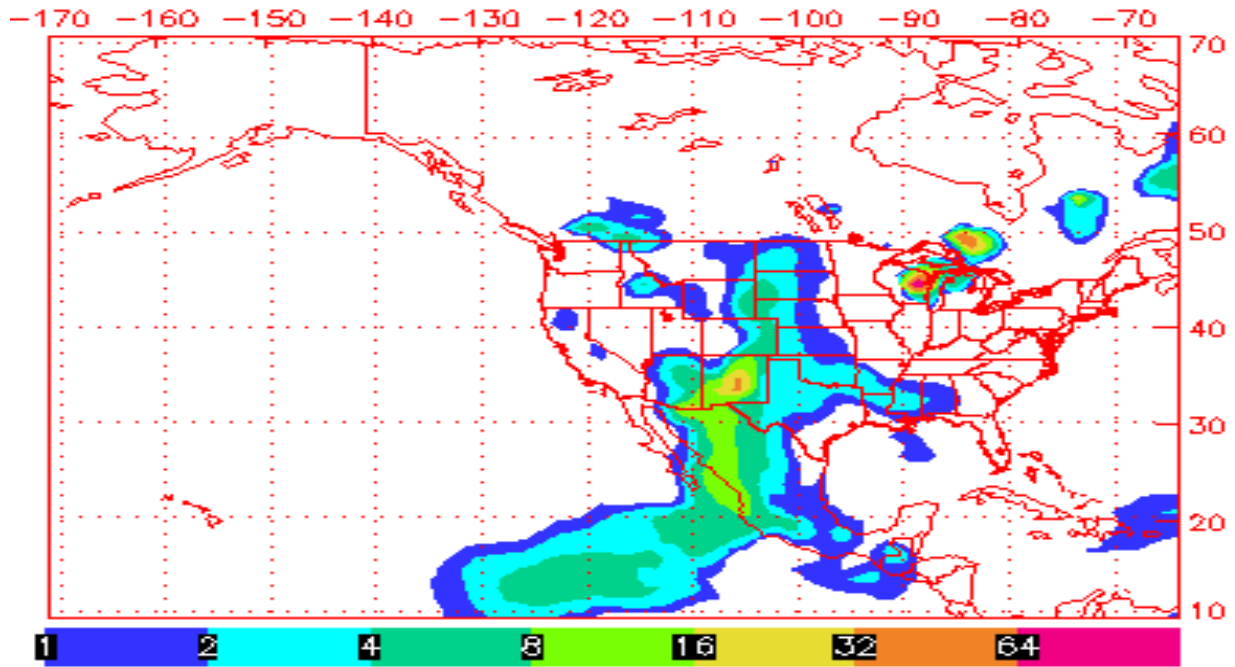


Figure 18-54. Smoke Surface Concentration for June 13, 2012 at 6:00 am MDT

Smoke Surface Concentration ( $\mu\text{g}/\text{m}^3$ )  
for 12:00Z 14 Jun 2012

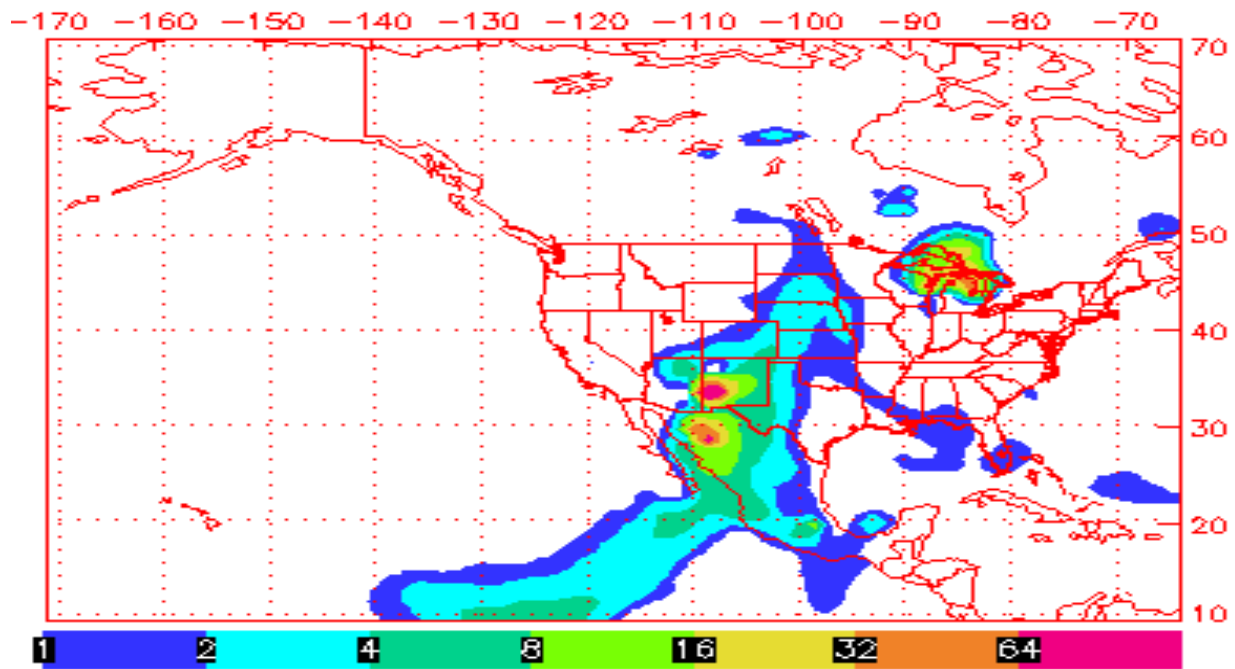


Figure 18-55. Smoke Surface Concentration for June 14, 2012 at 6:00 am MDT

Smoke Surface Concentration ( $\mu\text{g}/\text{m}^3$ )  
for 00:00Z 17 Jun 2012

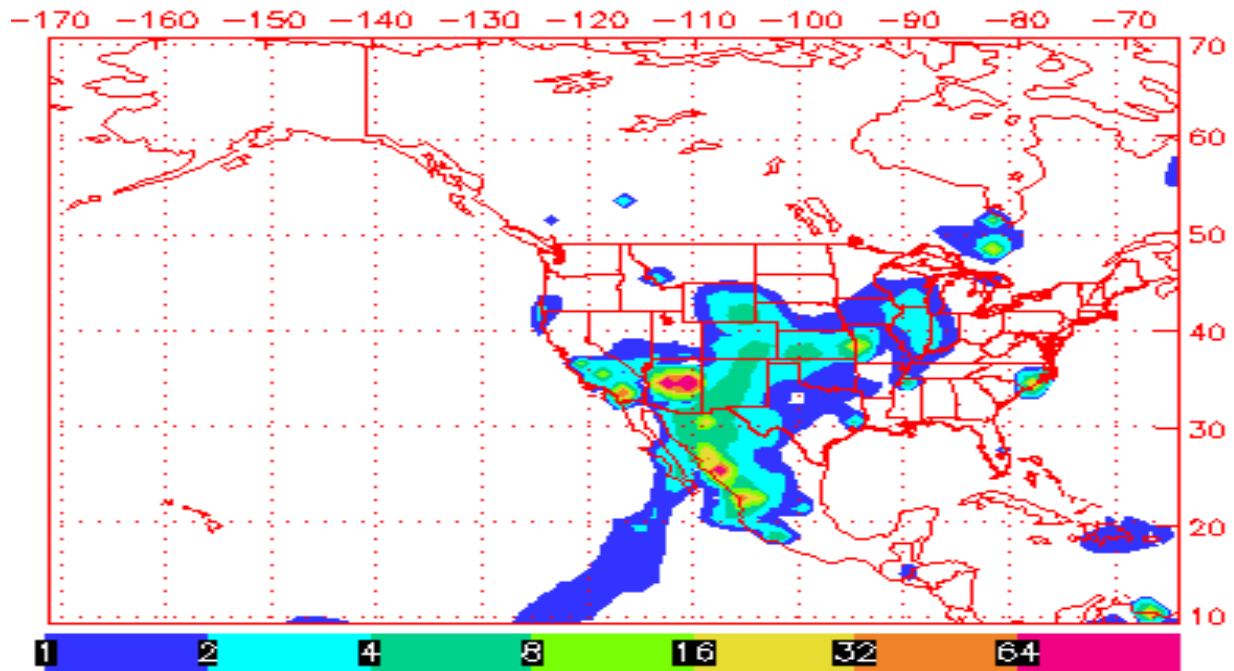


Figure 18-56. Smoke Surface Concentration for June 16, 2012 at 6:00 pm MDT

Smoke Surface Concentration ( $\mu\text{g}/\text{m}^3$ )  
for 12:00Z 21 Jun 2012

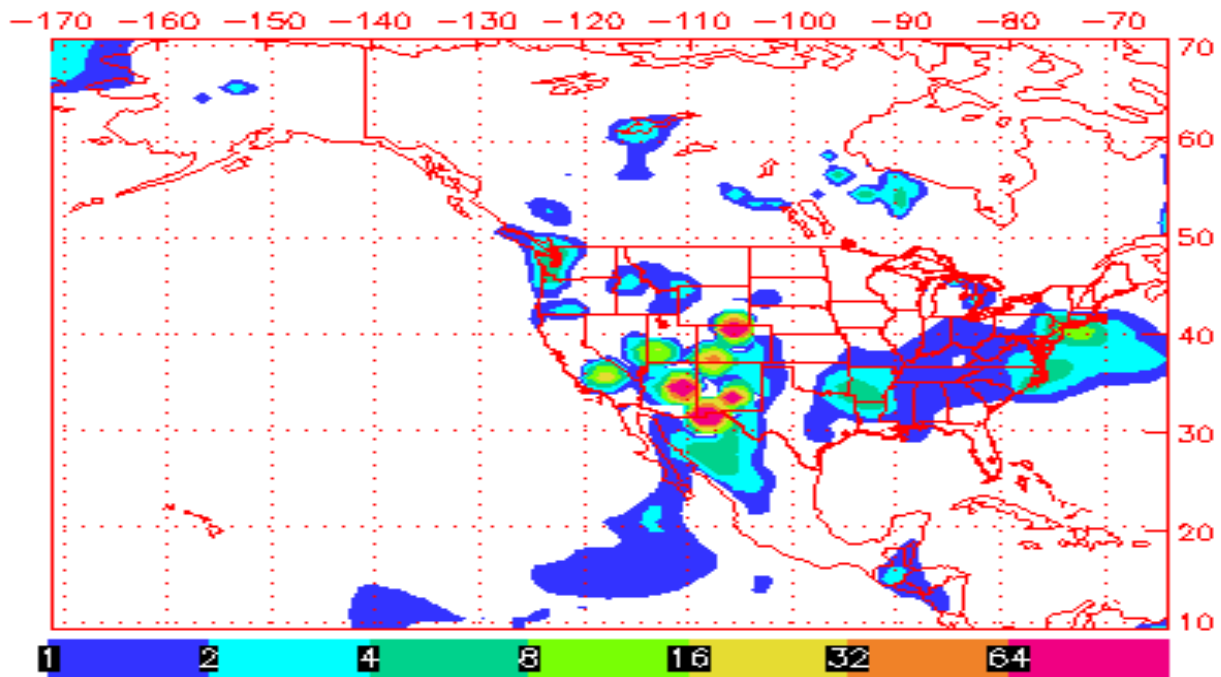


Figure 18-57. Smoke Surface Concentration for June 21, 2012 at 6:00 am MDT

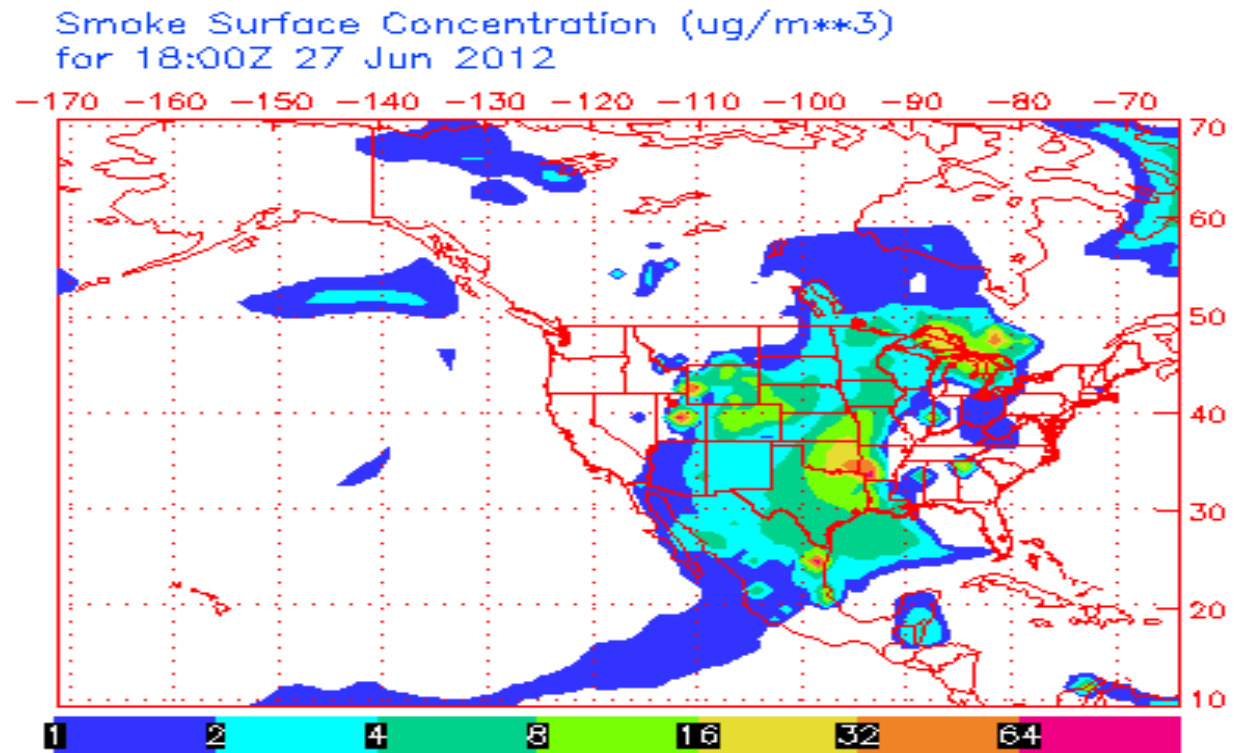


Figure 18-58. Smoke Surface Concentration for June 27, 2012 at 12:00 pm MDT

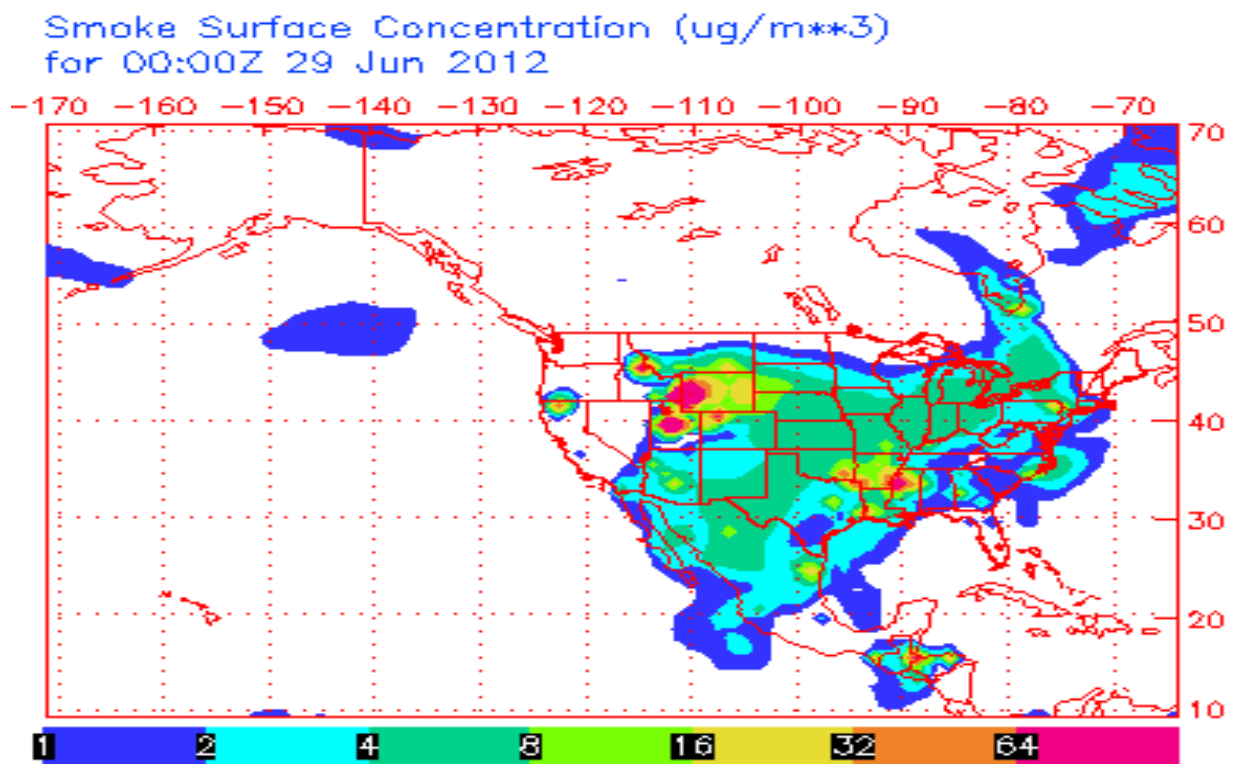


Figure 18-59. Smoke Surface Concentration for June 28, 2012 at 6:00 pm MDT

Smoke Surface Concentration (ug/m\*\*3)  
for 00:00Z 13 Aug 2012

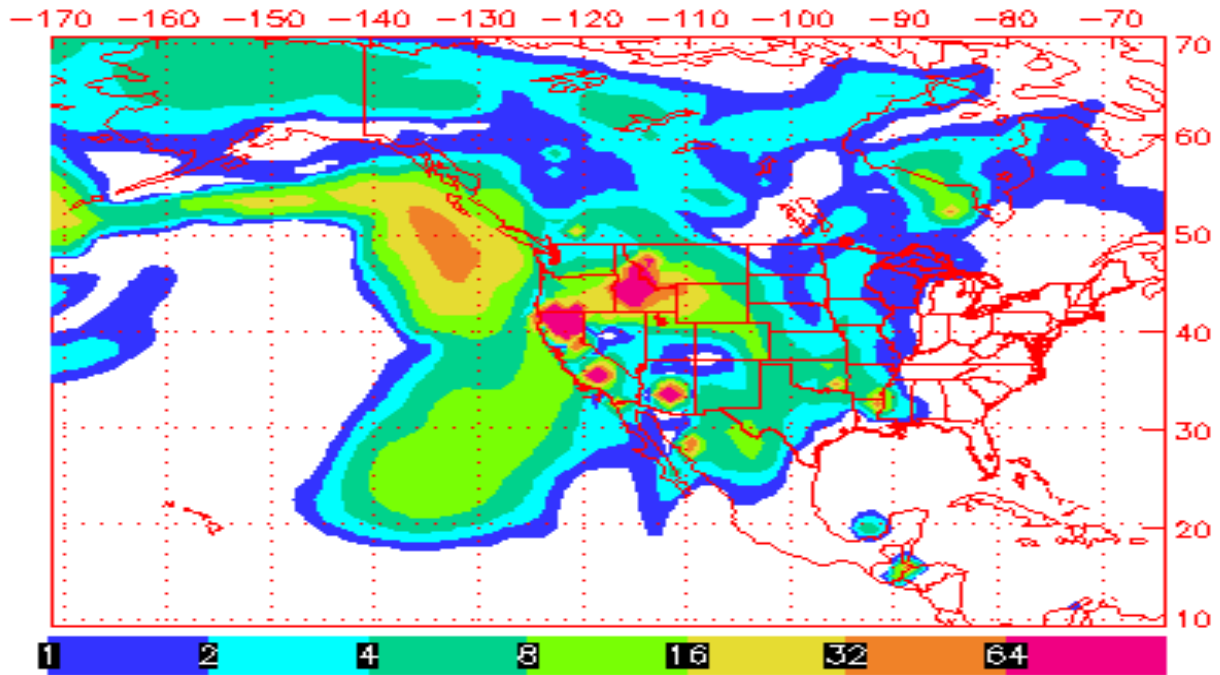


Figure 18-60. Smoke Surface Concentration for August 12, 2012 at 6:00 pm MDT

Smoke Surface Concentration (ug/m\*\*3)  
for 18:00Z 06 Sep 2012

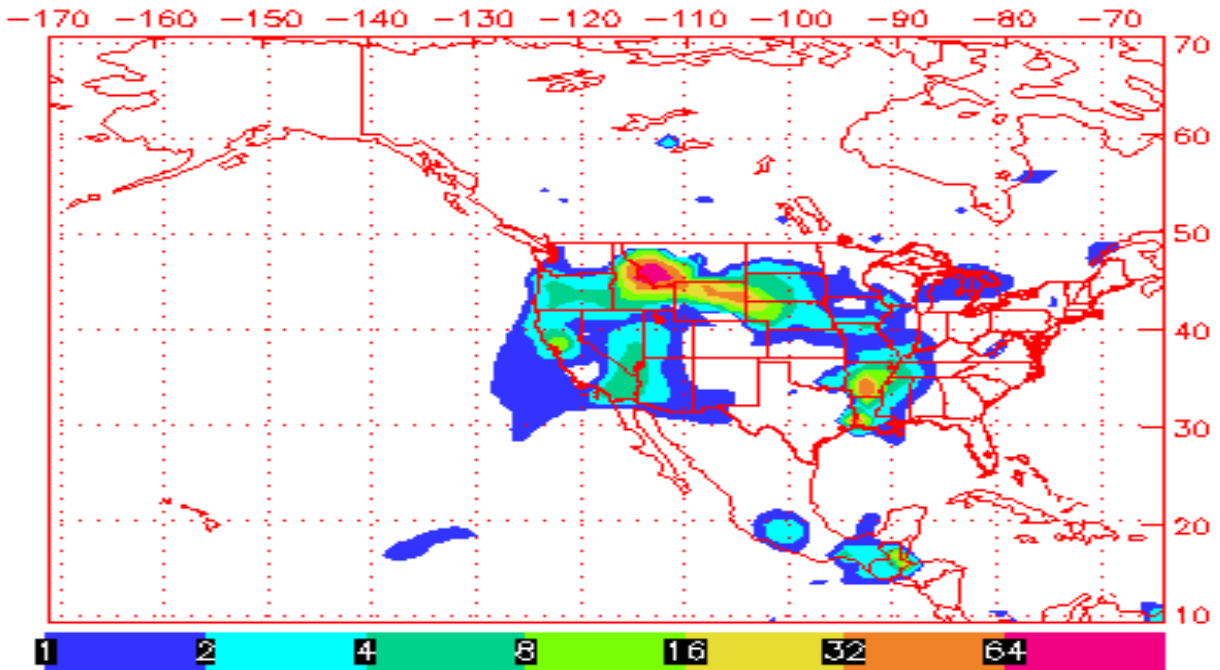


Figure 18-61. Smoke Surface Concentration for September 6, 2012 at 12:00 pm MDT

Smoke Surface Concentration ( $\mu\text{g}/\text{m}^3$ )  
for 00:00Z 08 Sep 2012

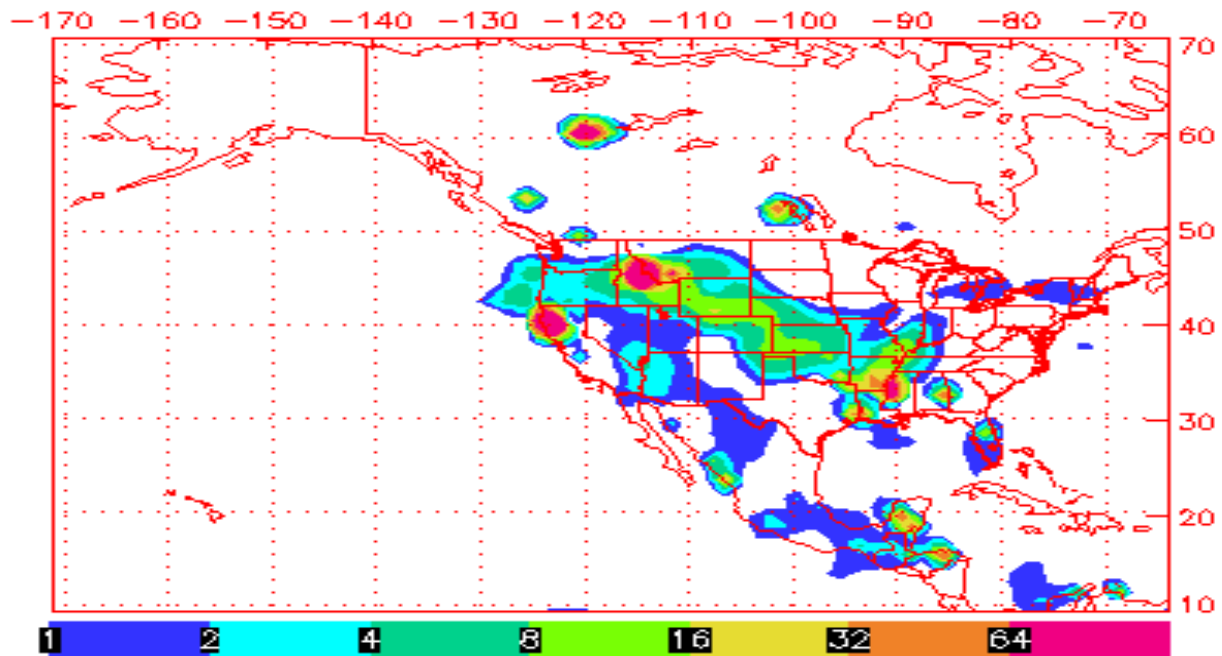


Figure 18-62. Smoke Surface Concentration for September 7, 2012 at 6:00 pm MDT

Smoke Surface Concentration ( $\mu\text{g}/\text{m}^3$ )  
for 12:00Z 17 Sep 2012

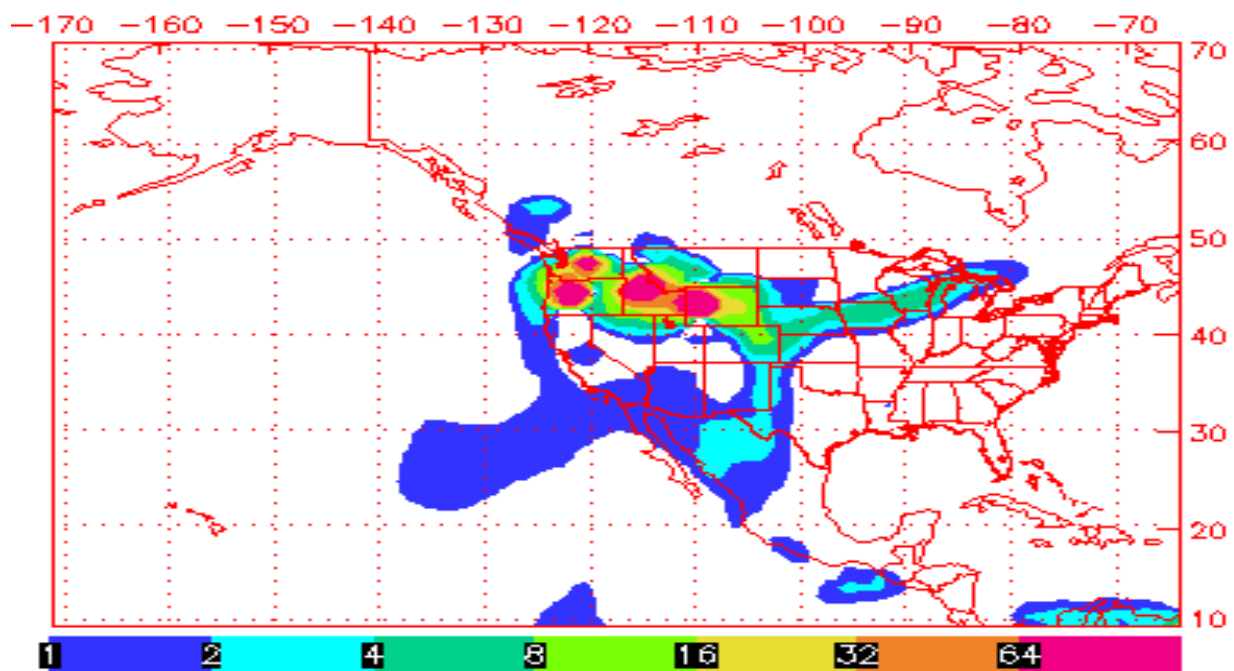


Figure 18-63. Smoke Surface Concentration for September 17, 2012 at 6:00 am MDT

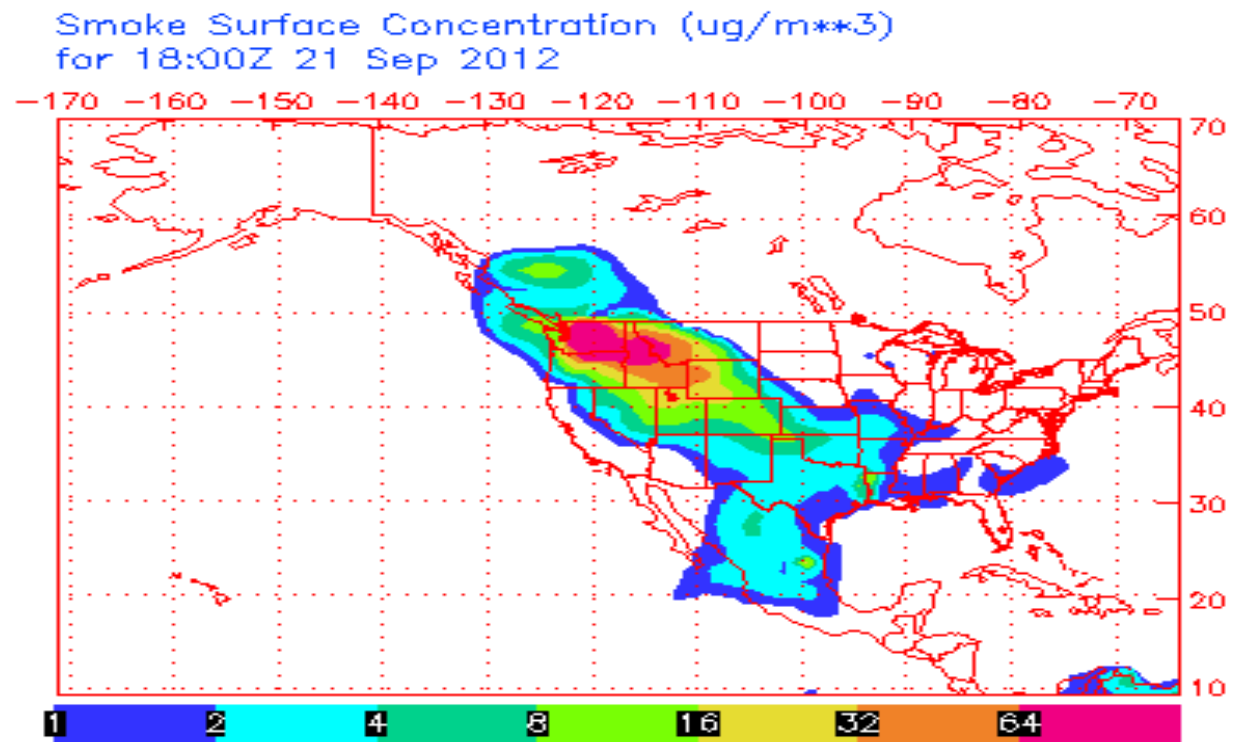


Figure 18-64. Smoke Surface Concentration for September 21, 2012 at 12:00 pm MDT

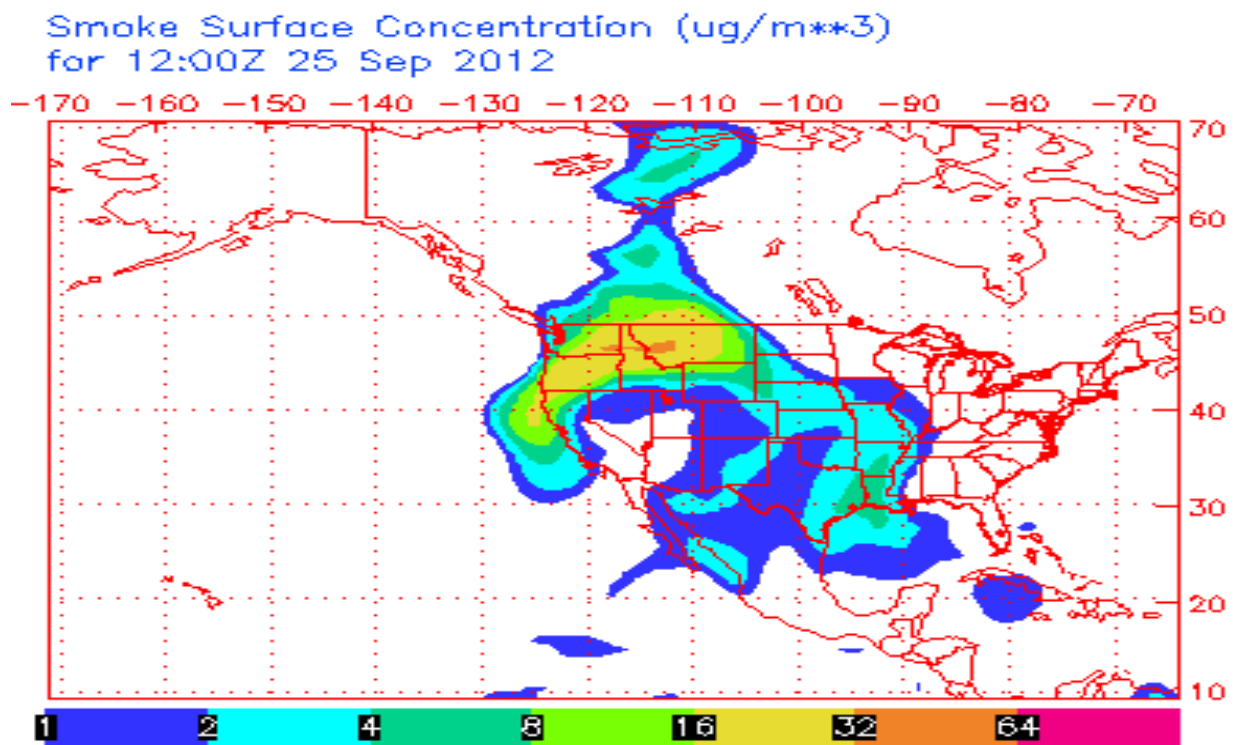


Figure 18-65. Smoke Surface Concentration for September 25, 2012 at 6:00 am MDT

Typically, when smoke effects are present, the ratio of  $PM_{2.5}$  to  $PM_{10}$  increases. The average ratio for non- smoke event days is .32648. For smoke-flagged event days, the average rises to .46757, indicating that these events did indeed see an effect from smoke.

At night, the land cools quickly, allowing the air above it to cool relatively quickly as well. During the night and morning hours, when winds are low, cool air descends, carrying with it the smoke that was aloft. Because the winds are low, the entrained particles build up near the ground. When the winds increase somewhat, the smoke may be blown out of the area. For this reason, we see a general inverse pattern between wind speed and  $PM_{2.5}$  in the morning and night hours.  $PM_{2.5}$  peaks are typically found during periods of low winds. In general, the reverse applies to midday hours as the land heats the air above it. During the late morning and afternoon hours, when winds increase,  $PM_{2.5}$  levels generally increase as smoke is blown in from the surrounding areas, following the terrain into the valley at Sunland Park. When peaks occur during midday, they usually occur when winds increase somewhat. Figures 18-66 to 18-93 show these relationships, using  $PM_{10}$  as a proxy at the SPCY TEOM monitor.

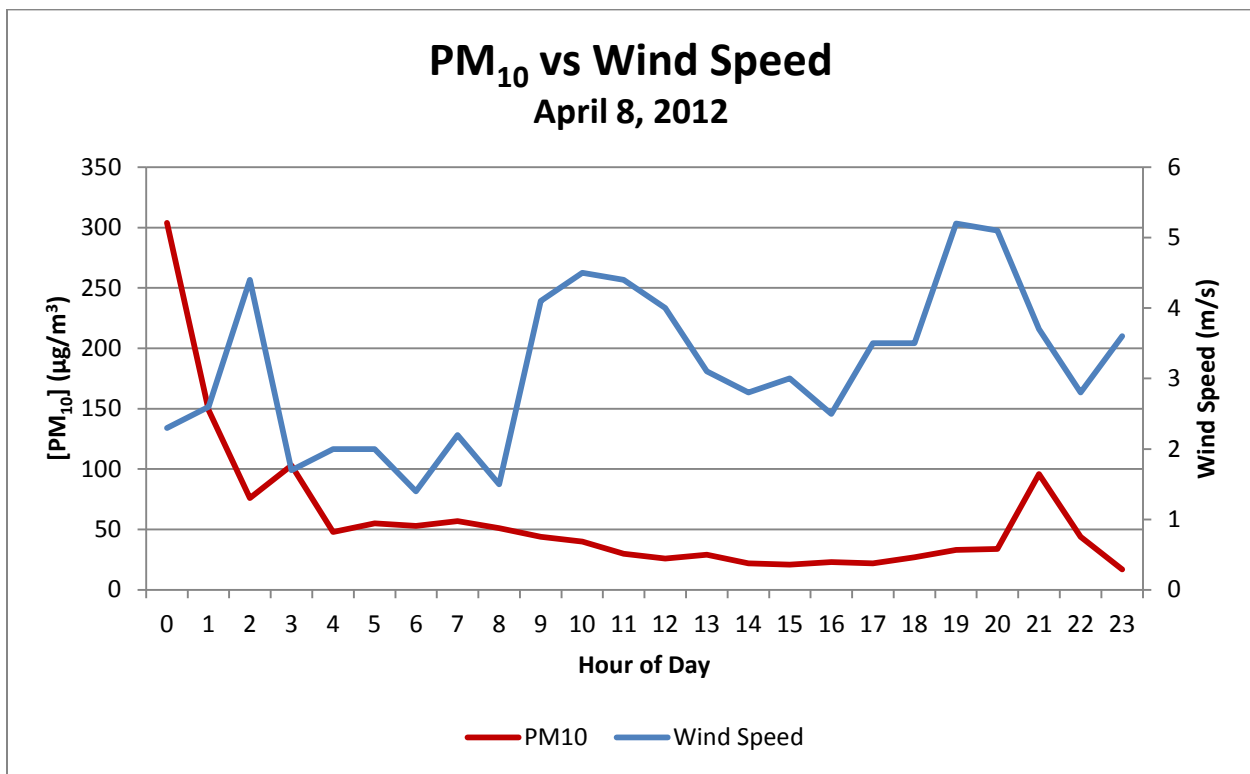


Figure 18-66. Wind speed vs. hourly  $PM_{10}$  concentrations at the SPCY TEOM monitor. The three peaks occurred in the early morning hours and the evening, as wind speeds decreased.

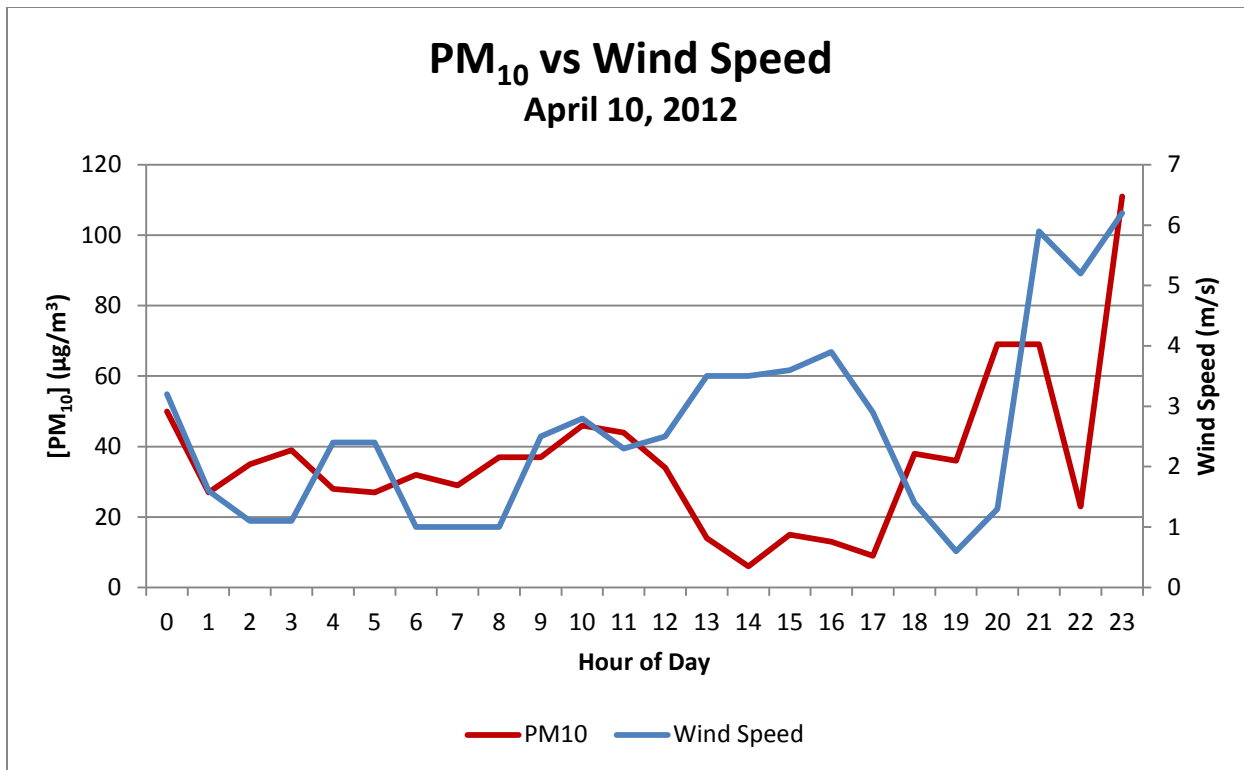


Figure 18-67. Wind speed vs. hourly PM<sub>10</sub> concentrations at the SPCY TEOM monitor. The first PM<sub>10</sub> peak occurred as wind speed decreased in the evening. The second peak which occurred at 11:00 pm corresponds to a change in wind direction from easterly to southerly as shown in Figure 18-94.

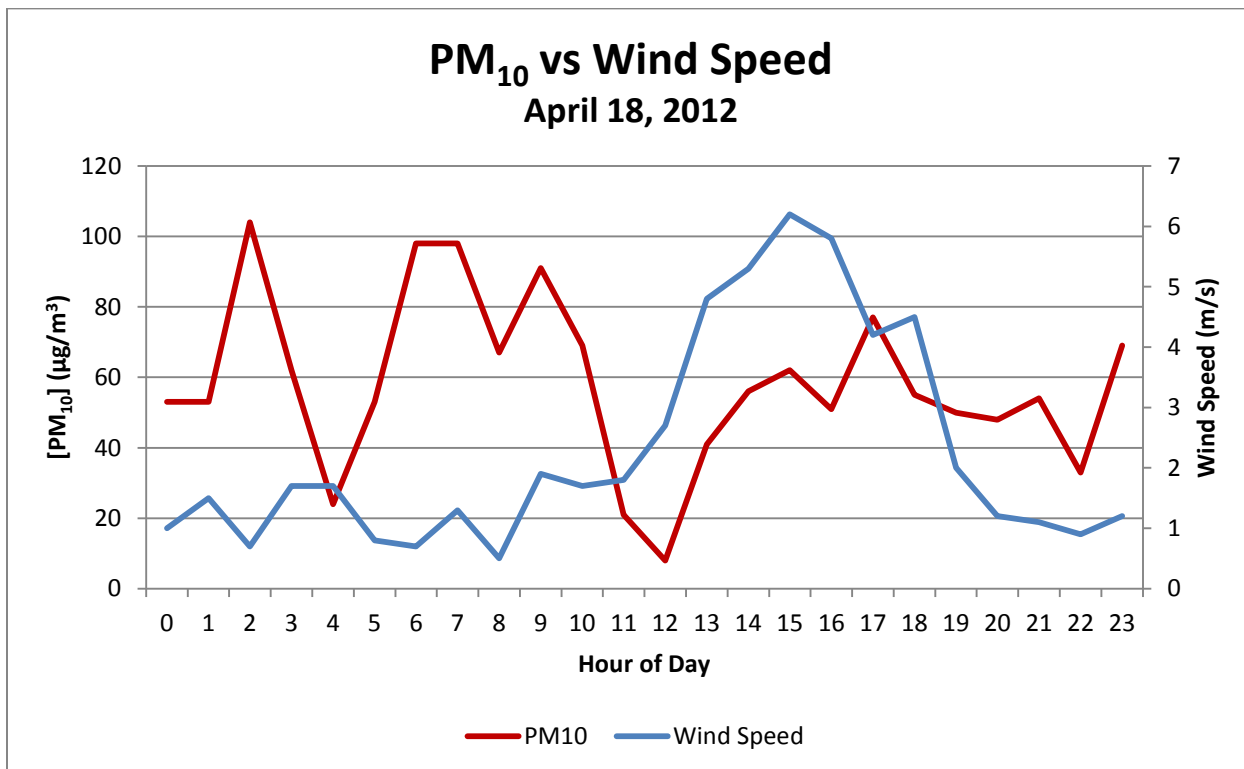


Figure 18-68. Wind speed vs. hourly PM<sub>10</sub> concentrations at the SPCY TEOM monitor. The morning PM<sub>10</sub> peaks occur when wind speeds are low, as do evening PM<sub>10</sub> peaks. The afternoon peaks roughly correspond to increased wind speeds.

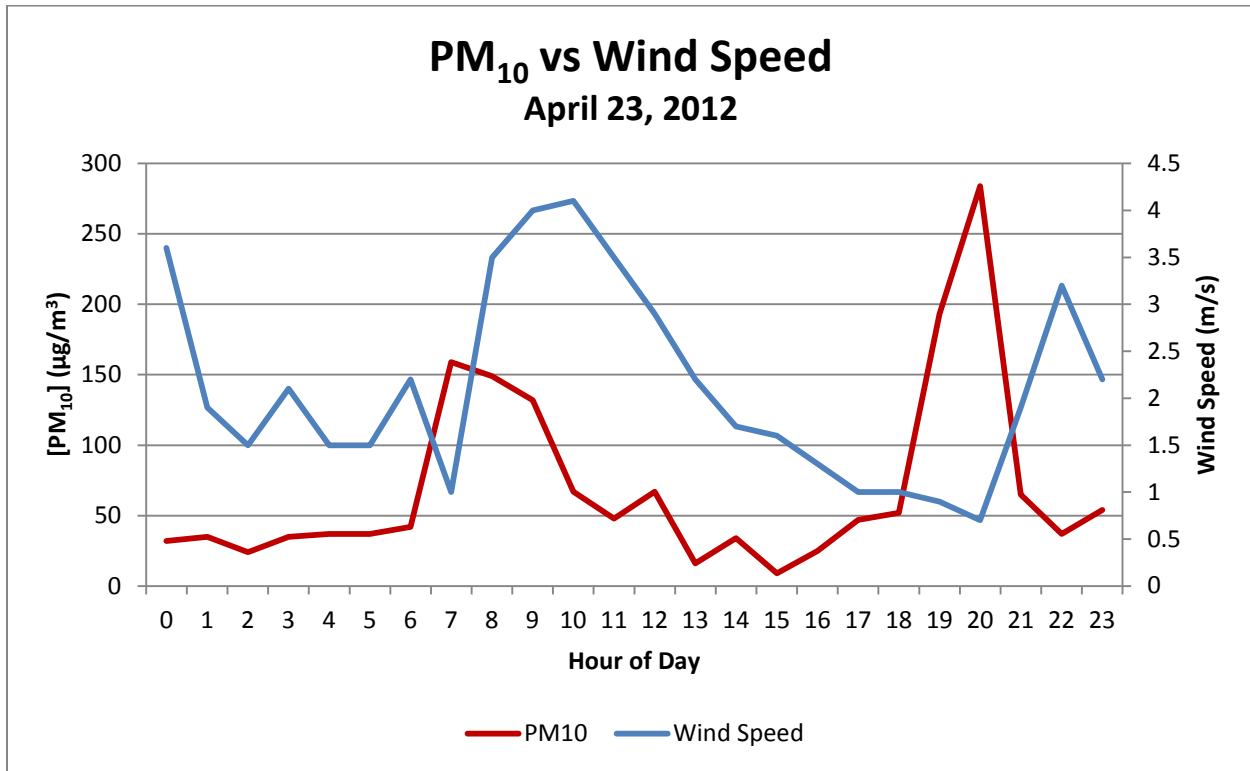


Figure 18-69. Wind speed vs. hourly PM<sub>10</sub> concentrations at the SPCY TEOM monitor. Major PM<sub>10</sub> peaks occur in the morning and evening as wind speeds decrease.

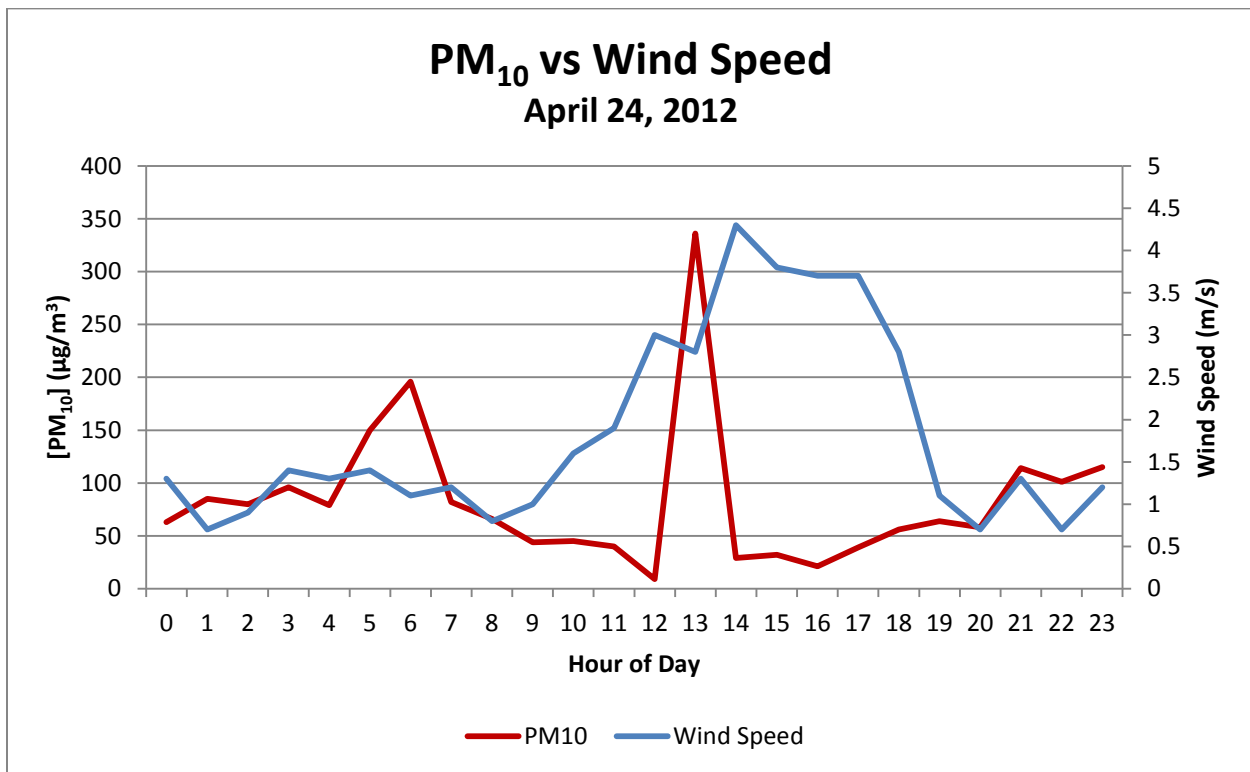


Figure 18-70. Wind speed vs. hourly PM<sub>10</sub> concentrations at the SPCY TEOM monitor. Two major PM<sub>10</sub> peaks occur, one in the morning and one mid-afternoon. Wind speeds are low in the morning and higher in the afternoon.

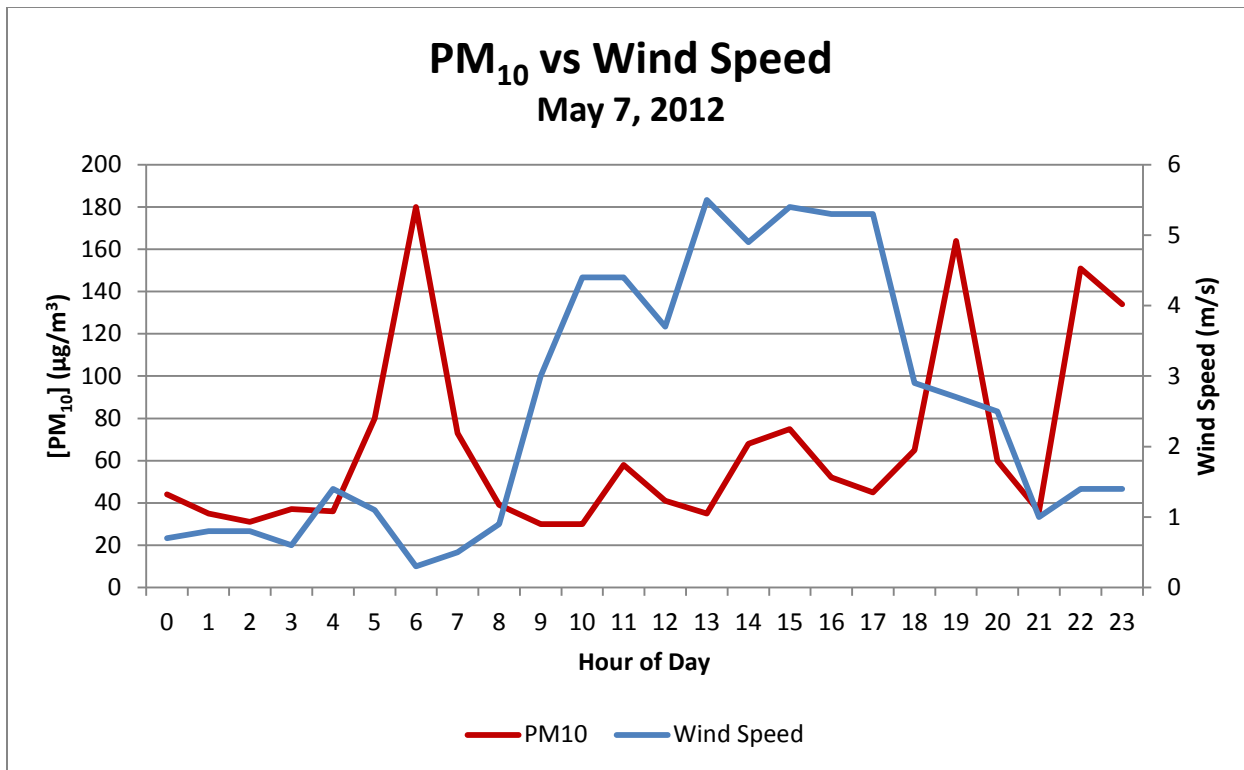


Figure 18-71. Wind speed vs. hourly PM<sub>10</sub> concentrations at the SPCY TEOM monitor. Major PM<sub>10</sub> peaks occur in the morning, early evening and late evening. These spikes roughly correspond to low winds.

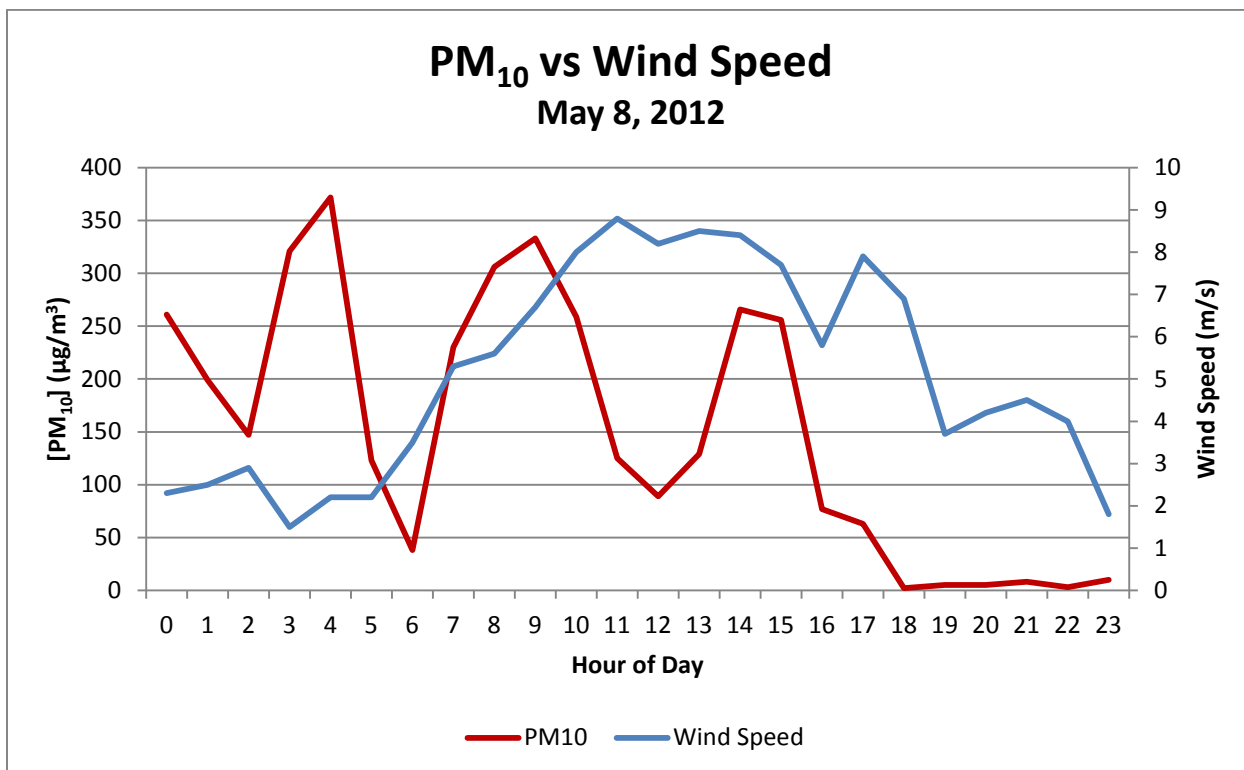


Figure 18-72. Wind speed vs. hourly PM<sub>10</sub> concentrations at the SPCY TEOM monitor. The first two PM<sub>10</sub> peaks occur in the morning when winds are low. The third major PM<sub>10</sub> peak occurs mid- to late morning as winds are rising. This peak requires further explanation, which follows this series of charts. The fourth peak occurs mid-afternoon with increased wind speed as expected.

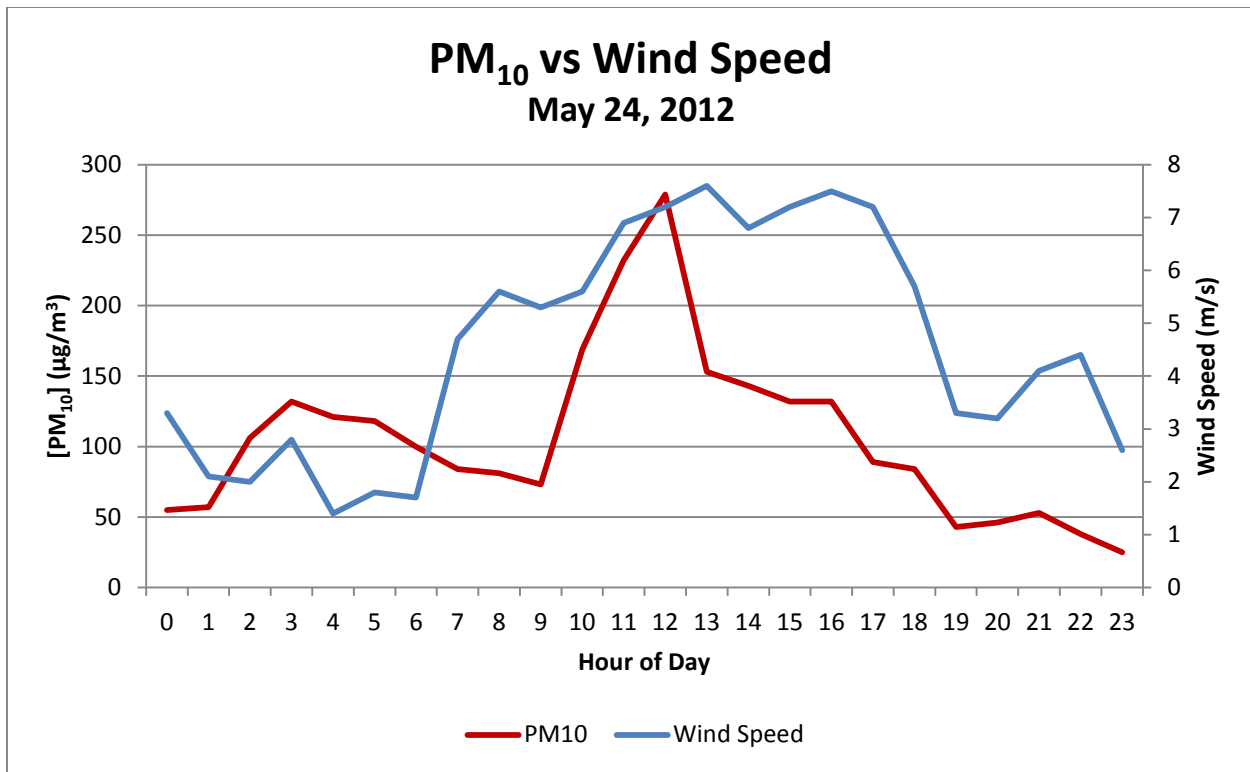


Figure 18-73. Wind speed vs. hourly PM<sub>10</sub> concentrations at the SPCY TEOM monitor. The only major PM<sub>10</sub> peak occurs midday as wind speeds increase.

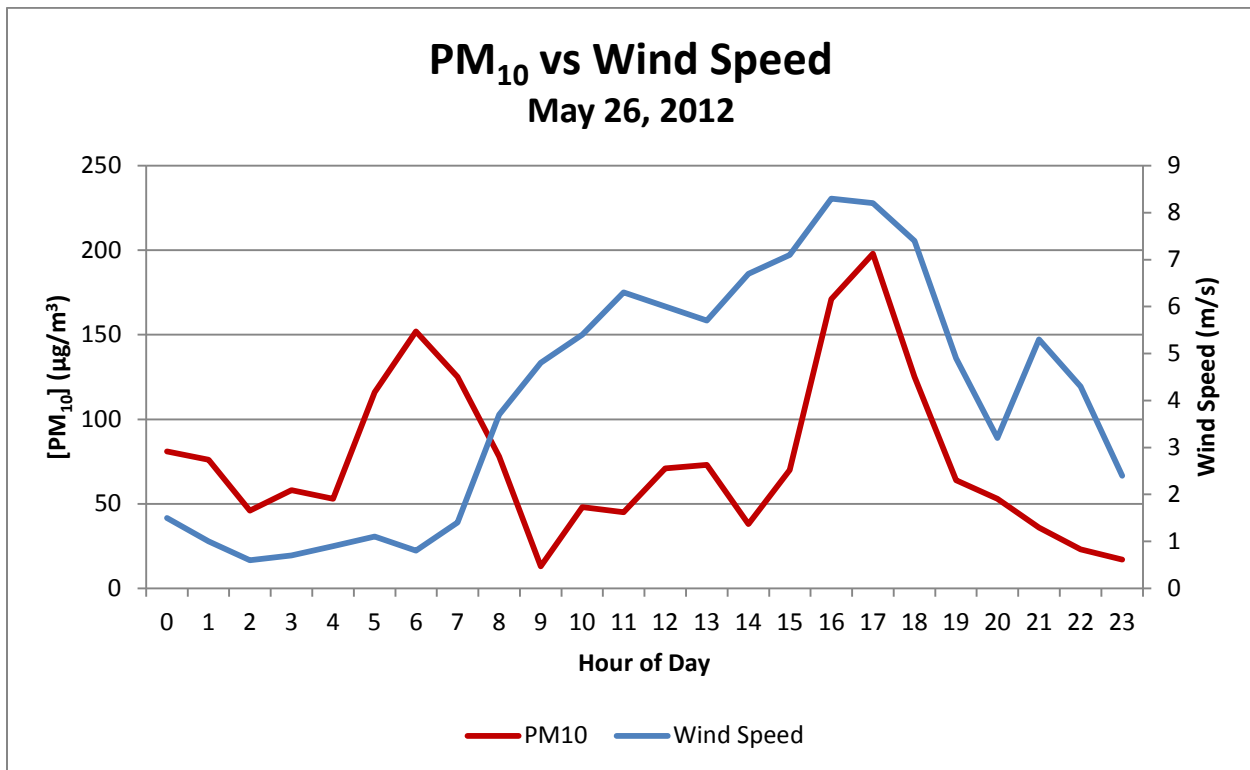


Figure 18-74. Wind speed vs. hourly PM<sub>10</sub> concentrations at the SPCY TEOM monitor. Two major peaks occur: one in the morning as wind speeds are low and one in the late afternoon when wind speeds increase.

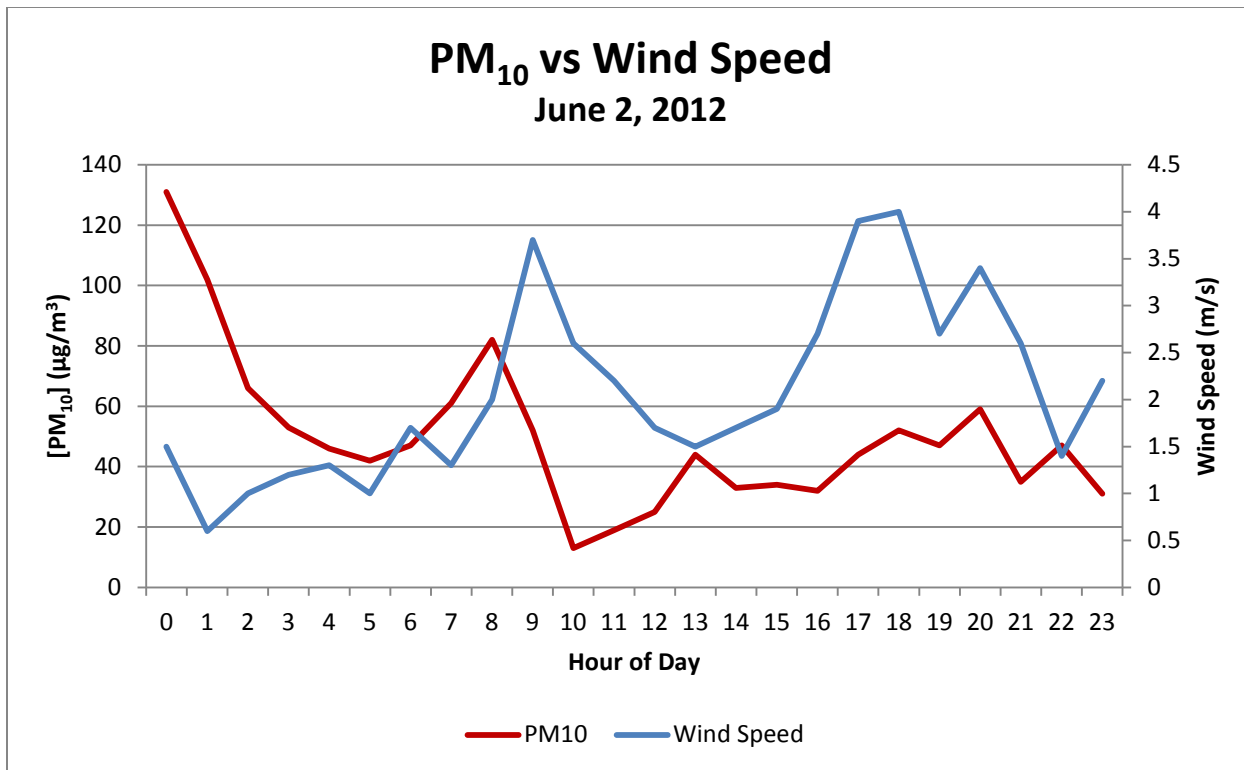


Figure 18-75. Wind speed vs. hourly PM<sub>10</sub> concentrations at the SPCY TEOM monitor. The major peaks occur in the morning when wind speeds are low.

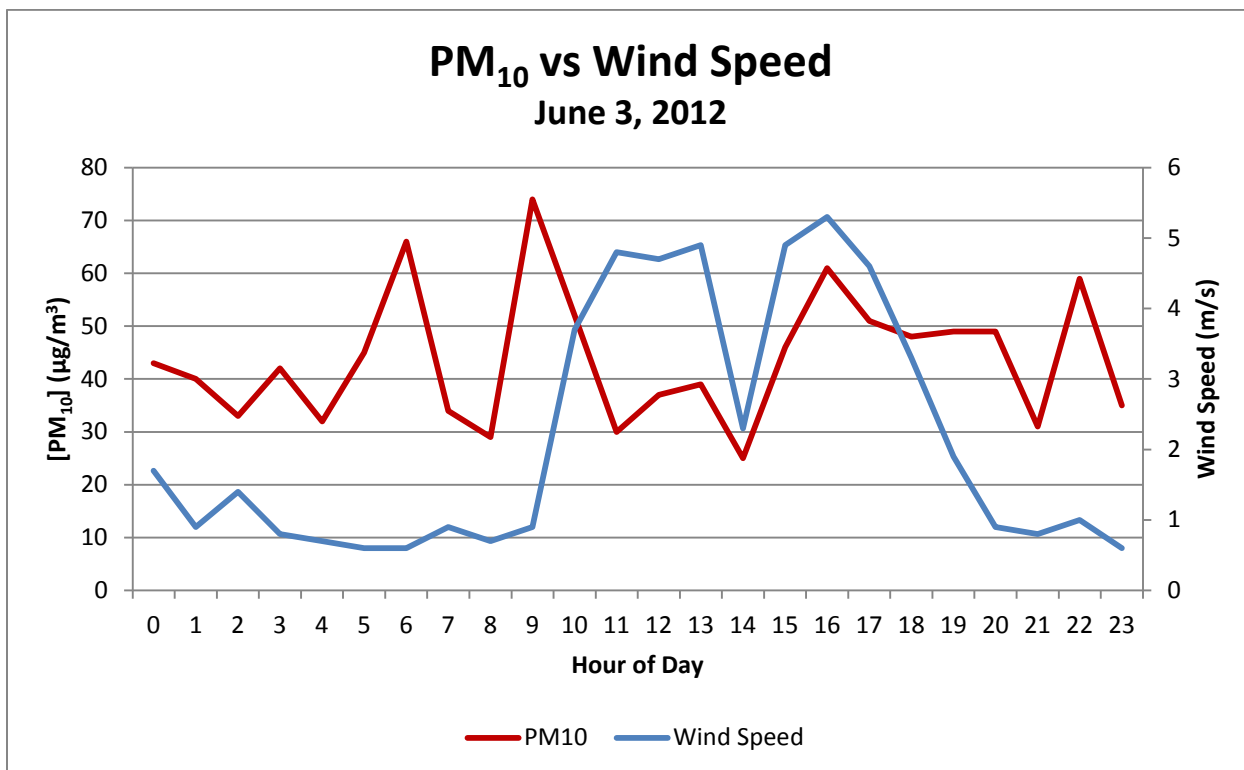


Figure 18-76. Wind speed vs. hourly PM<sub>10</sub> concentrations at the SPCY TEOM monitor. Morning and evening PM<sub>10</sub> peaks occur when wind speeds are low. The afternoon peak occurs when wind speed is relatively higher.

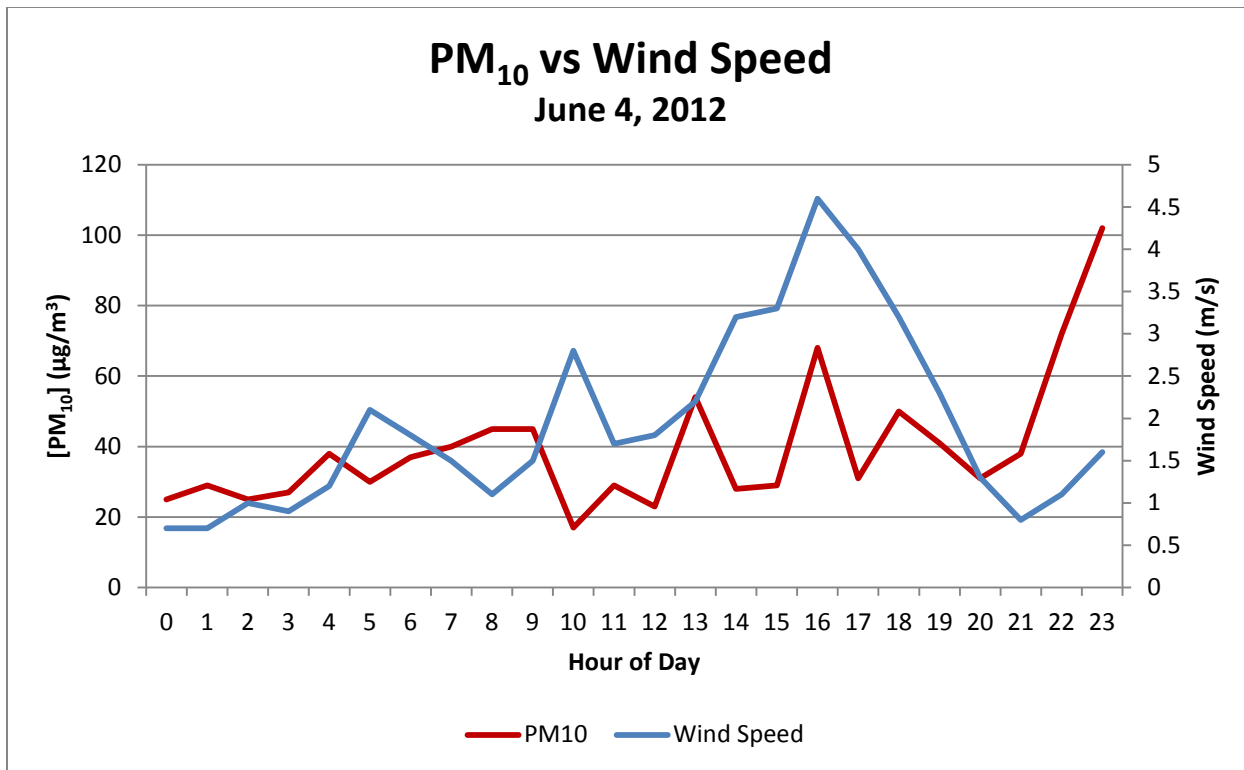


Figure 18-77. Wind speed vs. hourly PM<sub>10</sub> concentrations at the SPCY TEOM monitor. The major PM<sub>10</sub> peak occurs at night as wind speed is low.

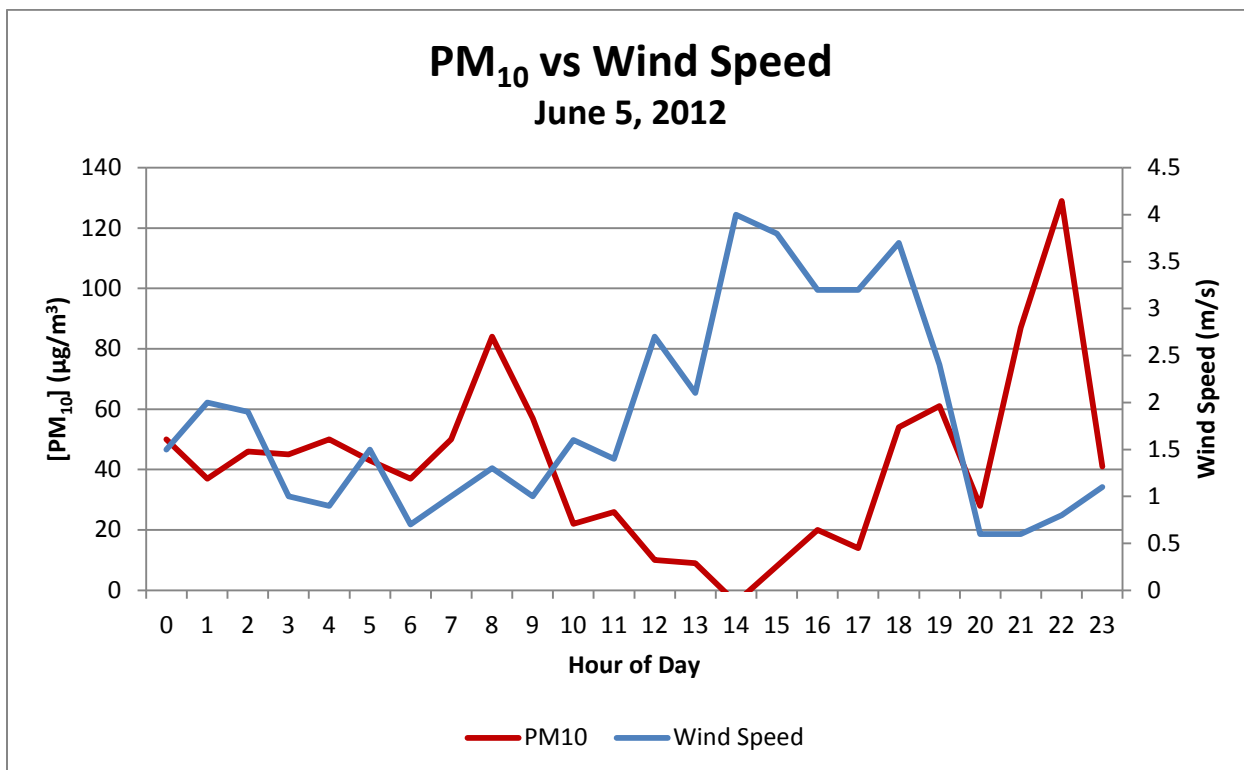


Figure 18-78. Wind speed vs. hourly PM<sub>10</sub> concentrations at the SPCY TEOM monitor. The major PM<sub>10</sub> peaks occur in the morning and evening when wind speeds are low.

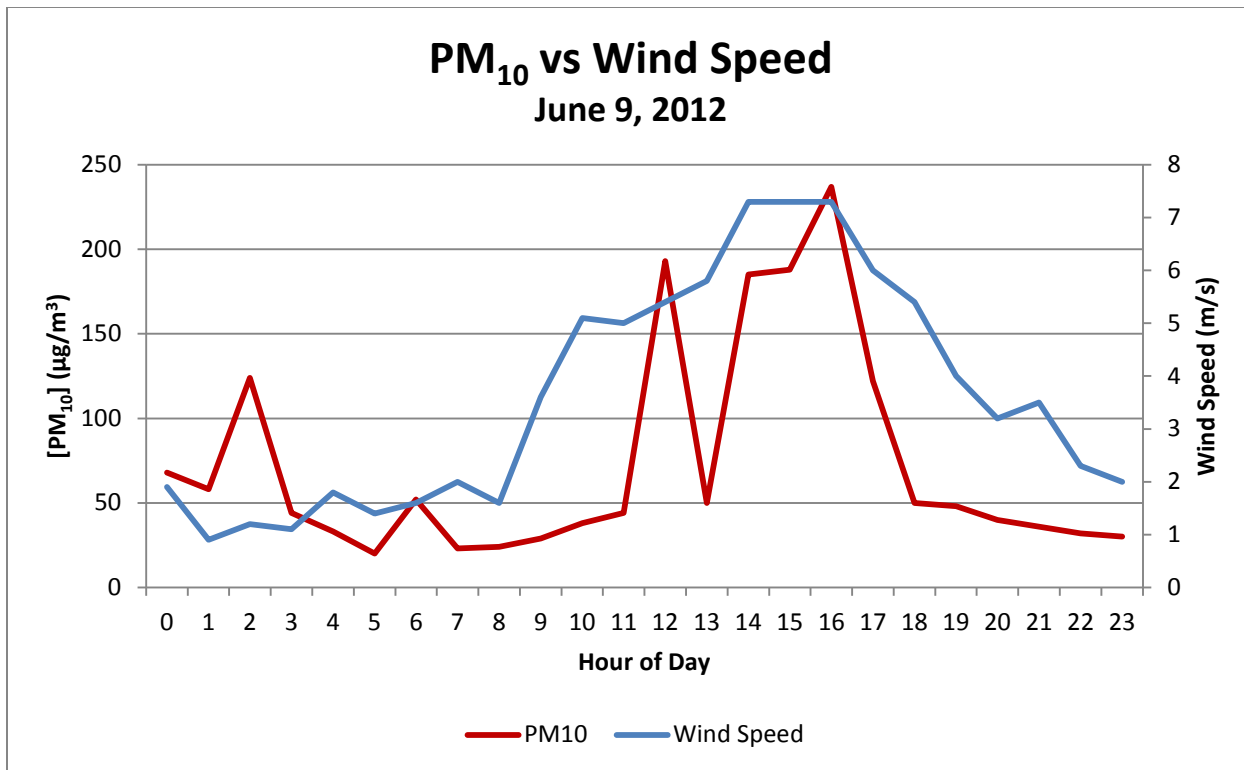


Figure 18-79. Wind speed vs. hourly PM<sub>10</sub> concentrations at the SPCY TEOM monitor. The major PM<sub>10</sub> peaks occur in the morning when winds are low, and the afternoon when wind speeds are relatively higher.

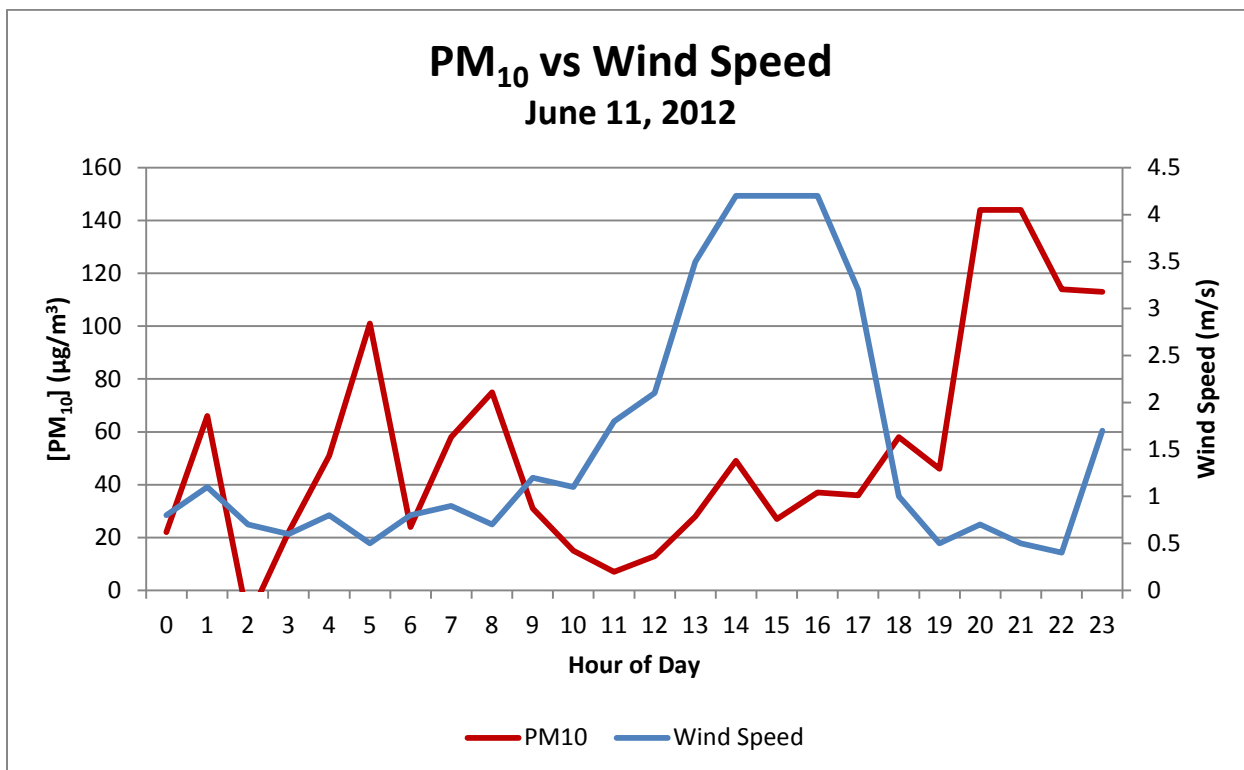


Figure 18-80. Wind speed vs. hourly PM<sub>10</sub> concentrations at the SPCY TEOM monitor. The major PM<sub>10</sub> peaks occur in the morning and evening when wind speeds are low.

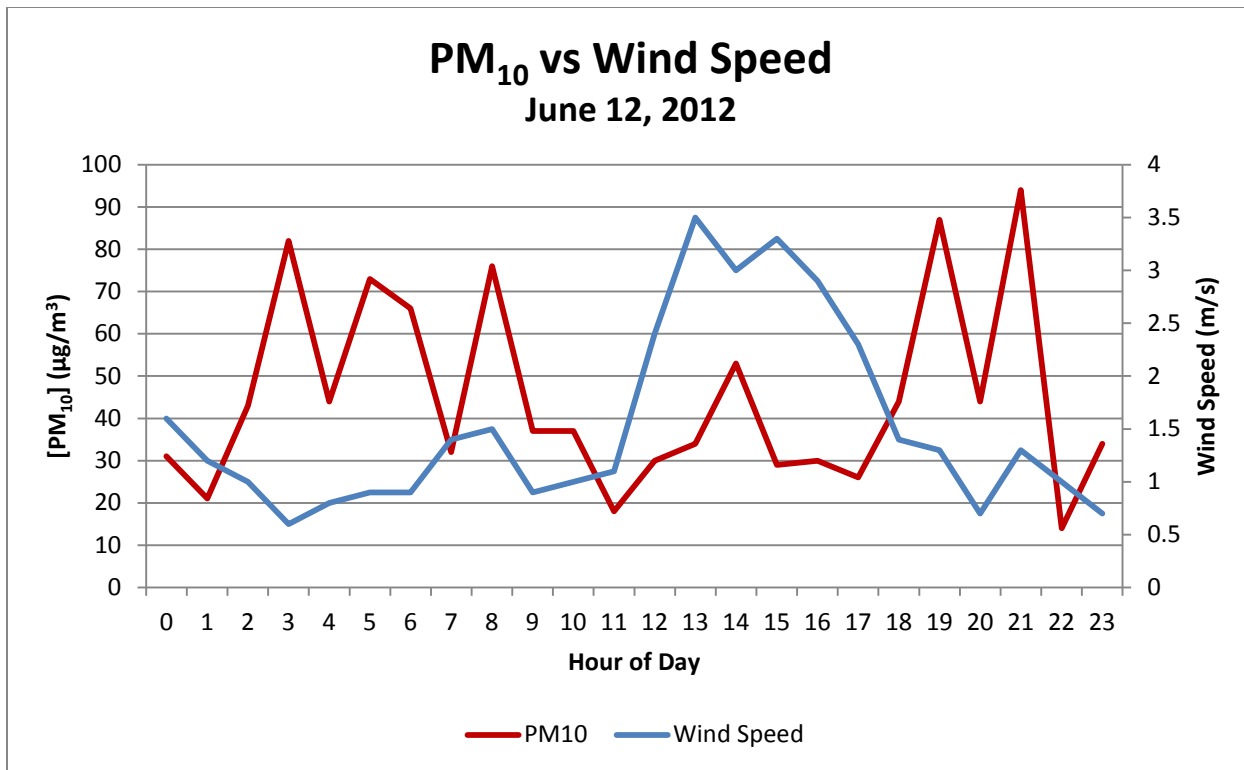


Figure 18-81. Wind speed vs. hourly PM<sub>10</sub> concentrations at the SPCY TEOM monitor. All major PM<sub>10</sub> peaks occur in the morning and evening when wind speeds are low. A minor peak occurs in the afternoon when wind speed is higher.

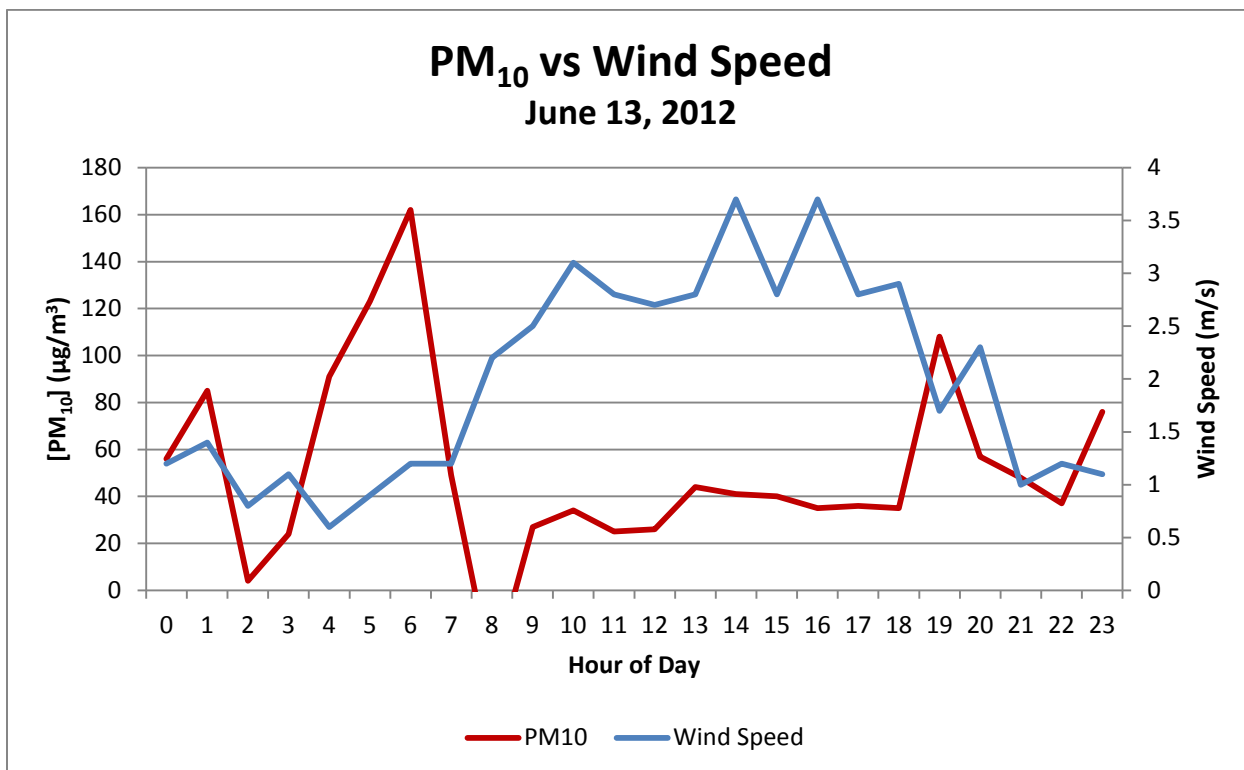


Figure 18-82. Wind speed vs. hourly PM<sub>10</sub> concentrations at the SPCY TEOM monitor. The major PM<sub>10</sub> peak occurs in the morning when wind speed is low. One minor peak occurs after midnight when wind speed is low. Another minor peak occurs in the evening and responds inversely to wind speed.

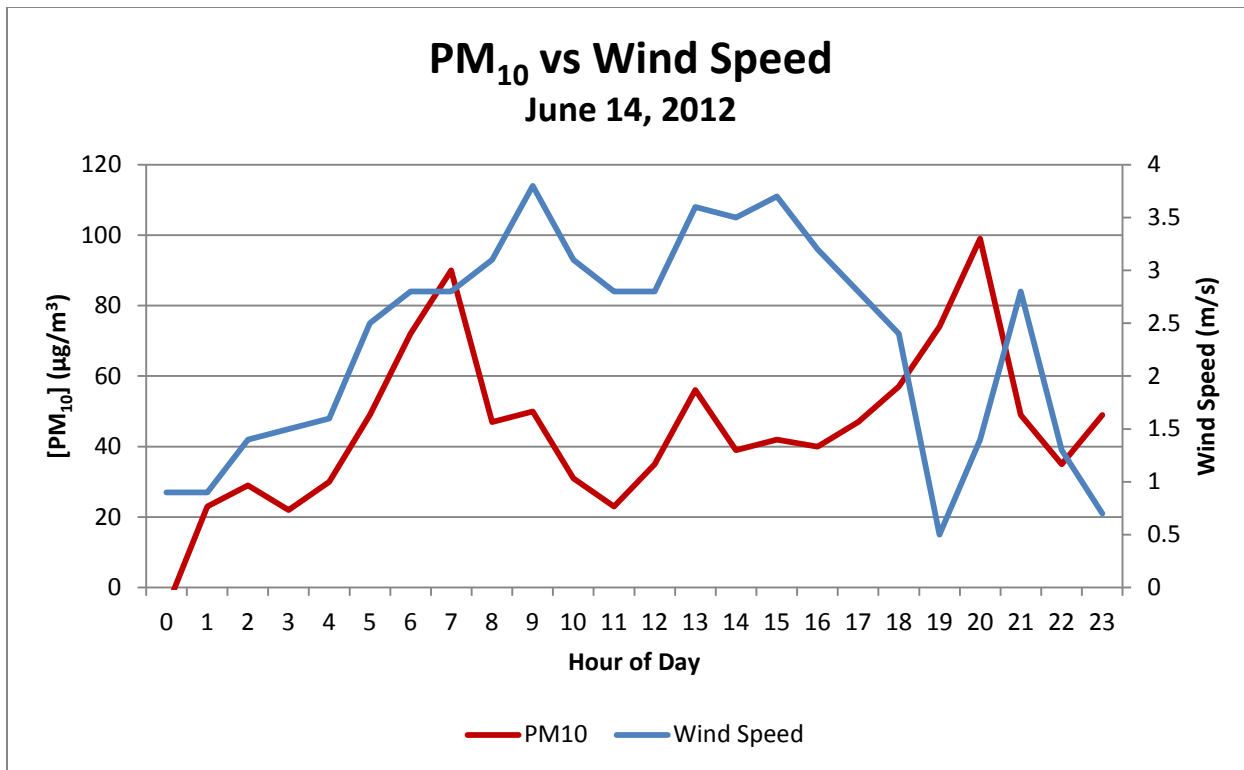


Figure 18-83. Wind speed vs. hourly PM<sub>10</sub> concentrations at the SPCY TEOM monitor. The largest PM<sub>10</sub> peak occurs in the evening as wind speed drops. The other peak occurs in the morning when wind speed is increasing, although less than 3 m/s.

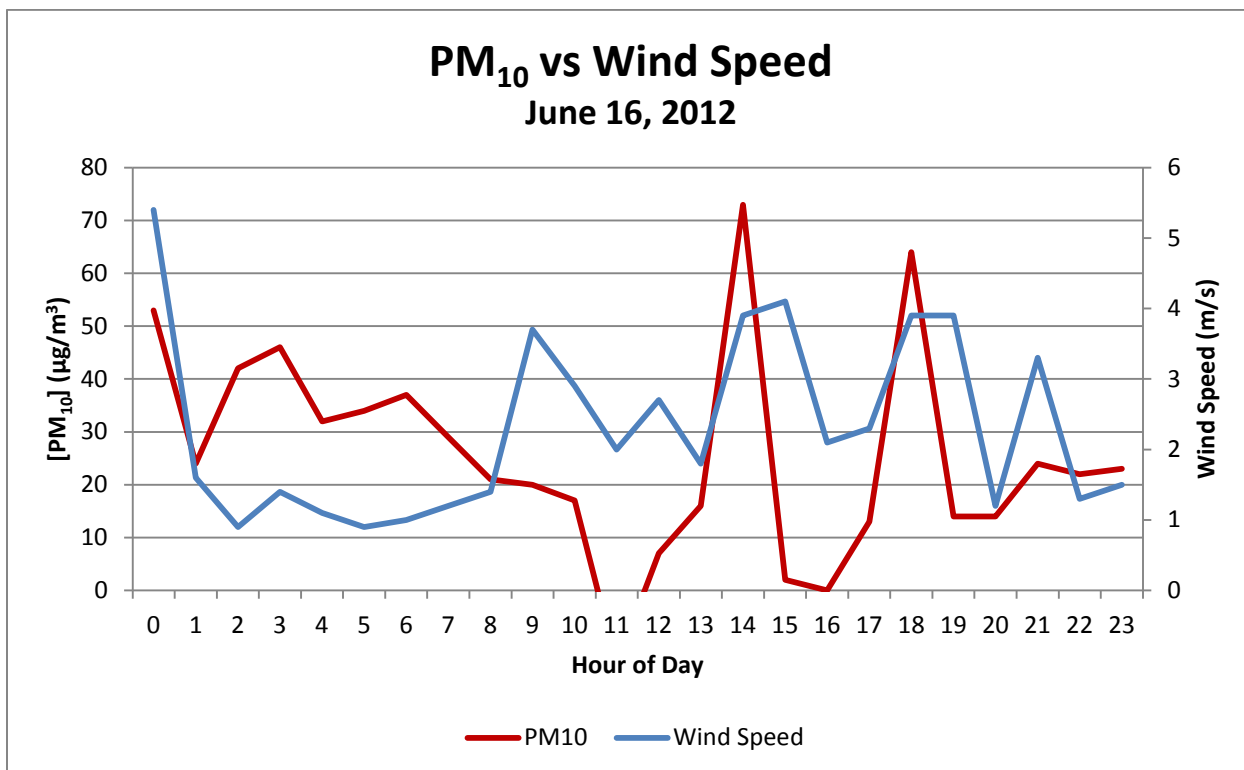


Figure 18-84. Wind speed vs. hourly PM<sub>10</sub> concentrations at the SPCY TEOM monitor. The first PM<sub>10</sub> peak occurs at midnight following a high wind dust event. The other peaks occur mid- and late afternoon as wind speeds increase.

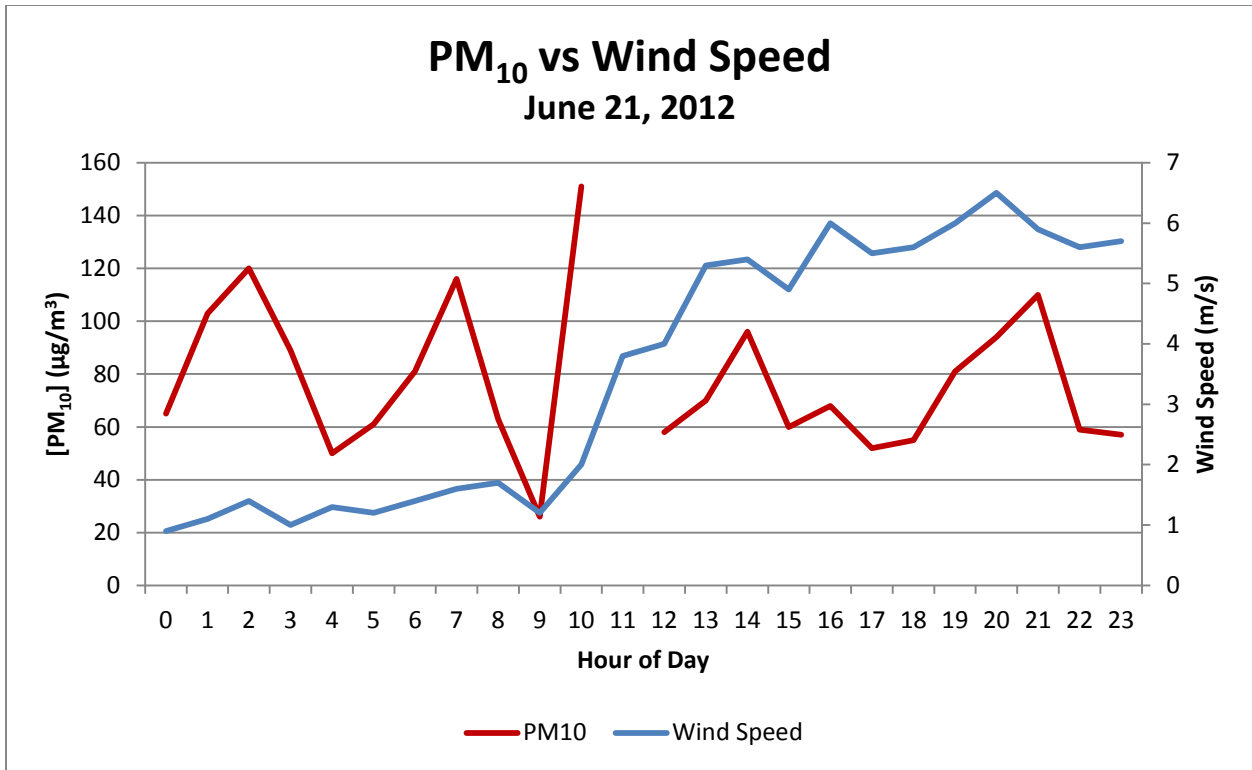


Figure 18-85. Wind speed vs. hourly PM<sub>10</sub> concentrations at the SPCY TEOM monitor. The largest peak occurs late morning as wind speeds increase. The other peaks occur in the (earlier) morning as winds are low, and mid-afternoon as wind speeds increase, and late evening as wind speeds decrease slightly. As Figure 18-99 shows, the evening did not cool to a normal extent.

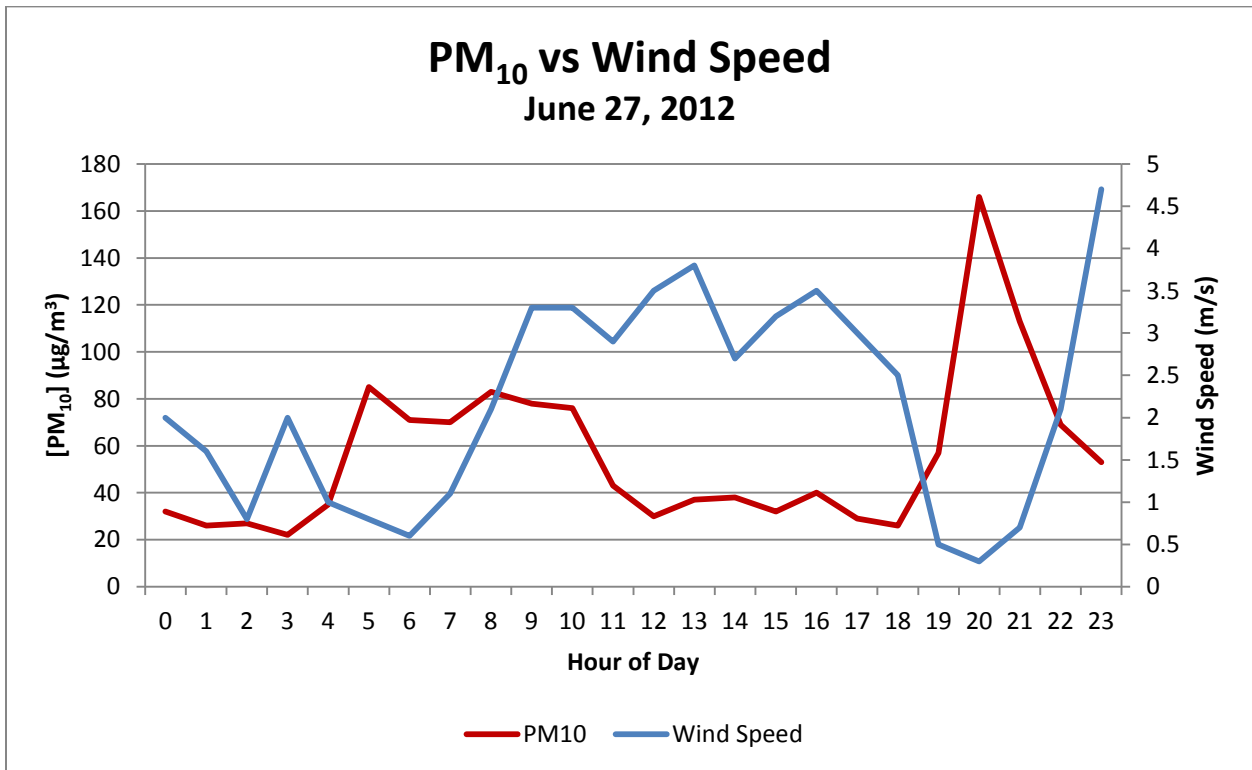


Figure 18-86. Wind speed vs. hourly PM<sub>10</sub> concentrations at the SPCY TEOM monitor. The major PM<sub>10</sub> peak occurs in the evening as wind speed drops.

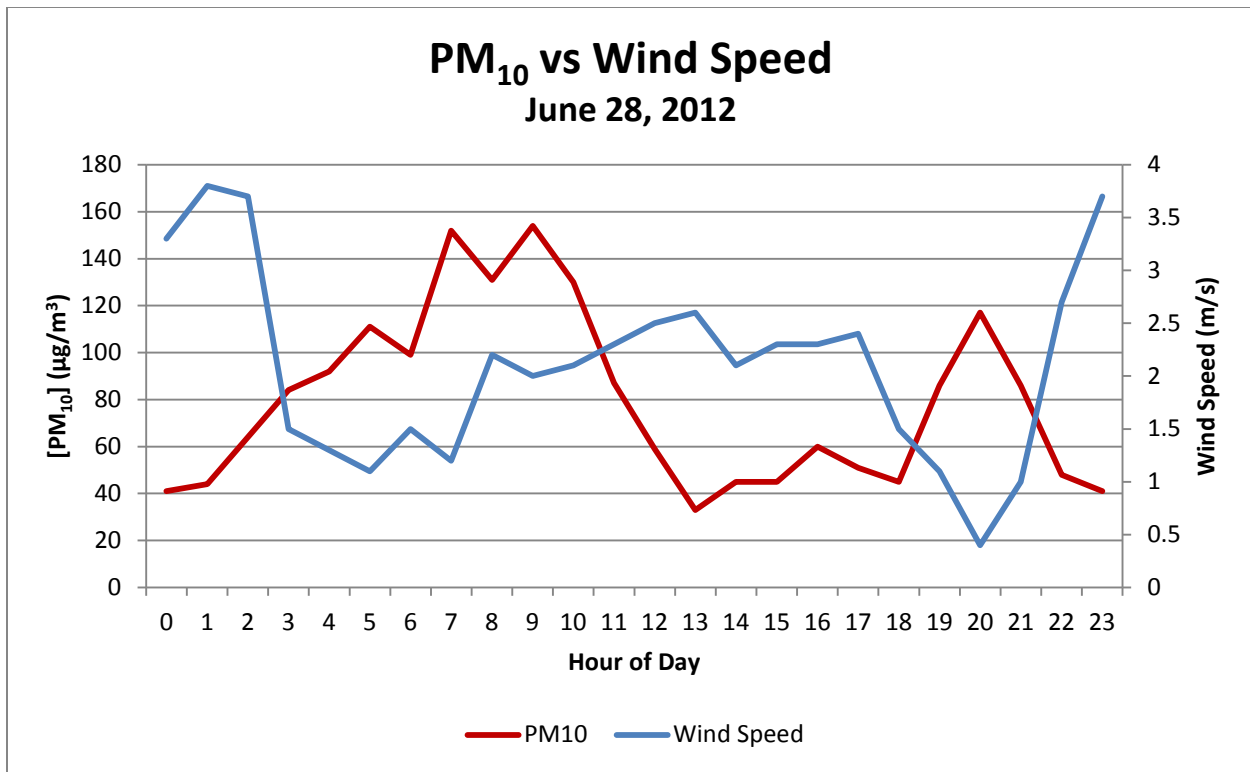


Figure 18-87. Wind speed vs. hourly PM<sub>10</sub> concentrations at the SPCY TEOM monitor. The first set of PM<sub>10</sub> peaks occurs early to mid-morning when wind speeds are low. The other peak occurs in the evening as wind speed drops.

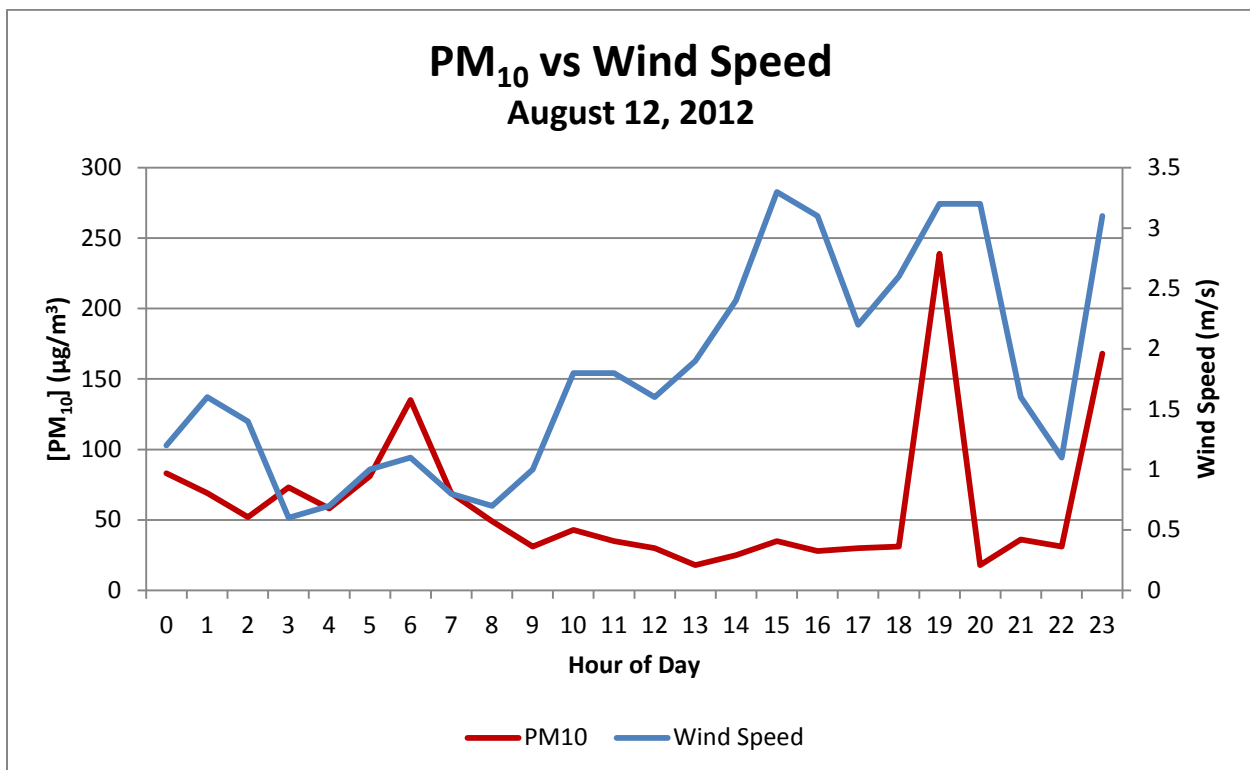


Figure 18-88. Wind speed vs. hourly PM<sub>10</sub> concentrations at the SPCY TEOM monitor. The first PM<sub>10</sub> peak occurs in the morning when wind speed is low. The two evening peaks occur when wind speed is relatively higher, although still relatively low.

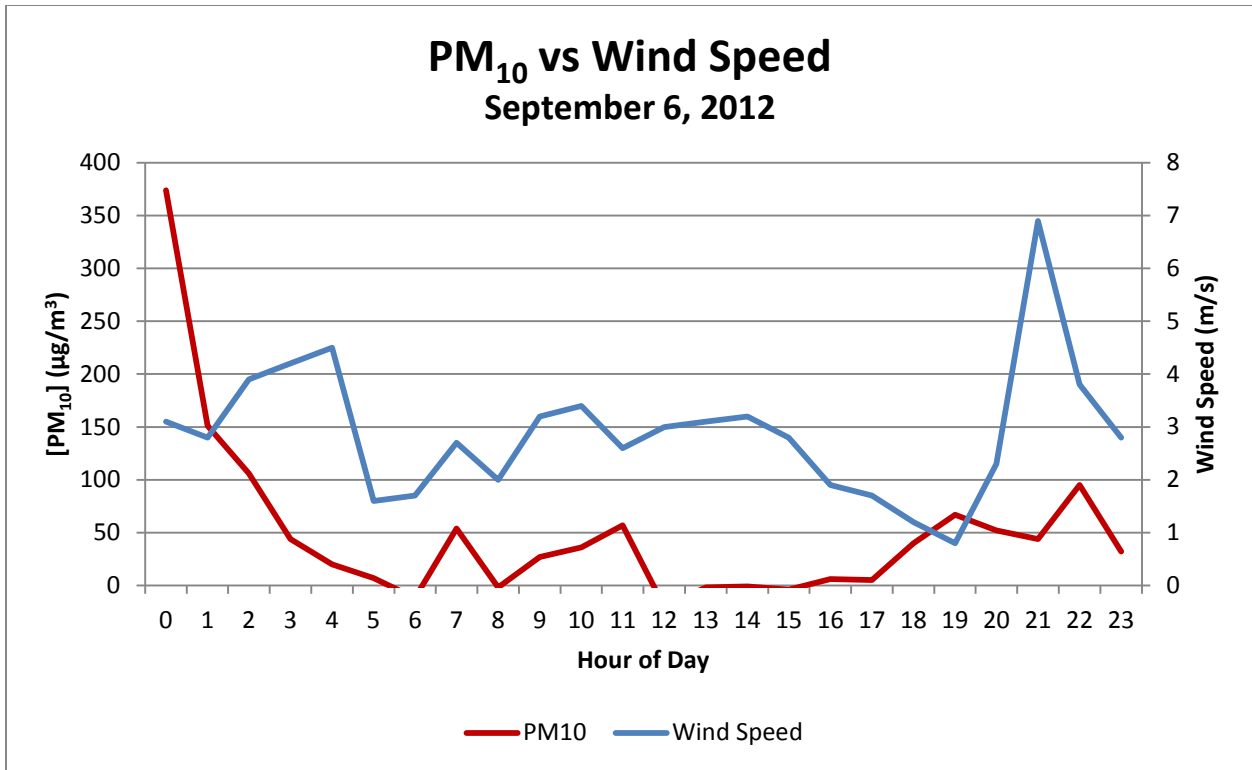


Figure 18-89. Wind speed vs. hourly PM<sub>10</sub> concentrations at the SPCY TEOM monitor. The only major PM<sub>10</sub> peak occurs at midnight. Wind data cannot explain this peak, but the smoke analysis shown in Figure 18-61 above indicates that smoke was arriving from as far away as California on this date.

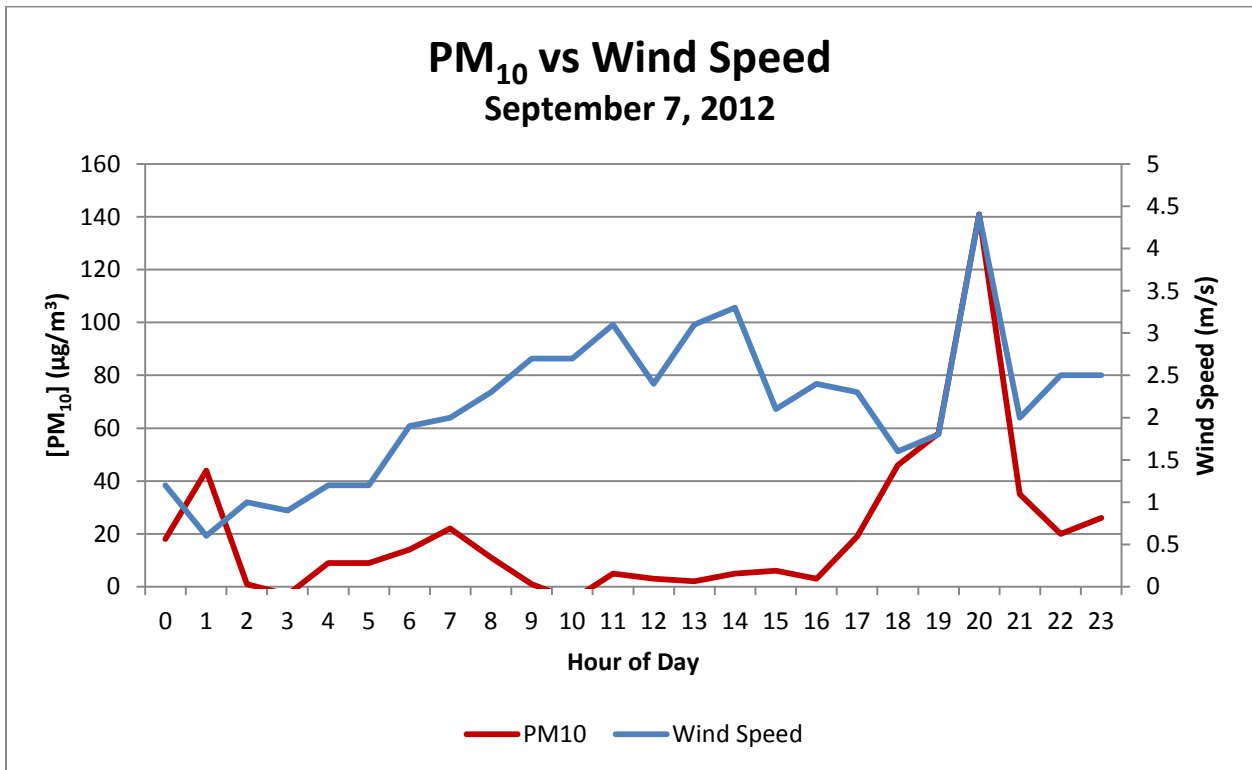


Figure 18-90. Wind speed vs. hourly PM<sub>10</sub> concentrations at the SPCY TEOM monitor. The major PM<sub>10</sub> spike occurs in the early evening as wind speed increases.

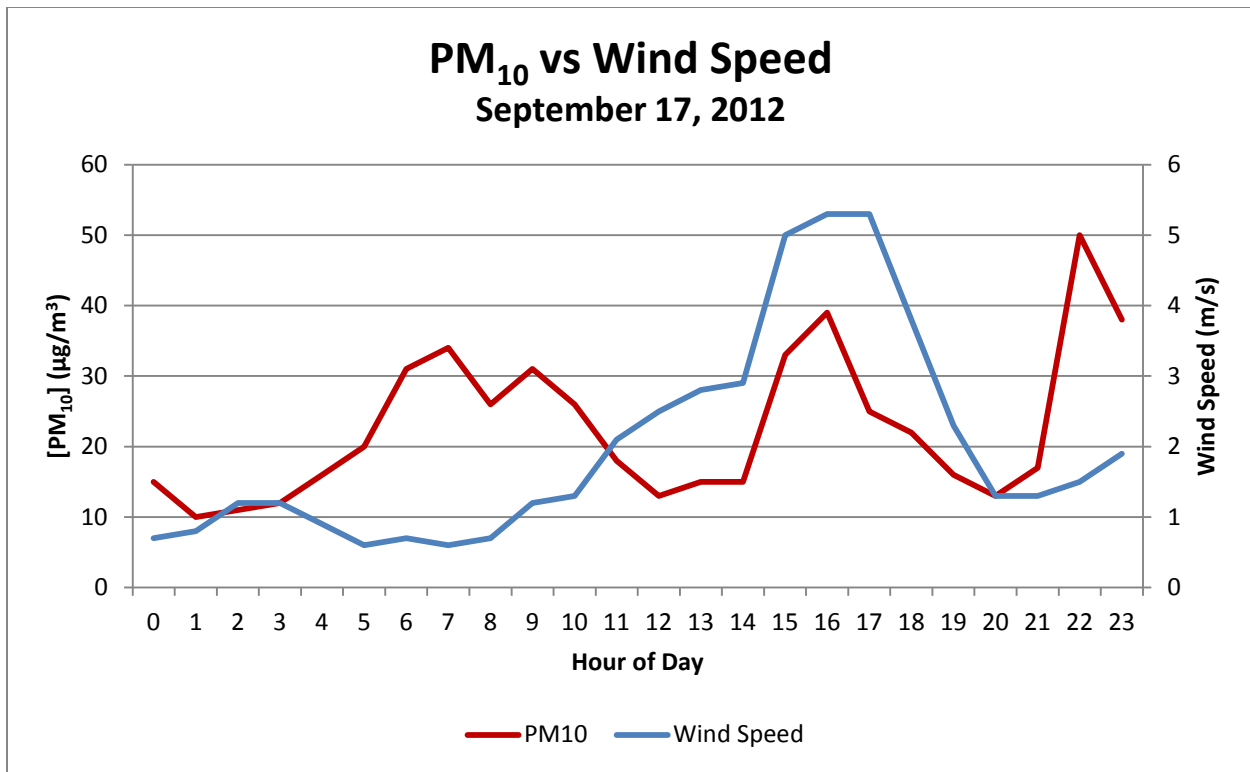


Figure 18-91. Wind speed vs. hourly PM<sub>10</sub> concentrations at the SPCY TEOM monitor. The first set of PM<sub>10</sub> peaks occurs in the morning as wind speeds are low. Another peak occurs in the afternoon as wind speeds increase. The evening peak also occurs as wind speeds are low.

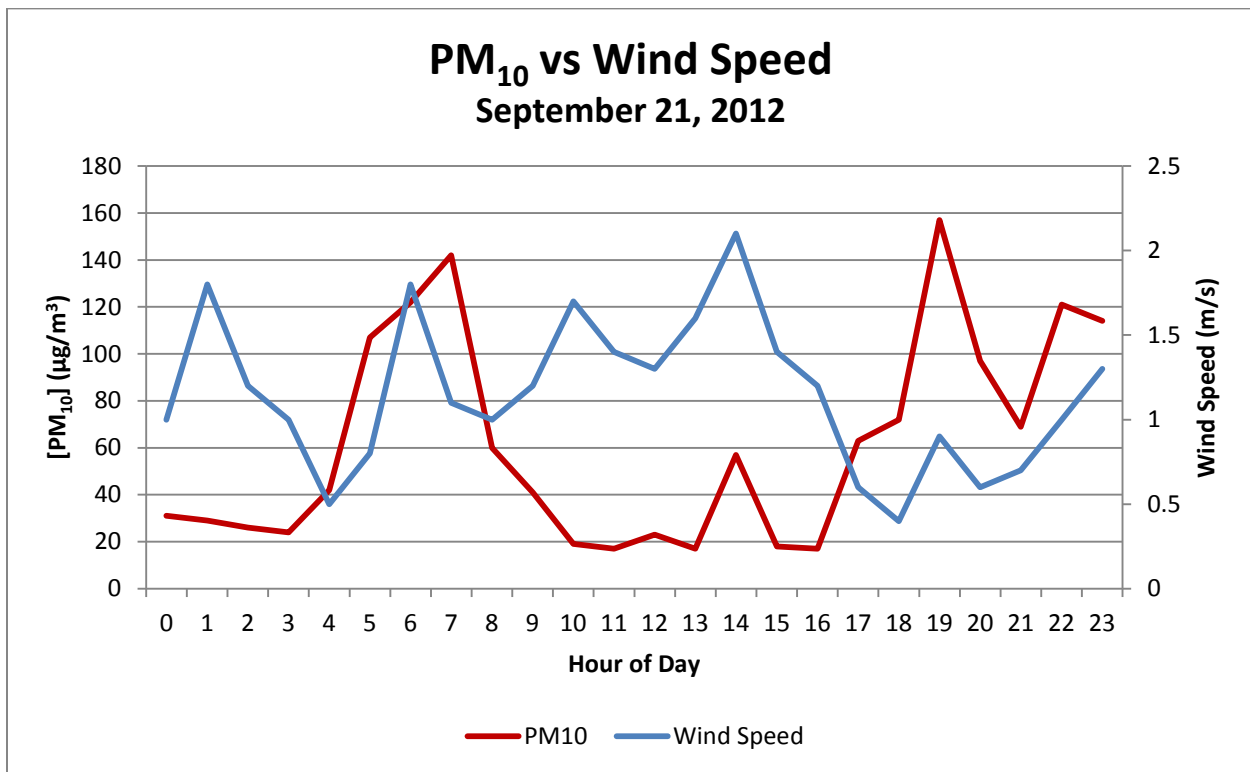


Figure 18-92. Wind speed vs. hourly PM<sub>10</sub> concentrations at the SPCY TEOM monitor. Wind speeds were low all day. The morning peak followed extremely low wind, allowing smoke to concentrate. As the wind picked up slightly, settled smoke was likely blown into the valley. The evening peak also occurred following low wind speeds.

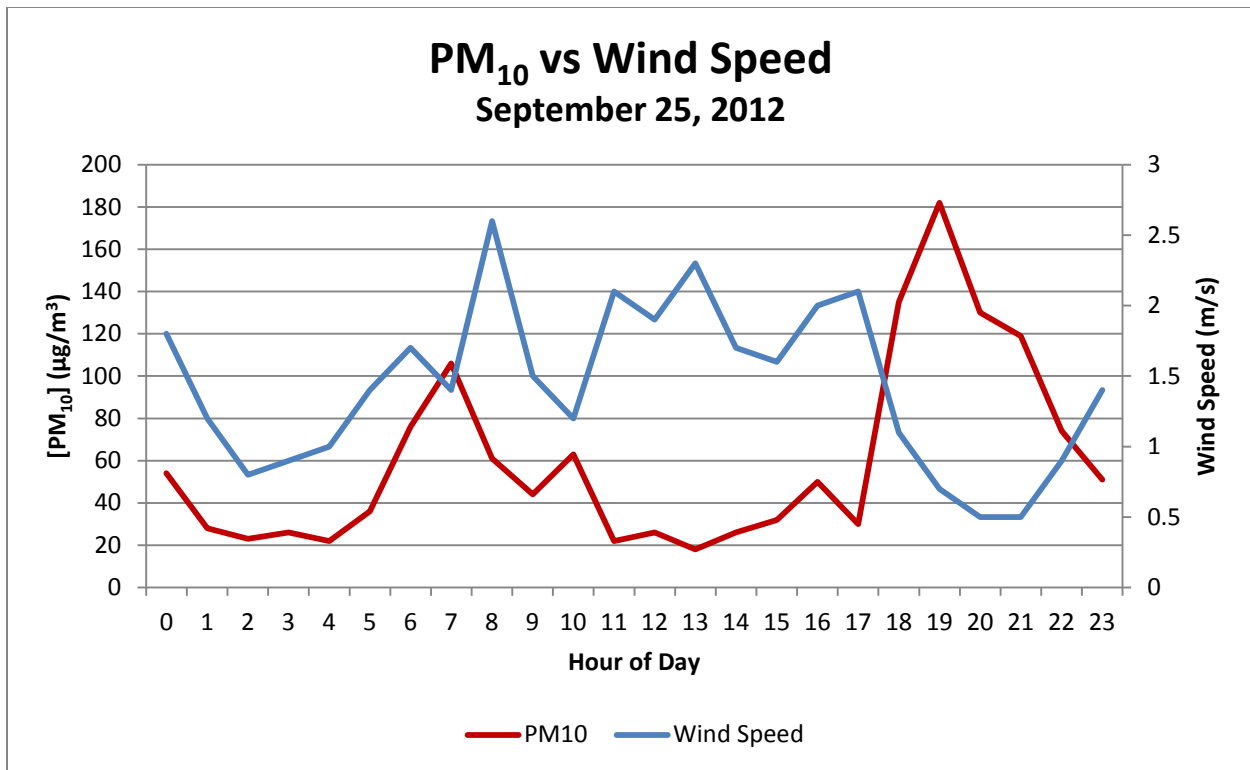


Figure 18-93. Wind speed vs. hourly PM<sub>10</sub> concentrations at the SPCY TEOM monitor. The morning and evening PM<sub>10</sub> peaks correspond roughly to lowered wind speeds.

The exceptions noted in the captions for April 10, May 8, June 21, and September 6 are explained here with supporting documentation provided in Figures 18-94 to 18-99 below. El Paso climate data is included in several explanations because it is the nearest weather station (approximately 13 miles from the SPCY Partisol monitor) with information on barometric pressure and wind direction.

April 10, 2012 – Between 10:00 pm and 11:00 pm, the winds at the El Paso, Texas weather station reported a change in direction from easterly to westerly, then southerly (Figure 18-94). The peak seen at 11:00 pm while wind speeds were relatively high can be explained by smoke being blown in from fires in Mexico, eastern Arizona and western New Mexico as shown in Figure 18-2 above.

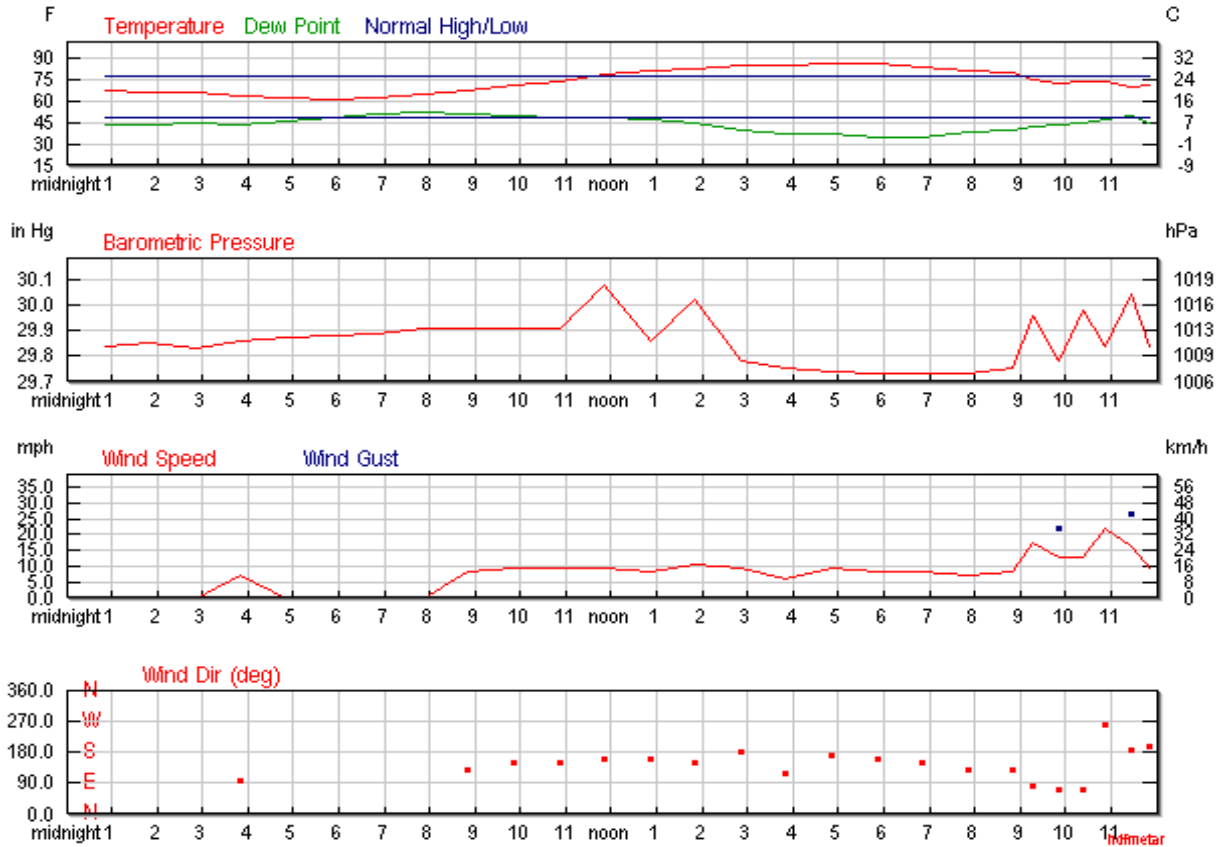


Figure 18-94. Data from the El Paso, Texas weather station showing late evening wind direction changes from easterly to westerly, then southerly on April 10, 2012. This directional change corresponds to an exception noted in Figure 18-67 above. Figure 18-39, above, further confirms the large areas in Mexico and the United States with smoke available for transport.

April 22, 2012 – The normal low temperature for this time of year is less than 60 °F. As Figure 18-95 shows, from 7 – 10 pm MDT the times of peaks noted as exceptions in Figure 18-68 above, the temperature remained at or above 80 °F, making the conditions more likely to follow afternoon patterns.

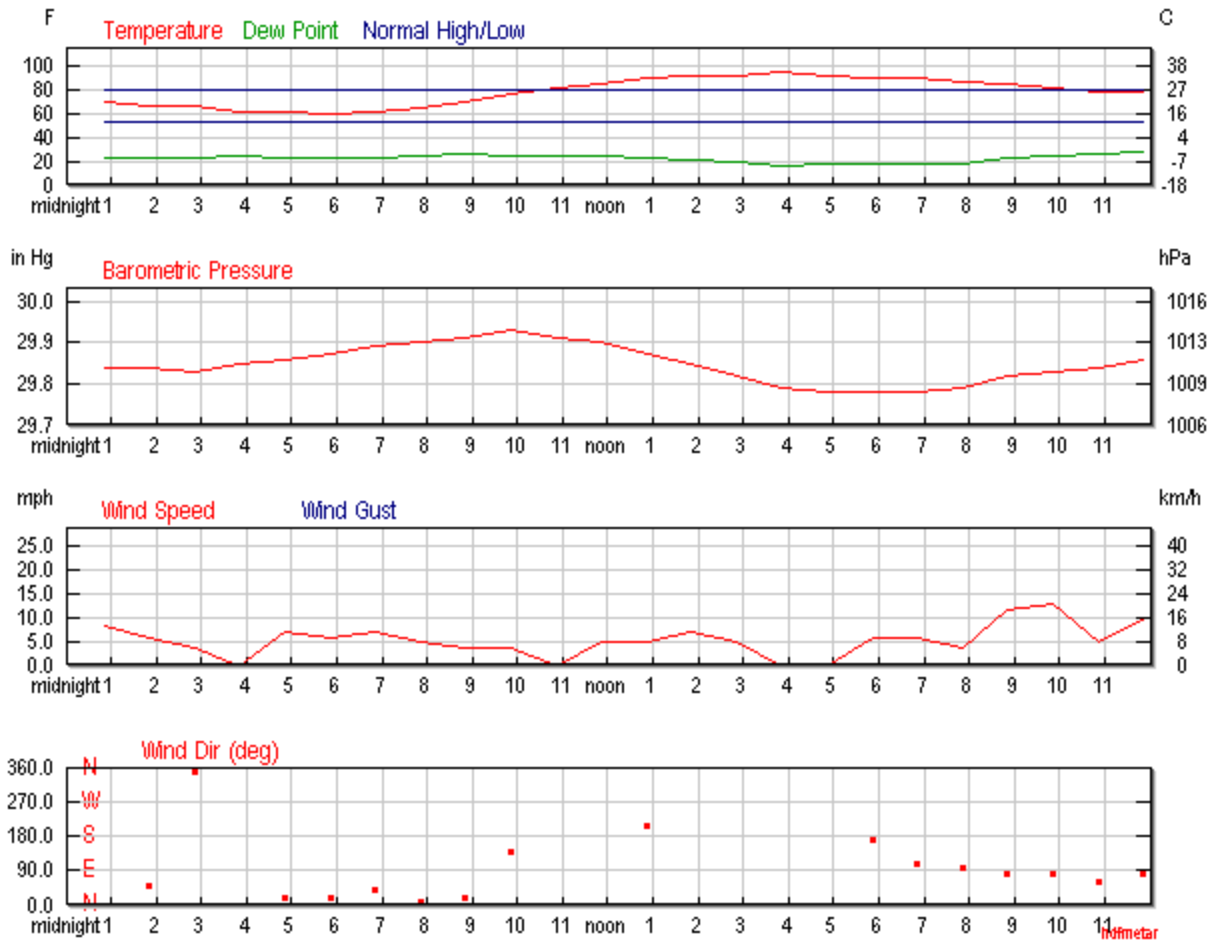


Figure 18-95. April 22, 2012 El Paso, Texas climate data showing the lack cooling that normally occurs at this time of year. Lack of cooling caused the evening hours' moderate winds to blow smoke into the valley, similar to afternoon patterns.

May 8, 2012 – The exception noted in the caption in Figure 18-72 above occurs between 7 and 10 am. A HYSPLIT 24-hour smoke dispersion analysis simulation shows smoke effects at the SPCY Partisol monitor during this time period, taking into account meteorological conditions and aerosol data. Figures 18-96 and 18-97, below, show the analysis at 7 am and 10 am respectively. This may have been due to the mostly easterly wind directions shown in Figure 18-98 below.

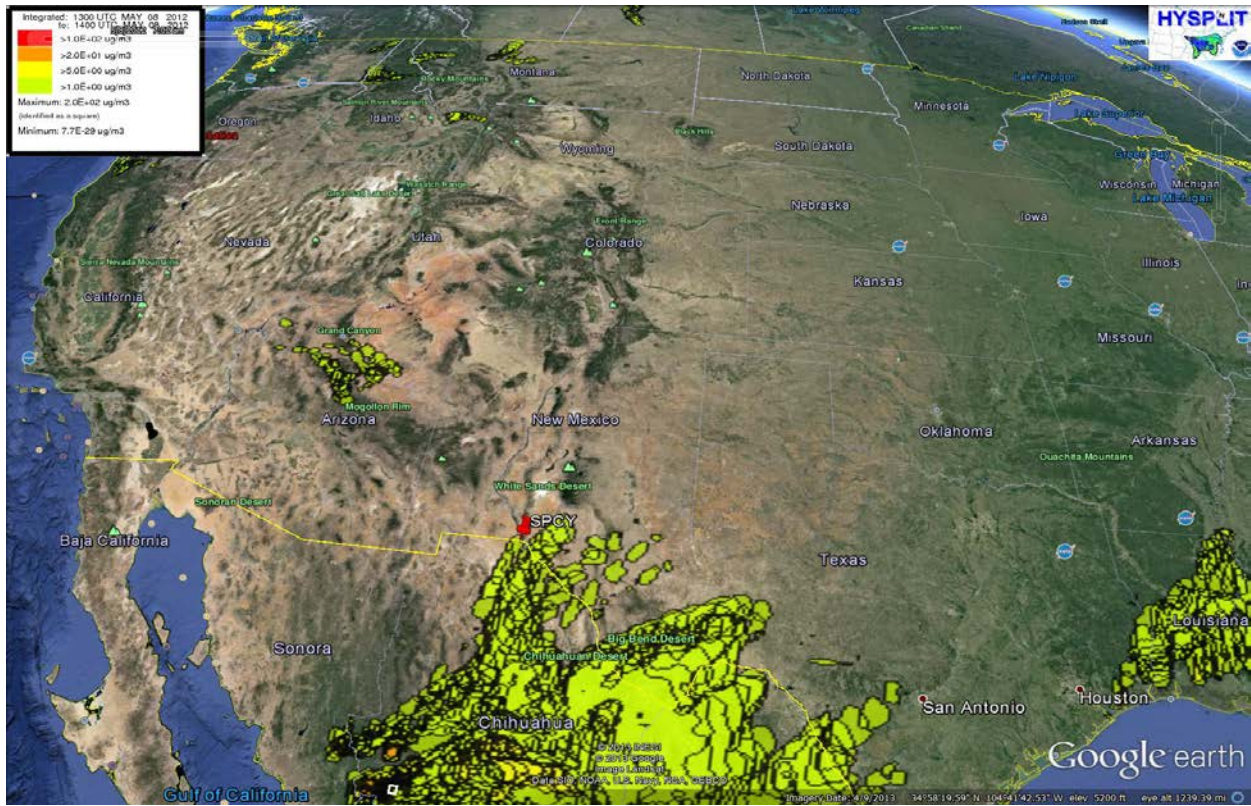


Figure 18-96. HYSPLIT smoke dispersion 24-hour analysis simulation based on aerosol data and meteorological conditions. At 7:00 am (MDT), the SPCY monitor was affected by smoke.

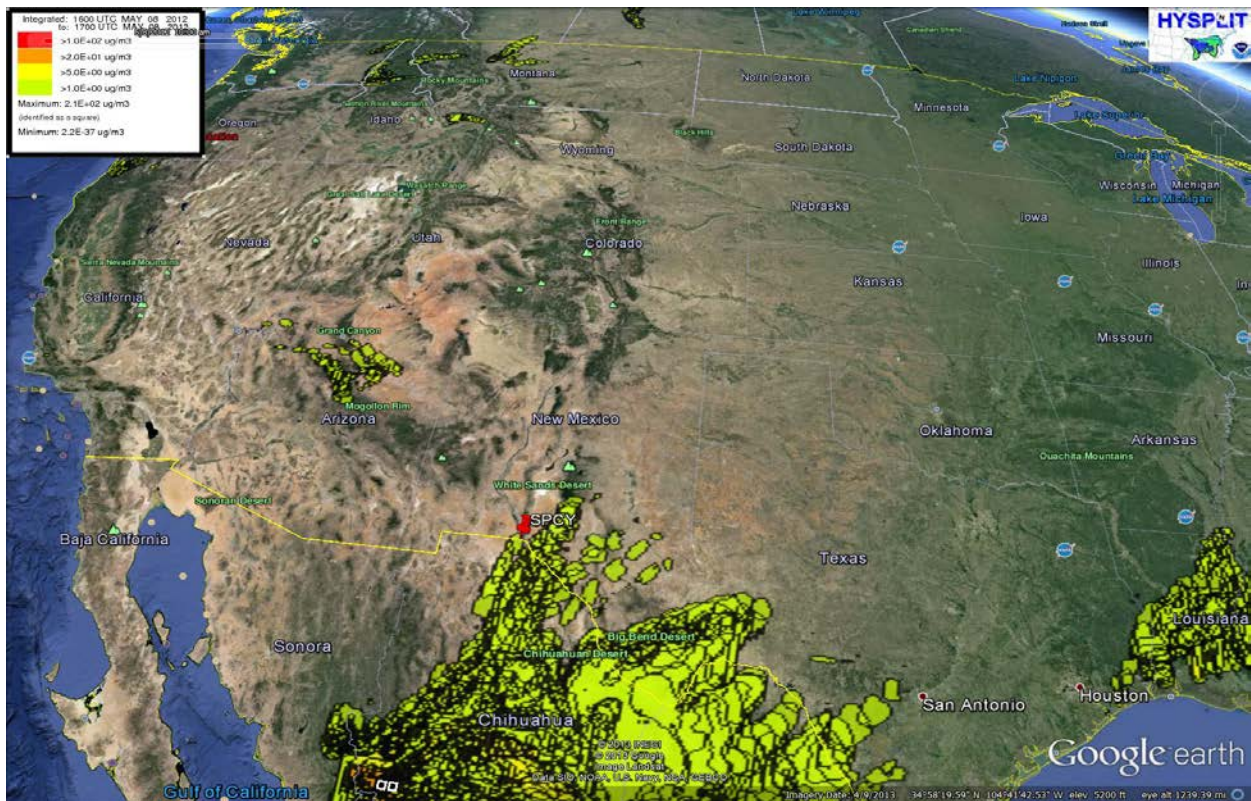


Figure 18-97. HYSPLIT smoke dispersion 24-hour analysis simulation based on aerosol data and meteorological conditions. At 10:00 am (MDT), the SPCY monitor was still affected by smoke.

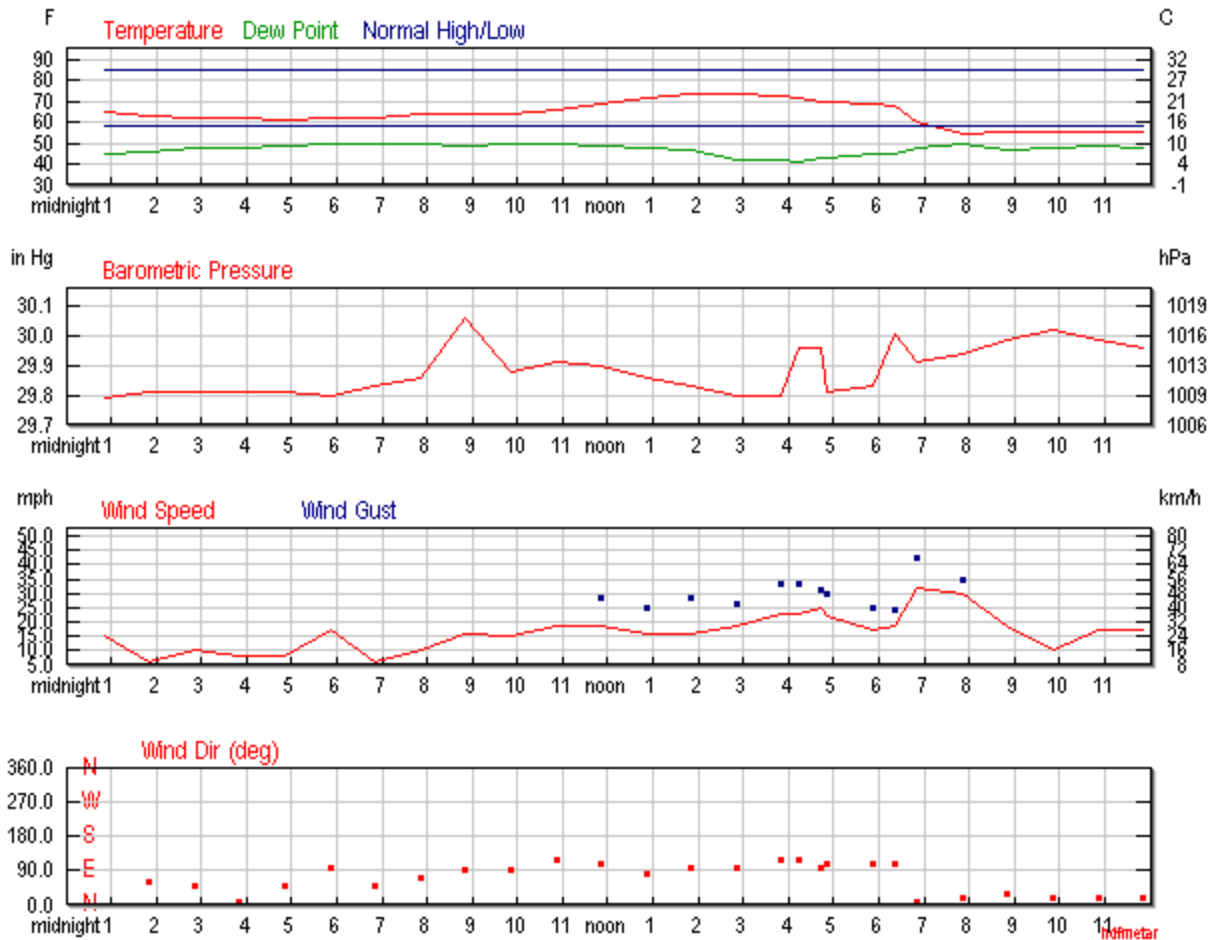


Figure 18-98. El Paso, Texas climate data May 8, 2012, showing that between the hours of 7 and 10 am MDT (between 8 and 11 am CDT), winds changed from east northeast to east southeast, confirming the smoke dispersion analysis images in Figures 18-96 and 18-97 above.

June 21, 2012 – The peak noted in the caption of Figure 18-85 above occurred at approximately 7 – 9 pm (MDT). As the El Paso climate data shown in Figure 18-99 below shows, the temperature remained at or above 85 °F during these hours. This may have caused the fluctuation pattern to mimic those of afternoon. In addition, high wind gusts were seen during this time, likely contributing dust to the high PM<sub>10</sub> readings.

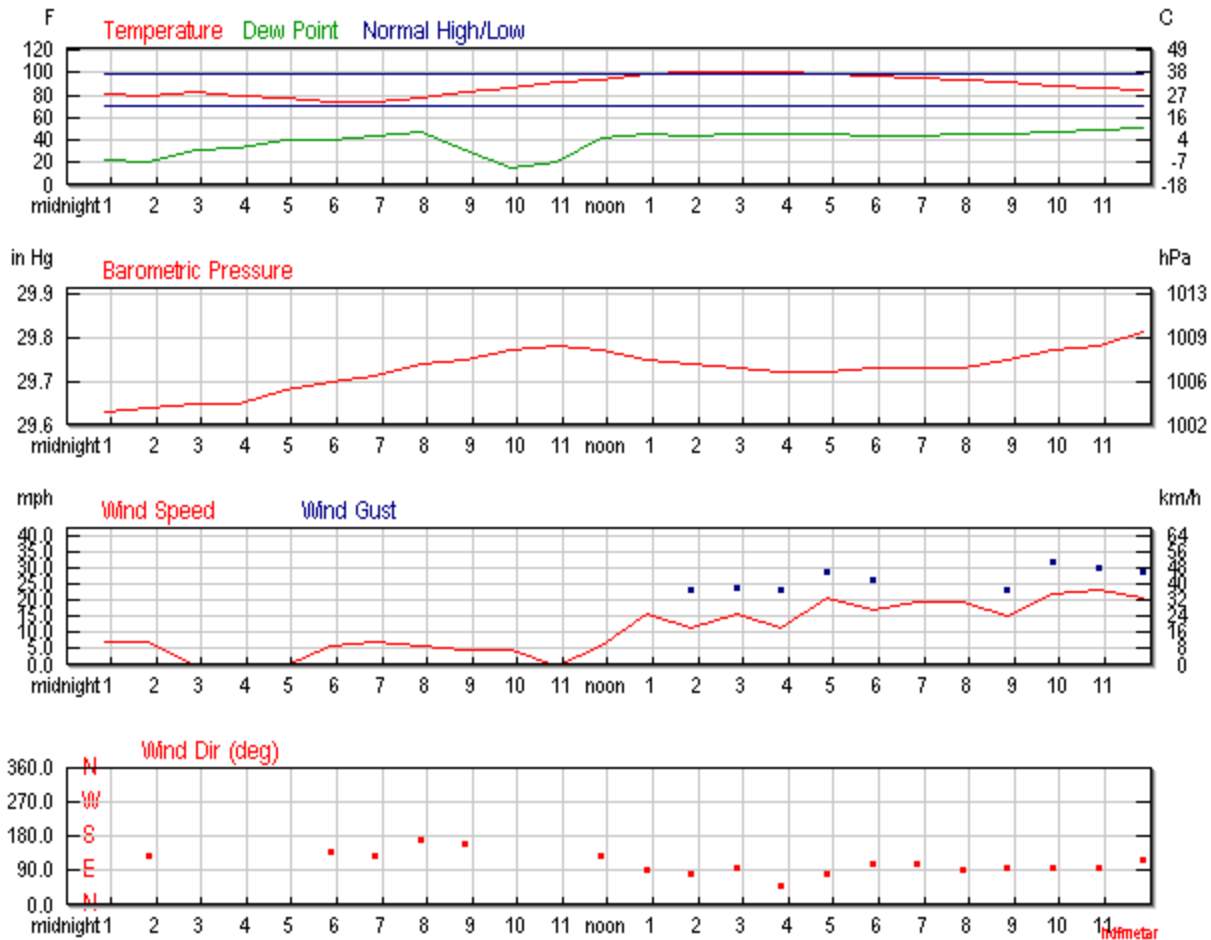


Figure 18-99. El Paso, Texas climate data June 21, 2012, showing that the temperature remained relatively high during the hours of 7 – 9 pm (MDT). Also shown are high wind gusts which may have contributed dust to the PM<sub>10</sub> readings.

September 6, 2012 – The only major peak on this date occurred at midnight. Examination of Figure 18-61 above, shows that smoke was likely reaching the monitor from California. Readings at the SPCY monitor were elevated (116) and the PM<sub>2.5</sub> to PM<sub>10</sub> ratio was over 2.3, indicating that smoke was indeed a factor.

## 18.5 Affects Air Quality

Smoke undoubtedly affected air quality on all dates listed in Table 18-1, as each of these dates had a smoke impact. The NM Border Air Quality Blog confirms that air quality was affected. Full reports for fire season (and other) months may be viewed at <http://nmborderaq.blogspot.com/search?updated-min=2012-01-01T00:00:00-07:00&updated-max=2013-01-01T00:00:00-07:00&max-results=50>.

## 18.6 Natural Events

The Clear Causal Relationship and not Reasonably Controllable or Preventable analyses show that these were natural events caused mainly by wildfire smoke. 80% of the fires were

attributable to lightning in 2012. Natural conditions (including severe drought conditions, winds, and remote or rugged terrain) in many fire locations make control of these fires difficult.

## **18.7 No Exceedance but for the Event**

As the previous sections of this chapter have shown, the exceedances shown in Table 18-1 were caused by natural events – specifically, wildfires in Arizona, New Mexico, northern Mexico and even southern California, which put significant amounts of smoke (and therefore PM<sub>2.5</sub>) into the atmosphere when low winds and cooling land mass caused increases in particle concentrations near the ground, or when moderate winds caused smoke to be blown into the valley. The only other possible source for PM<sub>2.5</sub> would have been from Ciudad Juarez as reports to EPA have previously shown and which were not analyzed for this demonstration.

2012 average PM<sub>2.5</sub> concentration at the SPCY Partisol monitor is 14.8 micrograms per cubic meter. However, the average for the dates included in Table 18-1 for which smoke was a factor is 23.84 micrograms per cubic meter. Excluding this data lowers the average to 13.3 micrograms per cubic meter. As fine dust is also a factor for PM<sub>2.5</sub> readings, another average was calculated which also excluded the high wind events described in previous chapters. This average drops even further, to 11.3 micrograms per cubic meter. Therefore, the SPCY PM<sub>2.5</sub> Partisol monitor would have had no exceedance but for the smoke due to wildfires.